CONF-9305310--

NREL/CP-420-6032
DE94000218

PROCEEDINGS OF THE DOE/NREL/ORNL WORKSHOP

LOW COST MATERIALS OF CONSTRUCTION FOR BIOLOGICAL PROCESSES

MAY 13, 1993

HELD AT THE 15TH SYMPOSIUM ON BIOTECHNOLOGY FOR FUELS & CHEMICALS COLORADO SPRINGS, COLORADO

Sponsored By:
Department of Energy Alternative Fuels - Compatible Materials Program

National Renewable Energy Laboratory
1617 Cole Blvd., Golden, CO 80401 (303) 231-7000

NOTICE

TABLE OF CONTENTS

Page

Executive Summary 1-1

Workshop Arrangements

Agenda 2-1

List of Attendees 2-2

Abstracts/Presentations

DOE Alternative Fuels - Compatible Materials Perspective (Joe Perez, DOE) . . 3-1

Materials Selection for the Biomass to Ethanol Process (Cindy Riley, NREL) . . 3-18

Overview of Fuel Ethanol Industry (Raphael Katzen, RKAII) 3-35

Fuel Infrastructure Concerns (Joe Perez, DOE) 3-37

Corrosion (James R. Keiser, ORNL) 3-49

Corrosion Research (Richard C. Alkire, U. of IL) 3-67

High Resolution Molecular Emission Spectroscopy For Material Characterization and Corrosion Studies (George Andermann, U. of HI) 3-104

Electro Chemical Engineering & Manufacturing Co., Background and Capabilities (Dale Heffner, Electro Chem) 3-127

Chemical-Resistant Non-Metallic Materials of Construction for Biomass-to-Ethanol Process (Norman Huxley, Elf Atochem) 3-141

Work Session Topics

Standards for Biomass from ASTM Committee E-48 on Biotechnology (Larry Eitel, Wolder) 4-1

Discussion Summary 4-17

Questionnaire Summary 5-1

Appendix 6-1

DOE/NREL/ORNL WORKSHOP

LOW COST MATERIALS OF CONSTRUCTION FOR BIOLOGICAL PROCESSES

EXECUTIVE SUMMARY

This represents an informal account of the DOE/NREL/ORNL workshop, "Low Cost Materials of Construction for Biological Processes." The workshop was held Thursday, May 13, 1993, at the Antlers Hotel in Colorado Springs, Colorado, in conjunction with the 15th Symposium on Biotechnology for Fuels and Chemicals. There were 22 attendees in all, representing a variety of companies and institutions. The purpose of this workshop was to present information on the biomass to ethanol process in the context of materials selection and through presentation and discussion, identify promising avenues for future research.

Six technical presentations were grouped into two sessions: process assessment and technology assessment. The technical sessions were followed by a work session in which key issues and ideas raised during the workshop were examined. In addition, input was solicited from the attendees through a questionnaire distributed at the workshop. This information will be used to give direction to future materials research for biomass processing in the areas of materials selection, testing procedures and correlation/interpretation of results. Following is a brief summary of the key issues and discussions taken from the proceedings and questionnaire responses.

Based on the information presented in the process assessment session, the group felt that the pretreatment area would require the most extensive materials research due the complex chemical, physical and thermal environment. Considerable discussion centered around the possibility of metals being leached into the process stream and their effect on the fermentation mechanics. Linings were a strong option for pretreatment assuming the economics were favorable. Fermentation was considered an important area for research also, due to the unique complex of compounds and dual phases present. Again, linings were recommended, as well as stainless steel cladding over less expensive metals. Erosion in feedstock handling equipment was identified as a minor concern.

In the technology assessment session, methodologies in corrosion analysis were presented in addition to an overview of current coatings/linings technology. Widely practiced testing strategies, including ASTM methods, as well as novel procedures for micro-analysis of

corrosion were discussed. Various coatings and linings, including polymers and ceramics, were introduced.

The prevailing recommendations for testing included keeping the testing simple until the problem warranted a more detailed approach and developing standardized testing procedures to ensure the data was reproducible and applicable. The need to evaluate currently available materials such as coatings/linings, carbon/stainless steels, or fiberglass reinforced plastic was emphasized. It was agreed that economic evaluation of each material candidate before, during and after testing must be an integral part of any research plan.

On behalf of the U.S. Department of Energy, Oak Ridge National Laboratory and the National Renewable Energy Laboratory, I want to thank each of you for your participation in the workshop. The information gathered will be useful in determining the focus of future materials research for the biomass to energy process.

Thank you for your interest.

Kelly N. Ibsen
NREL

WORKSHOP ARRANGEMENTS

DEPARTMENT OF ENERGY ALTERNATIVE FUELS - COMPATIBLE MATERIALS PROGRAM

DOE/NREL/ORNL WORKSHOP
LOW COST MATERIALS OF CONSTRUCTION FOR BIOLOGICAL PROCESSES

15TH SYMPOSIUM ON BIOTECHNOLOGY FOR FUELS AND CHEMICALS
THURSDAY, MAY 13, 1993, 1-5 PM
COLORADO SPRINGS, CO

WORKSHOP AGENDA

INTRODUCTION (15 MIN.)

•Welcome	C. Wyman (NREL)
•DOE Alternative Fuels - Compatible Materials Perspective	J. Perez (DOE)
•Workshop Format/Goals	Wyman (NREL)

PROCESS ASSESSMENT (1 HR.)

•Overview of Biomass Processes (30 min):	C. Riley (NREL)
•Overview of Fuel Ethanol Industry (15 min):	R. Katzen (RKAII)
•Fuel Infrastructure Concerns (15 min):	J. Perez (DOE)

TECHNOLOGY ASSESSMENT (1 HR., 15 MIN.)

•Corrosion Research:	- Government	J. Keiser (ORNL)
	- Universities	R. C. Alkire (U. of IL)
		G. Andermann (U. of HI)
•Coatings Technology:		D. Heffner (Electro-Chem)
		N. Huxley (Elf-Atochem)

WORK SESSION TOPICS (1 HR., 30 MIN.)

•Materials:	-Available Technologies and Costs
Chairman: L. Eitel (Wolder)	-Coating Alternatives
Recorder: D. Schell (NREL)	
•*Fuel Infrastructure:	-Processing
Chairman: J. Perez (DOE)	-Storage
Recorder: K. Kadam (NREL)	-Vehicles
•*Test Methods:	-Bench Tests (Coupons)
Chairman: J. Keiser (ORNL)	-Pilot Plant
Recorder: B. Duff (NREL)	

*Due to the number of participants and their areas of expertise, one combined work session was held instead of the three originally planned.

ATTENDEES

DOE/NREL/ORNL Workshop

LOW COST MATERIALS OF CONSTRUCTION FOR BIOLOGICAL PROCESSES

May 13, 1993

AGCHEM Biosynthesis
Roger Warren
830 48th St. E.
Saskatoon, S7K 3Y4
CANADA
(306) 934-2434

AMOCO Corp.
Keith Blanchard
Mail Code B4
P.O. Box 3011
Naperville, IL 60566
(708) 420-5771
Fax: (708) 420-5988

Colorado State University
Jim Linden
Dept. of Agricultural & Chem. Eng.
Ft. Collins, CO 80523
(303) 491-7065 or 491-3122
Fax: (303) 491-7369

Dedini S/A Adm. & Part
Antonio Hilst
Av Limeira, 222
Piracicaba, S. Paulo
Priacicaba, 13414-902
BRAZIL
(019) 421-1122

Electro Chemical Engr. & Mfg.
Dale Heffner
750 Broad St.
Emmaus, PA 18049-0509
(215) 965-9061
Fax: (215) 965-2595

Elf Atochem North America
Norman Huxley
3 Park Way, Room 807
Philadelphia, PA 19102
(215) 587-7137
Fax: (215) 587-7469

Genencor International, Inc.
Steve Lewis
1000 41st Ave., SW
Cedar Rapids, IA 52404
(319) 368-2971

Interep, Inc.
Carl Horecky
P.O. Box 123
Golden, CO 80401
(303) 277-0401
Fax: (303) 277-0452

Meridian Corporation
Rene Tshiteya
4300 King Street
Suite 400
Alexandria, VA 22302
(703) 998-3716

National Renewable Energy Laboratory
(NREL)
Cindy Riley
1617 Cole Boulevard
Golden, CO 80401

Office of Transportation Materials
Joe Perez
Department of Energy EE-34
1000 Independence Ave., SW
Washington D C. 20585
(202) 586-8060
Fax: (202) 586-1600

ATTENDEES (Cont'd.)

Oak Ridge National Laboratory (ORNL)
Jim Keiser
P.O. Box 2008, Bldg. 4500-S, MS-6156
Oak Ridge, TN 37831-6156
(615) 574-4453
Fax: (615) 574-5118

ORNL
Ralph McGill
Bear Creek Road
Building 9108, MS-8087
Oak Ridge, TN 37831-8087

Process Equipment Company (PEC)
Norm Klapper
2653 Spruce Street
Boulder, CO 80302-3808
(303) 449-5702

Raphael Katzen Assoc. Int'l, Inc.
Raphael Katzen
7162 Reading Rd., Ste. 1200
Cincinnati, OH 45237
(513) 351-7500
Fax: (513) 351-0810

Starch Processing (Ethanol) Consultant
Tom Wallace
4426-C Simsbury Rd.
Charlotte, NC 28226
(704) 366-6864

University of Missouri
Rakesh Bajpai
Chemical Engineering
W2030, EBE
Columbia, MO 65211
(314) 882-3708

University of Illinois
Richard Alkire
Dept. of Chemical Eng.
1209 W. California St.
Urbana, IL 61801
(217) 333-3640
Fax: (217) 244-8068

University of Hawaii at Manoa
George Andermann
Dept. of Chemistry
2545 The Mall
Honolulu, HI 96822
(808) 956-8174
Fax: (808) 956-5908

WA Energy Office
Jim Kerstetter
P.O. Box 43165
Olympia, WA 98504
(206) 956-2069 or 956-2030

Wolder Engineers/Constructors
Larry Eitel
Denver West, Bldg. 4
1536 Cole Blvd., Golden, CO 80401
(303) 235-0300
Fax: (303) 235-0066

Xylan Inc.
George J. Tyson
6320 Monona Dr.
Madison, WI 53716
(608) 222-7340

NREL Coordinating Staff

Kelly Ibsen, Process Engineer
Vicky Putsche, Process Engineer
Kris Andrews, Administrative Assistant

ABSTRACTS/ PRESENTATIONS

DOE/NREL/ORNL WORKSHOP LOW COST MATERIALS OF CONSTRUCTION FOR BIOLOGICAL PROCESSES

MAY 13, 1993

Perspective on Low-Cost Materials of Construction for Biological Processing Facilities

Joseph Perez
Office of Transportation Materials
Department of Energy EE-34
1000 Independence Ave., SW
Washington D.C. 20585

ABSTRACT

This presentation focused on the Mission and Research and Development areas of the Office of Transportation Materials. The technical issues and near term needs of industry in the Alternate Fuels - Compatible Materials Program area were discussed. Low cost materials are a critical need related to the biomass technology. With the current budgetary constraints, establishing priorities is critical to obtaining cooperative industry and government agency support to capitalize on the opportunities and achieve breakthroughs in the transfer of the technology. Materials are definitely one of the enabling priorities that will bring the economics of large scale production costs more in line with conventional fuels.

DOE/OFFICE OF TRANSPORTATION MATERIALS ALTERNATIVE FUELS-COMPATIBLE MATERIALS PROGRAM

PERSPECTIVE

Joseph M. Perez, Program Manager
Office of Transportation Materials
U.S. Department of Energy

DOE/NREL/ORNL Workshop on Low-Cost
Materials of Construction for Biological Processes
Colorado Springs, CO
May 13, 1993

Alternative Fuels Compatible Materials

Outline

- The Office of Transportation Materials
  - Mission
  - R&D Areas
- Alternative Fuel Biomass Processing
  - Technical Issues
  - Near-term Materials Needs

Office of Transportation Materials
Materials Development Program

Origin - DOE/CE * Reorganization April 1990

Action

- The Office of Transportation Materials (OTM) was created to provide a centralized materials development support to the programs of the Office of Transportation Technologies

* Now EE (Energy Efficiency & Renewable Energy)

Organization of the Office of Transportation Technologies

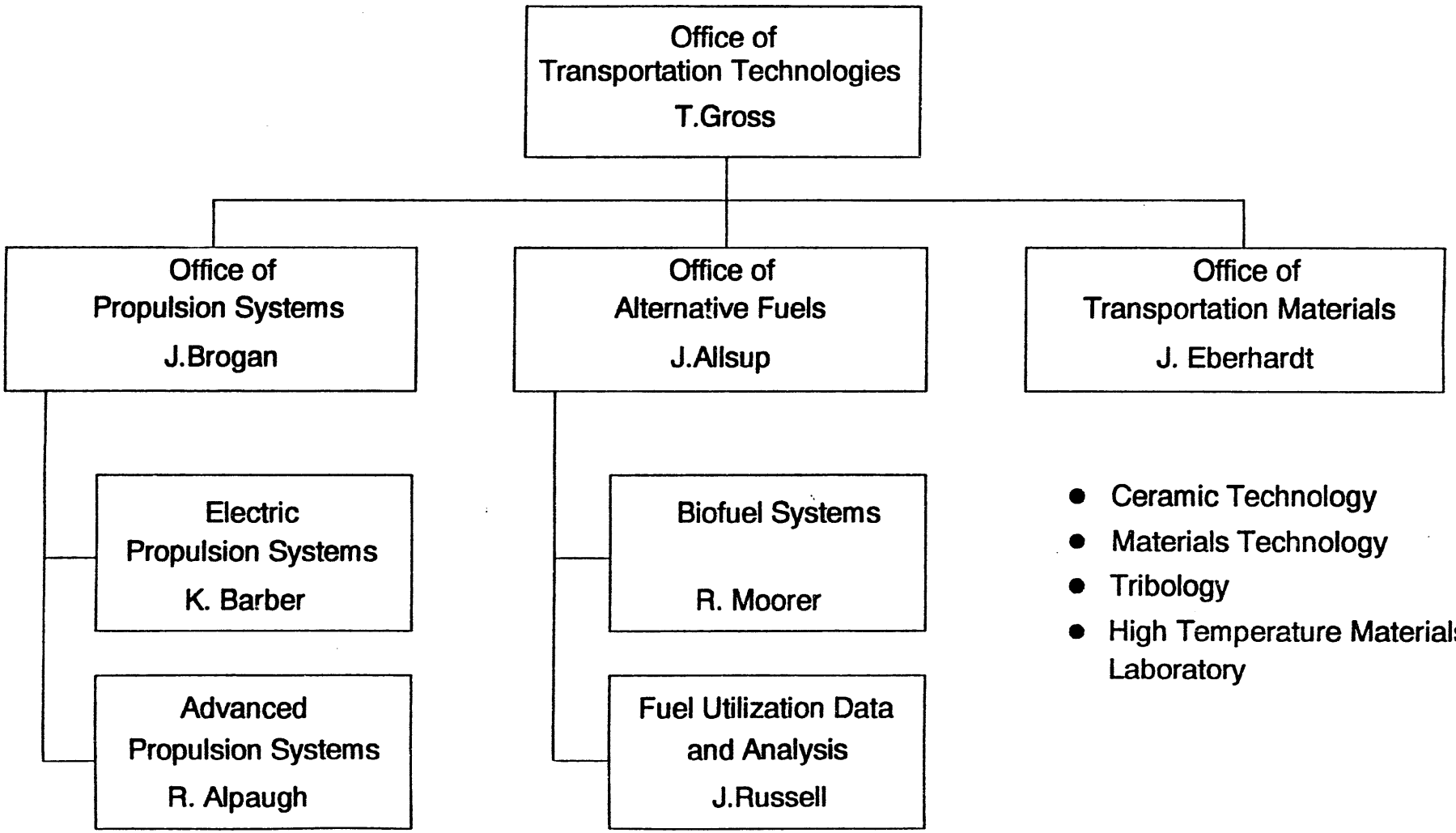

- Ceramic Technology
- Materials Technology
- Tribology
- High Temperature Materials Laboratory

Role and Mission

Office of Transportation Materials

The Office of Transportation Materials is developing a comprehensive R&D program which seeks to extend throughout the transportation sector of the economy the benefits of modern materials science and engineering.

- Materials technology enables components and systems to achieve their design performance capabilities.

- Improved materials of all types (metals, metal matrix composites, intermetallics, polymers, polymer matrix composites and ceramics) can be exploited so that their inherently superior properties can make the largest contribution to:

  - improving energy efficiency;
  - reducing environmental degradation; and
  - utilizing alternative fuels all at the lowest cost possible.

Proposed Program Structure of OTM

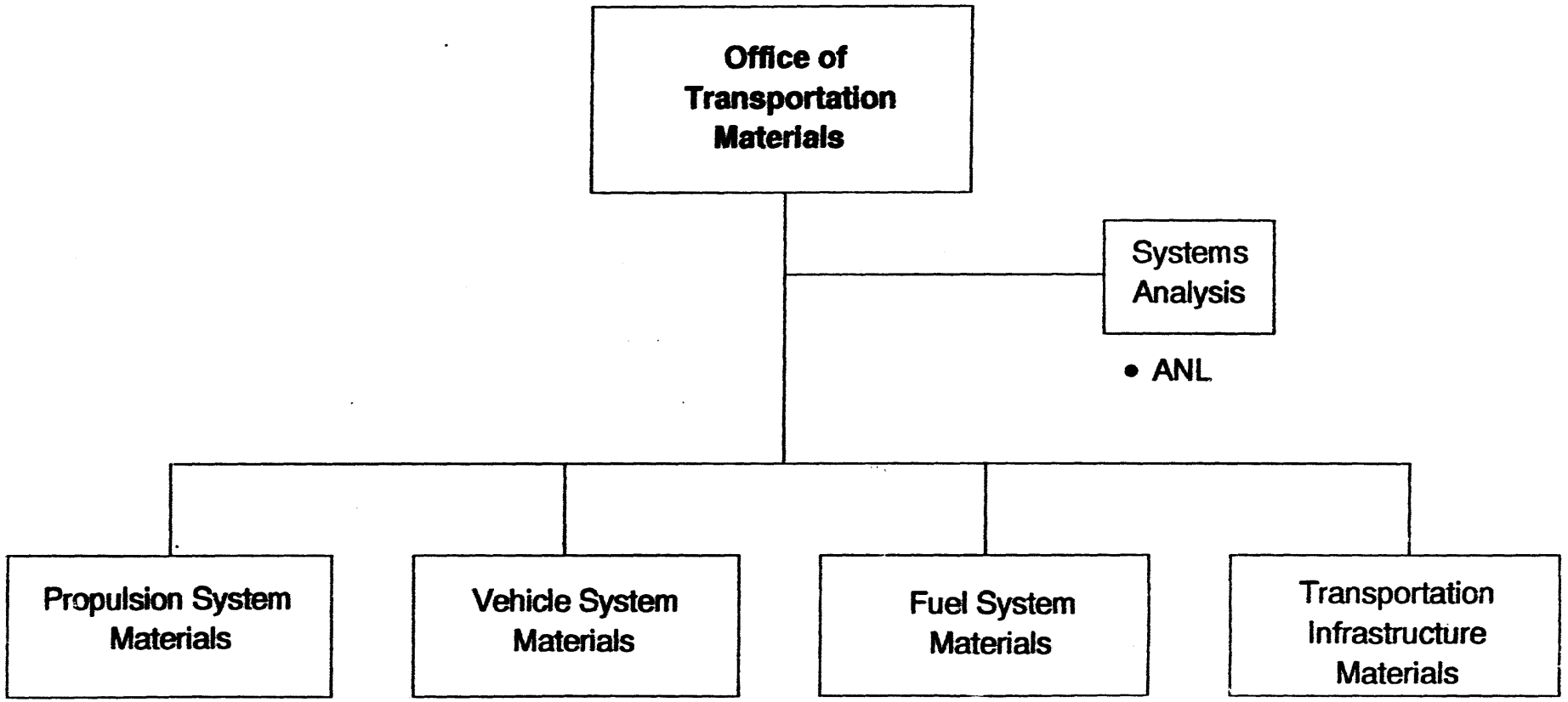

Office of Transportation Materials

Mission

- Develop an industrial technology base in advanced transportation-related materials and associated materials processing.

- Enable development and engineering of energy-efficient transportation systems that will allow the U.S. transportation sector to shift from near total dependence on petroleum to use of alternative fuels and electricity.

- Pursue excellence in environmental safety and health performance by incorporating ES&H issues into all aspects of materials development.

Office of Transportation Materials

Budget History

	FY 1990	FY 1991	FY 1992	FY 1993	FY 1994 (Request)
Ceramics Technology	14.2	16.0	15.8	17.8	19.6
Materials Technology	0.0	1.0	1.0	2.0	6.0
Tribology	3.0	3.0	3.0	1.6	0.6
AFCM	—	—	—	1.0	2.0
High Temperature Materials Laboratory	2.9	3.5	3.7	3.8	4.6
	20.1	23.5	23.5	26.2	32.8

Office of Transportation Materials

FY 1993 Budget: $26.2 Million

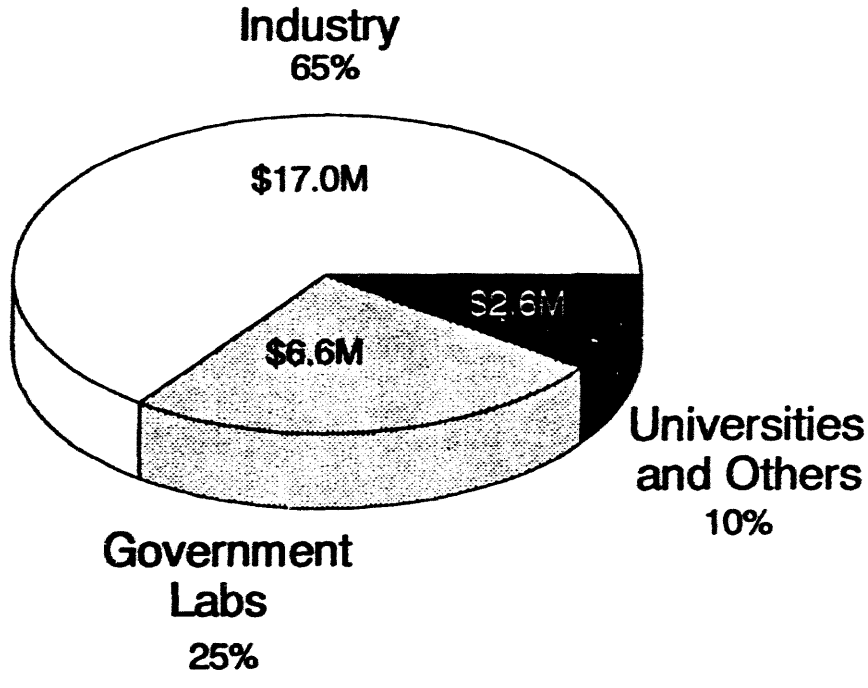

Advanced Materials and Processing Program (AMPP)

Goal

Improve manufacture and performance of materials to enhance U.S. quality of life, national security, industrial productivity and economic growth

Importance of Materials

Materials is a KEY "enabling technology"

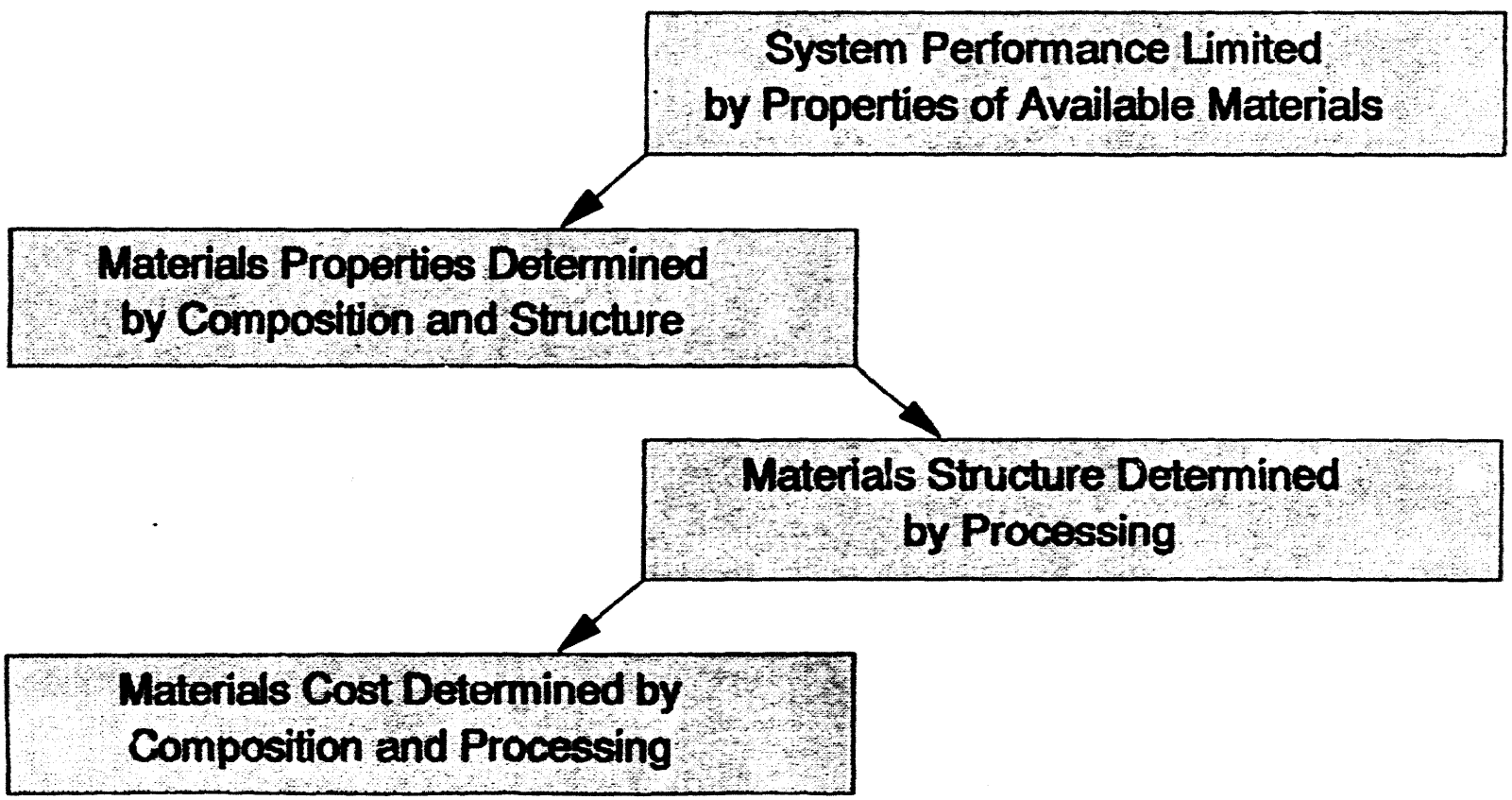

Biomass Processes

Are Materials a Major Factor?

Biocatalysis Hierarchy of Models

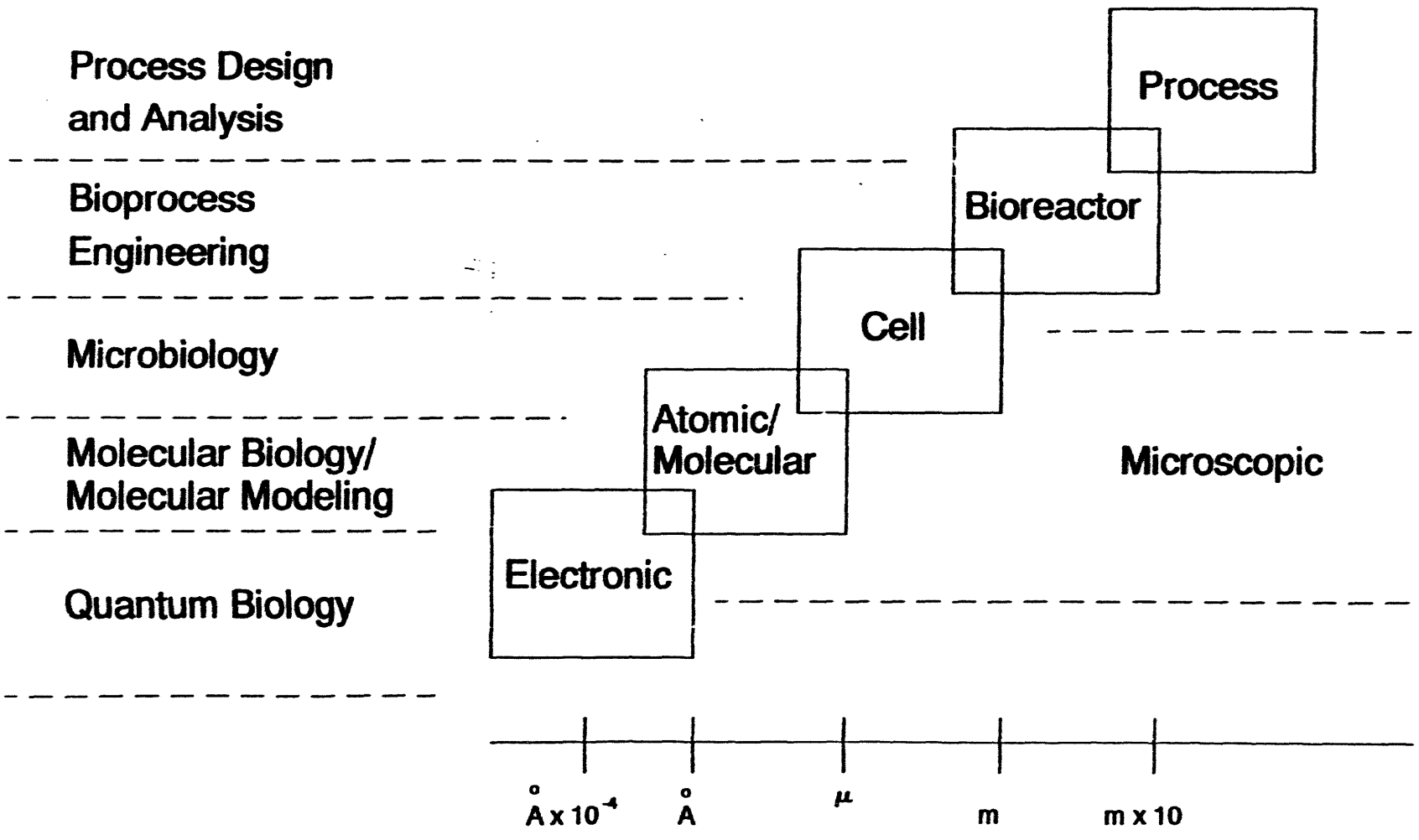

Strategy

- Establish a systematic planning framework and process
- Establish priorities reflecting private sector input (workshops, visits, etc)
- Solicit agency support for enhancement opportunities while taking into consideration budgetary constraints
- Conduct additional planning with private sector on applied programs
- Effect a multi-year phase-in to capitalize on opportunities and achieve breakthroughs

Office of Transportation Materials

Goals

- Improve competitiveness
- Reduce energy dependence
- Environmentally friendly
- Produce U.S. jobs

DOE/NREL/ORNL WORKSHOP LOW COST MATERIALS OF CONSTRUCTION FOR BIOLOGICAL PROCESSES

MAY 13, 1993

Materials Selection for the Biomass to Ethanol Process

Cindy Riley
NREL
1617 Cole Blvd.
Golden, CO 80401

ABSTRACT

This presentation provided an overview of the conditions of service and economic aspects of materials selection for biomass conversion. The general process for converting biomass to ethanol is comprised of the following steps: feedstock handling, pretreatment, biocatalyst production, fermentation, and ethanol recovery. The conversion of biomass to biofuels is relatively well-researched in some aspects; other aspects are much less understood. One of the latter areas is materials selection for the process. Often, construction materials are chosen solely on the basis of past experience. Of the process areas, the highest percentage of installed equipment costs are in the pretreatment and the fermentation areas (source: the NREL design case). These areas represent the greatest potential for savings from reduced equipment costs.

MATERIALS SELECTION FOR THE BIOMASS TO ETHANOL PROCESS

The Conditions of Service and
Economic Aspects of
Materials of Construction Selection
for Biomass Conversion

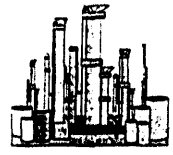

National Renewable Energy Laboratory

GENERAL COMPOSITION OF LIGNOCELLULOSIC MATERIALS

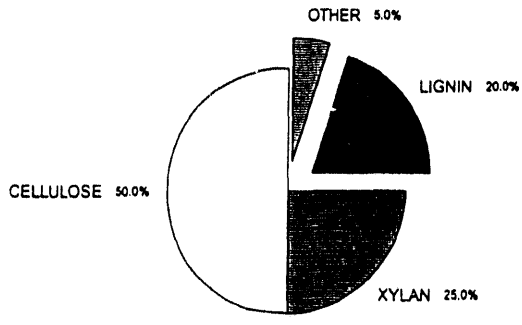

Example: Hardwoods

RELATIVE TOTAL INSTALLED COST OF PROCESS AREAS

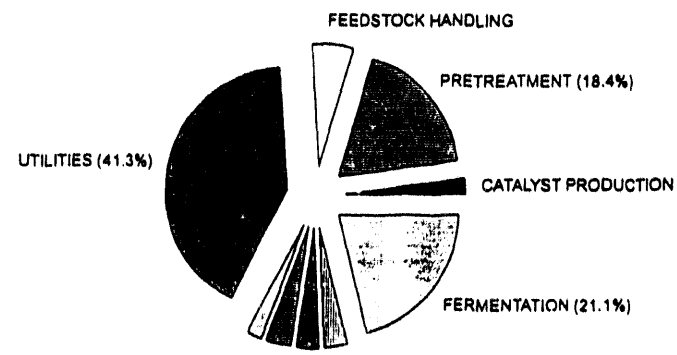

SOURCE: NREL DESIGN CASE, WOOD TO ETHANOL

BIOMASS TO ETHANOL GENERAL PROCESS CONDITIONS

- ABRASIVE SOLIDS
- MODERATE TO HIGH SOLIDS LEVEL
- pH EXTREMES
- ACIDIC, AQUEOUS MEDIUM
- AMBIENT TO MODERATE TEMPERATURES
- ATMOSPHERIC TO LOW PRESSURES

OTHER INDUSTRIES USING SIMILAR TECHNOLOGIES

- GRAIN TO ETHANOL INDUSTRY
  - FERMENTATION
  - RECOVERY
  - WASTE TREATMENT
- WINE/BREWING INDUSTRY
  - ASEPTIC CONDITIONS
  - FERMENTATION
  - WASTE TREATMENT
- PULP/PAPER INDUSTRY
  - FEEDSTOCK HANDLING
  - PRETREATMENTS
- PHARMACEUTICALS
  - ASEPTIC CONDITIONS
  - PRODUCTION OF BY-PRODUCTS
  - NOT A LOW VALUE PRODUCT

PRETREATMENT

- PURPOSE: TO HYDROLYZE THE XYLAN TO XYLOSE AND INCREASE THE DIGESTABILITY OF THE LIGNOCELLULOSIC STRUCTURE FOR SUBSEQUENT ENZYMATIC HYDROLYSIS

ACID PREHYDROLYSIS

- FEED: MILLED WOOD CHIPS (GRASSES, PAPER, MSW)
- SOLIDS: 35%
- AGENT: 0.73 - 0.95 WT. % SULFURIC ACID
- TEMPERATURE: 140 - 180 C
- PRODUCT pH: 1.3 - 1.4

ACID PREHYDROLYSIS

BY-PRODUCTS OF WOOD SUBSTRATES

- IDENTIFIED — FOR 80% CONVERSION OF XYLAN TO XYLOSE:
  - FURFURAL — 13 WT. % OF XYLAN
  - HMF — 0.1 WT. 5 OF CELLULOSE
  - ACETIC ACID — 3 WT. % OF BIOMASS

- THEORETICAL
  - LIGNIN DERIVATIVES
  - FORMIC ACID
  - HYDROGEN GAS
  - CARBON DIOXIDE

ACID PREHYDROLYSIS

- EQUIPMENT
  - FEEDERS
  - IMPREGNATORS/REACTORS
  - FLASH TANK/AGITATOR
  - PUMPS
  - ACID HANDLING EQUIPMENT
- PROCESS CONSIDERATIONS
  - VERY LOW pH
  - HIGH SOLIDS CONCENTRATION
  - MODERATE TEMPERATURE AND PRESSURE
  - EROSION BY SUBSTRATE
  - LEACHING OF METALS
  - CORROSION PRODUCTS
  - SHORT RESIDENCE TIME

OTHER PRETREATMENT PROCESSES

- 2-STAGE ACID PREHYDROLYSIS
  - HIGH XYLAN CONVERSION
  - 2 WT. % XYLAN TO FURFURAL
- AMMONIA FIBER EXPLOSION (AFEX)
  - AMBIENT TEMPERATURE
  - FEW BY-PRODUCTS FORMED
  - NO NEUTRALIZATION NEEDED
  - LOW XYLAN CONVERSION
- ACID HYDROLYSIS
  - REPLACES ENZYMATIC HYDROLYSIS
  - HIGH TEMPERATURES (265 C)
  - DEGRADATION PRODUCTS - TARS, ALPHA-PINENE, OLEIC ACID, LEVULINIC ACID

OTHER PRETREATMENT PROCESSES

- STEAM EXPLOSION
  - HIGH PRESSURE (650 PSIG)
  - EXPLOSIVE DECOMPRESSION
  - LOW XYLAN CONVERSION
  - DEGRADATION PRODUCTS FORMED
- ACID CATALYZED STEAM EXPLOSION
  - USES SULFUR DIOXIDE
  - PRODUCES SULFURIC ACID
  - REQUIRES RECOVERY SYSTEM

NEUTRALIZATION

- FEED: HYDROLYZATE/SOLIDS FROM ACID PRETREATMENT
- SOLIDS: 12%
- AGENT: LIME
- TEMPERATURE: 100 C
- PRODUCT pH: 5.0

BY-PRODUCTS OF WOOD SUBSTRATES

- IDENTIFIED
  - GYPSUM

NEUTRALIZATION

- EQUIPMENT
  - LIME HANDLING
  - NEUTRALIZATION TANK
  - HEAT EXCHANGERS
  - SLURRY PUMPS

- PROCESS CONSIDERATIONS
  - LARGE pH SWING
  - PRECIPITATE FORMATION
  - MAINTENANCE OF ASEPTIC CONDITIONS
  - MODERATE TEMPERATURES
  - SHORT RESIDENCE TIME

NEUTRALIZATION

OTHER NEUTRALIZATION TECHNIQUES

- OVERLIMING
  - ADDITIONAL GYPSUM FORMED
  - REQUIRES ADDITIONAL ACID UTILIZATION
  - MAY REMOVE ACID PRETREATMENT BY-PRODUCTS

FERMENTATION

- PURPOSE: TO CONVERT SUGARS TO ETHANOL THROUGH METABOLIC PATHWAYS OF SELECTED ORGANISMS

FERMENTATION

- FEED: STREAM FROM PRETREATMENT
- SOLIDS: 12%
- AGENT: YEASTS, ENZYMES (BACTERIA, FUNGI)
- TEMPERATURE: 37 C
- PROCESS MODE: CONTINUOUS FERMENTATION
- PRODUCT pH: 3.0 - 5.0
- pH CONTROL AGENTS:
  - CALCIUM SALTS
  - AMMONIUM HYDROXIDE
  - SODIUM HYDROXIDE
  - POTASSIUM HYDROXIDE

FERMENTATION

BY-PRODUCTS OF WOOD SUBSTRATES

• IDENTIFIED	FOR 3.0 WT. % ETHANOL PRODUCED
- CARBON DIOXIDE	3.0 WT. %
- GLYCEROL	0 - 0.05 WT. %
- ACETIC ACID	0 - 0.4 WT. %
- LACTIC ACID	TRACE AMTS.

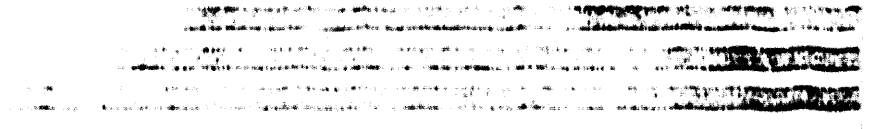

FERMENTATION

BY-PRODUCTS OF WOOD SUBSTRATES

- THEORETICAL
  - ACETALDEHYDE
  - FUSEL OILS (AMYL, ISOAMYL, PROPYL ALCOHOL)
  - SUCCINIC ACID (FROM E. COLI)
  - PROPIONIC ACID
  - FORMIC ACID
  - HYDROGEN GAS
  - AMMONIA (FROM pH CONTROL AGENTS)
  - CHLORIDE IONS (FROM SALTS)
  - XYLITOL, ARABITOL, MANNITOL

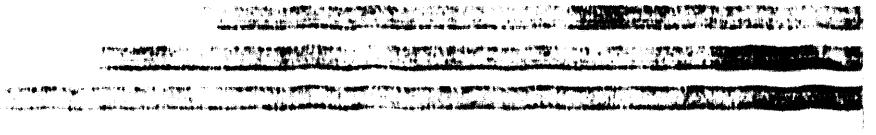

FERMENTATION

BY-PRODUCTS OF WOOD SUBSTRATES

- BY-PRODUCTS FROM POSSIBLE CONTAMINANTS
  - LACTIC ACID (FROM LACTOBACILLUS)
  - SUCCINIC ACID

FERMENTATION

- EQUIPMENT
  - FERMENTER TANKS (10,000 TO 1,000,000 GALLONS)
  - HOLD TANKS
  - AGITATORS
  - HEAT EXCHANGERS
  - PUMPS

- PROCESS CONSIDERATIONS
  - ACIDIC pH
  - AQUEOUS ENVIRONMENT
  - LONG RESIDENCE TIME
  - MAINTENANCE OF ASEPTIC CONDITIONS
  - EROSION FROM GYPSUM PRECIPITATE
  - LEACHING OF METALS
  - CORROSION PRODUCTS
  - LOW TEMPERATURE
  - ATMOSPHERIC PRESSURE

FEEDSTOCK HANDLING

- FEED: WOOD, GRASSES, PAPER, MSW
- MOISTURE: 10 - 50 WT. %
- TEMPERATURE: AMBIENT

FEEDSTOCK HANDLING

- EQUIPMENT
  - STORAGE AREAS
  - BINS/HOPPERS
  - FEEDERS
  - CONVEYORS, WATER FLUME
  - MILLS, GRINDERS, SHREDDERS

- PROCESS CONSIDERATIONS
  - ABRASIVE FEED/EROSION OF EQUIPMENT
  - POSSIBLE DROP IN FEEDSTOCK pH DUE TO POOR MANAGEMENT TECHNIQUES
  - LOW MOISTURE
  - AMBIENT TEMPERATURE

ETHANOL RECOVERY

- FEED: PRODUCT STREAM FROM FERMENTATION
- SOLIDS: 6 WT. %
- TEMPERATURE: 37 - 110 C
- PRODUCT pH: 3.0 - 5.0

ETHANOL RECOVERY

- EQUIPMENT
  - DISTILLATION COLUMNS
  - TANKS
  - HEAT EXCHANGERS
  - PUMPS
  - CENTRIFUGES
- PROCESS CONSIDERATIONS
  - CONCENTRATION OF BY-PRODUCTS
  - GYPSUM PRECIPITATION
  - SOLIDS FOULING
  - ORGANIC ACIDS
  - AQUEOUS SLURRY
  - ACIDIC pH
  - LOW PRESSURE
  - MODERATE TEMPERATURE

WASTE TREATMENT

- FEED: VARIED
- SOLIDS: DISSOLVED SOLIDS
- TEMPERATURE: 35 - 37 C
- PRODUCT pH: 6.8 - 7.4

WASTE TREATMENT

- EQUIPMENT
  - TANKS
  - HEAT EXCHANGERS
  - SLURRY PUMPS
- PROCESS CONSIDERATIONS
  - ALKALINE MEDIUM
  - GAS PRODUCTION (METHANE, CARBON DIOXIDE)
  - LOW TEMPERATURE
  - ATMOSPHERIC PRESSURE
  - WELL-DEFINED TECHNOLOGY

PROCESS VARIABLES THAT AFFECT MATERIALS SELECTION

- PRETREATMENT
  - SUBSTRATE TYPE
  - PRETREATMENT METHOD
    - AGENTS
    - TEMPERATURE
- FERMENTATION
  - pH
  - pH CONTROL AGENTS
  - SELECTION OF ORGANISM
  - WELD/LOAD STRESS
- OTHER AREAS
  - ABRASIVE NATURE OF SUBSTRATE
  - CIP/CS SYSTEM

CLEAN-IN-PLACE AND CHEMICAL STERILIZATION

- CIP PROCESS CONSIDERATIONS
  - TYPE OF CLEANING AGENT
  - CONCENTRATION
  - TEMPERATURE
  - pH
  - IMPINGEMENT/VELOCITY
- EQUIPMENT CONSIDERATIONS
  - SELF-DRAINING
  - SMOOTH, INERT, NON-POROUS INTERIOR SURFACE
  - NO HIDDEN/UNEVEN AREAS
  - EASY TO INSPECT

PURCHASED COST OF ACID PT REACTOR SHELL

TOTAL PURCHASED COST OF REACTOR-$1,830,000

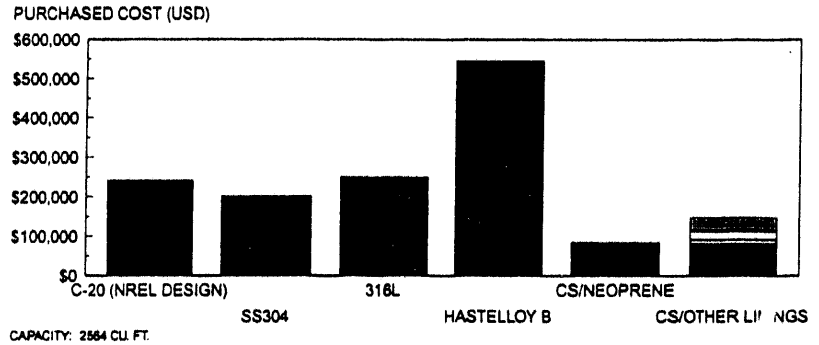

CAPACITY: 2564 CU. FT.
DP=175 PSIG, DT=400 F
SOURCE: NREL DESIGN CASE

PURCHASED COST OF ATMOSPHERIC TANKS

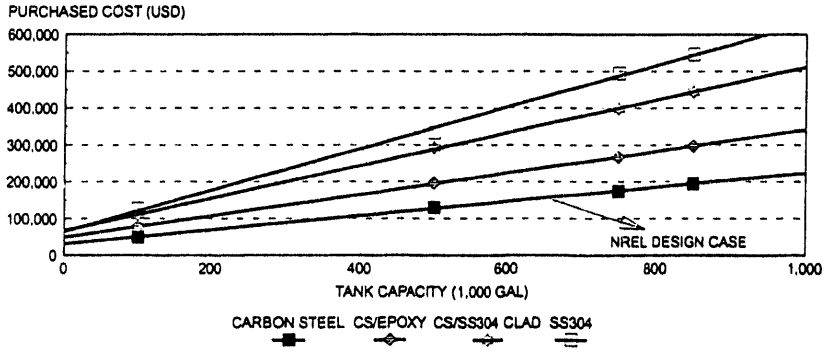

LOW-COST MATERIAL SELECTION NEXT STEPS

- DEVELOP TESTING PROGRAM
- IDENTIFY PARTICIPANTS
- IDENTIFY ADDITIONAL MATERIALS OPTIONS
  - SCREEN FOR POTENTIAL ECONOMIC IMPACT
- SUBJECT BEST ALTERNATIVES TO TESTING PROGRAM
  - CORROSION TESTING
  - IN-DEPTH ECONOMIC ANALYSIS
  - INHIBITION TESTING
- IDENTIFY CANDIDATES FOR LONG TERM VALIDATION
  - USE OF NREL PILOT DEVELOPMENT UNIT (PDU)

DOE/NREL/ORNL WORKSHOP LOW COST MATERIALS OF CONSTRUCTION FOR BIOLOGICAL PROCESSES

MAY 13, 1993

Overview of Fuel Ethanol Industry

Dr. Raphael Katzen
Raphael Katzen Assoc. Int'l., Inc.
7162 Reading Road, Suite 1200
Cincinnati, OH 45237

ABSTRACT

Dr. Katzen presented an overview of the processes used in the corn-to-ethanol industry including wet milling, dry milling and distillation. The typical conditions of service and materials used were outlined as well as material failures observed.

Ethanol is produced from grain, primarily corn, by two standard processes: wet and dry milling. Wet milling accounts for about 60 percent of total ethanol production. Dry milling plants cost less to build and have higher ethanol yields, but the value of the coproducts is less.

In the wet milling process, the corn is soaked in water and sulfur dioxide prior to milling. Following milling of the slurry, the starch is separated from the germ, fiber and gluten. These byproducts are further processed into gluten meal, gluten feed and corn oil. The gluten feed and gluten meal recovery areas are constructed of SS-304. Once the starch liquor has been separated from the other products it can be saccharified and fermented into ethanol, or it can be processed into high-fructose corn syrup. Ethanol fermentation in wet milling plants is usually carried out in SS-316 fermentation tanks. Ethanol is recovered from the fermentation broth, or beer, by distillation and then dehydrated. Equipment in the ethanol distillation area is usually constructed of SS-304.

The dry milling process begins with milling the dry corn prior to steam cooking. Milling the dry corn kernels is a very abrasive operation at a pH of about 6. Originally SS-304 was specified for milling equipment, however carbon steel with hardened surfaces is currently used. During the cooking process the starch is disaggregated, but not separated, from other grain components. The resulting slurry contains starch, fiber and gluten. The freed starch is then hydrolyzed by enzymes to produce fermentable sugars. Under anaerobic conditions yeast ferments the sugar to ethanol. Historically, there have been corrosion problems with carbon steel and SS-304 fermentation tanks, primarily as a result of low pH excursions due to bacterial contamination problems. Recently, there has been evidence that carbon steel tanks may be suitable in batch fermentations where contamination is controlled and the pH is maintained between 4.5 and 5.5. Continuous, or cascade, fermentations are often carried out at a lower pH of 3.5 to minimize bacterial infection. Stainless steel tanks may be required for

cascade fermentation operations. Ethanol is recovered by distillation and dehydrated. The unfermented materials are recovered, dried and sold as Distillers Dried Grains and Solubles (DDGS). The DDGS drying system is usually constructed of SS-316 because of the low pH, 3.0 - 3.5 and relatively high temperatures in this area.

Publications

- "Ethanol from Lignocellulosic Wastes with Utilization of Recombinant Bacteria", 1993.
- "Ethanol from Corn-State-of-the-Art Technology and Economics", 1992.
- "Fermentation Technology - Choices and Challenges", 1992.

DOE/NREL/ORNL WORKSHOP LOW COST MATERIALS OF CONSTRUCTION FOR BIOLOGICAL PROCESSES

MAY 13, 1993

Infrastructure Concerns Related to The Production, Storage and Use of Alternative Fuels from Biological Processes

Joseph M. Perez
Office of Transportation Materials
Department of Energy EE-34
1000 Independence Ave., SW
Washington D.C. 20585

ABSTRACT

This presentation was aimed at better defining the material needs related to biomass processing, storage and use of alcohol fuels. An overview of the impact of the technology and the real needs were discussed. To successfully solve many of the materials problems identified in previous discussions, a cooperative effort involving the best ideas of industry, university and government researchers will be required. In the laboratory phase of development, materials are of little concern since the objective is obtaining results regardless of cost. As the process advances to the pilot plant or development stage, materials are a factor but usually, they are not critical to the successful outcome of the process. However, if the pilot plant study is successful, the economics of up-scaling the process to commercialization and large scale production make materials and maintenance significant factors. To be competitive in the current business climate does not allow the leisure of long term drawn out edisonian type of research and development. The purpose of the workshop is to define the best path to rapid development and transfer of the technology to industry. This means new ideas regarding material needs for processing plants and storage facilities. There are even material needs for vehicles that will utilize the end product. The purpose of the workshop is to define the best path available to produce alcohols by the biomass process and to define alternative materials approaches to do so in a most economical process. The desired end result is in contributing to the DOE goals to reduce our dependence on foreign oil, improve engine emissions, conserve energy and ultimately create new jobs.

DOE/OFFICE OF TRANSPORTATION MATERIALS ALTERNATIVE FUELS-COMPATIBLE MATERIALS PROGRAM

INFRASTRUCTURE CONCERNS

Joseph M. Perez, Program Manager
Office of Transportation Materials
U.S. Department of Energy

DOE/NREL/ORNL Workshop on Low-Cost
Materials of Construction for Biological Processes
Colorado Springs, CO
May 13, 1993

"Infrastructure" Concerns

- Processing Materials
- Storage Systems
- Vehicles

"Big Fuels Picture"

- Energy Conservation
- Emissions Reduction
- Renewable Energy
- More Efficient Engines
- New Jobs

Workshop

Purpose: Define Real Needs

Input:
- Industry
- University
- Government

Result: Define Path(s)

Alternative Fueled Engines and Vehicles

Technical Issues

- Fuels: Alcohols, Natural Gas
- Engines: Light- & Heavy-duty
- Components
- Emissions & Catalysts
- Infrastructure

Alternative Fuels - Compatible Materials (AFCM) Program

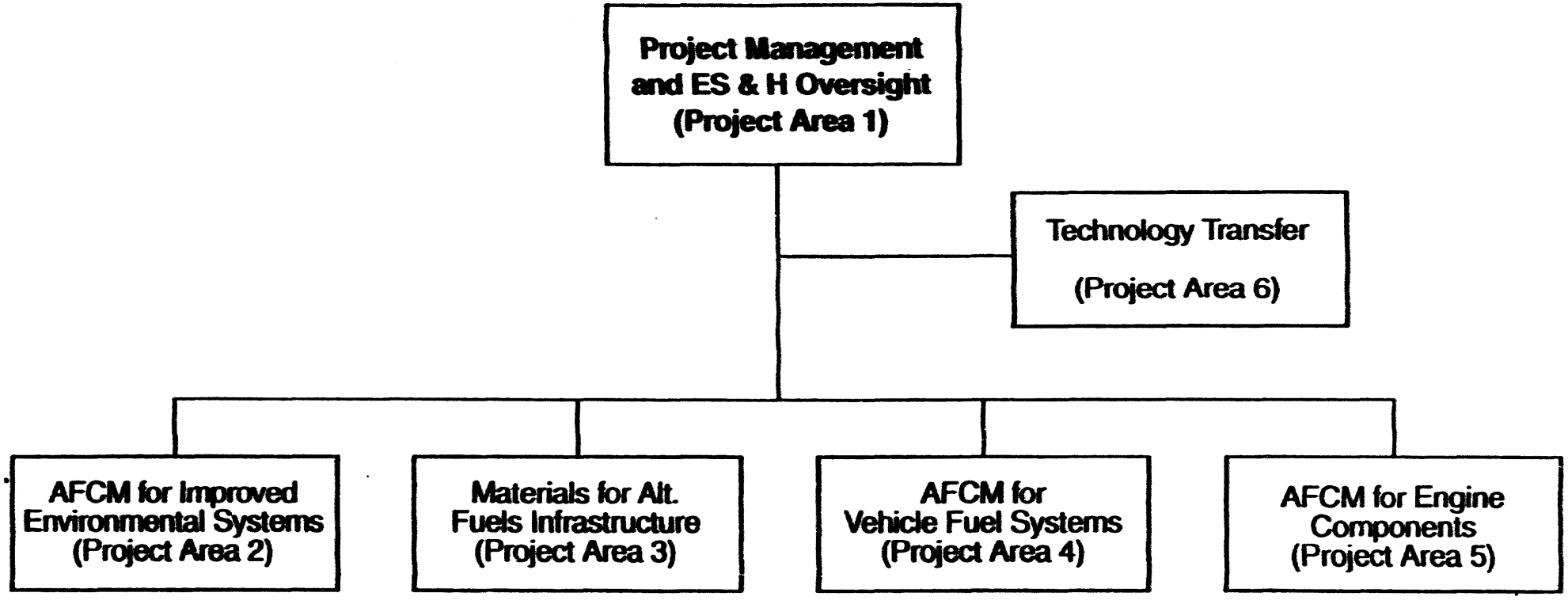

- 2.1 Improved Catalysts for Alternative Fuels
- 2.2 Aging and Testing Protocol for Alt. Fuel Catalysts

- 3.1 Materials for Processing of Biomass Fuels

- 4.1 All-Composite Fuel Tank Materials for Natural Gas
- 4.2 Impermeable Fuel Tank Materials for Alcohols

- 5.1 Friction and Wear of Alternative Fuel Materials

Materials for Alternative Fuels Infratructure

Biomass Process

- **Relevance of Materials of Construction**
  - Laboratory/Experimental Phase
    - Minimal Concern
  - Development/Pilot Plant Phase
    - Factor but Not Usually Critical
  - Commercialization/Production
    - Materials & Maintenence are Significant Factors

"Competitiveness"

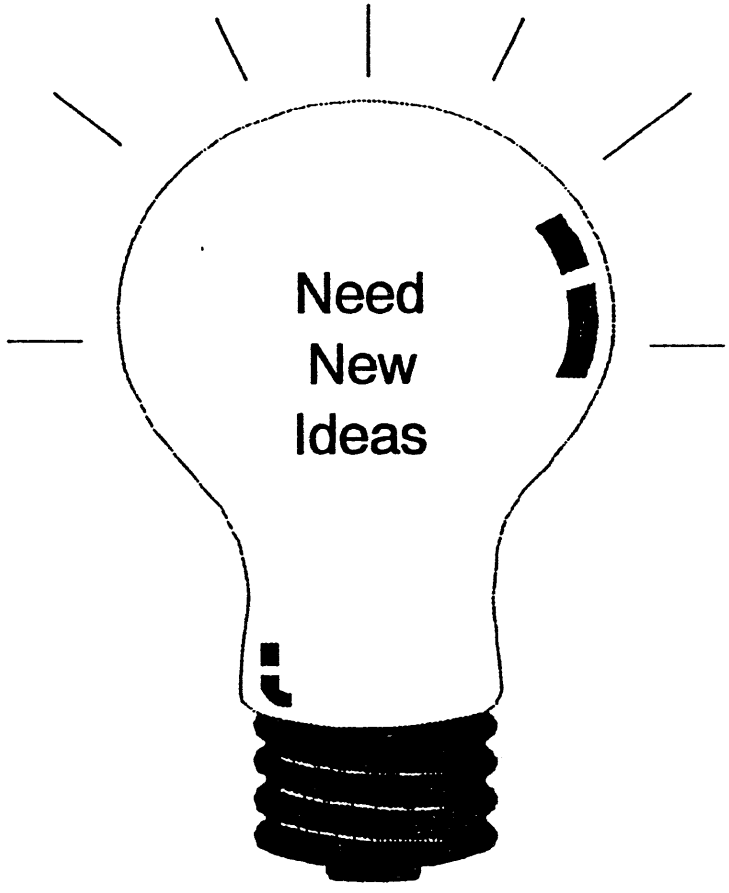

Example: Approach -1

- Data Base Searching
- Alternative Materials
- Experimental Evaluations
- Experimental Data Reduction
- Recommendations
- Productivity & Cost Impact
- Select

Time: 3-5 Years

Example: Approach-2

- Define Requirements/Theorize Needs
- Model Process
- "Tailor" Materials/"Best" Match
- Optimize Experiments
- Data Reduction/Refinements
- Recommendations
- Productivity & Cost Impact
- Select

Time: 1-3 Years

Renewable Energy/Alcohol

Workshop Strategy:

- Identify Material Needs
- Alternative Paths
- Draft Operating Plan (MYPP)
- Review & Revise
- Obtain Required Funding
- Execute Plan (AOP,FWP)

DOE/NREL/ORNL WORKSHOP LOW COST MATERIALS OF CONSTRUCTION FOR BIOLOGICAL PROCESSES

MAY 13, 1993

Corrosion

Dr. James R. Keiser
Oak Ridge National Laboratory
Bldg. 4500 S
P.O. Box 2008
Oak Ridge, TN 37831-6156

ABSTRACT

Dr. Keiser provided an overview of the Corrosion Science and Technology Group at ORNL including staffing and program diversity. Research capabilities such as Scanning Electron Microscopy and Electrochemical testing were discussed. Examples of corrosion in metals and changes in mechanical properties of ceramic composites were also presented.

CORROSION

DOE/NREL/ORNL WORKSHOP

LOW COST MATERIALS OF CONSTRUCTION FOR BIOLOGICAL PROCESSES

Dr. James R. Keiser
Corrosion Science and Technology Group
Metals and Ceramics Division
Oak Ridge National Laboratory

NATIONAL LABS HISTORICALLY HAVE SUPPORTED COMPLEX CHEMICAL PROCESSING ACTIVITIES

- Processing Of Nuclear Materials
- Coal Conversion (Gasification/Liquefaction)
- Battery And Fuel Cell Development
- Thermochemical H_2 Development
- Desalination
- Biomass
- Waste Treatment
- Industrial Support (Wood Pulping)

METALS AND CERAMICS DIVISION

- STAFF

  170 PROFESSIONALS

  154 TECHNICAL AND ADMINISTRATIVE SUPPORT

- PROGRAM MIX

  65% METALS

  35% CERAMICS

- FOCUS

  20% BASIC RESEARCH

  60% LONG-RANGE APPLIED RESEARCH

  20% DEVELOPMENT

CORROSION SCIENCE AND TECHNOLOGY GROUP

CONDUCTS EXPERIMENTAL AND ANALYTICAL STUDIES TO PROVIDE AN UNDERSTANDING OF THE EFFECTS OF ENVIRONMENT ON MATERIALS FOR A BROAD RANGE OF ENERGY APPLICATIONS

- Mechanistic Studies
- Evaluation Tests
- Engineering System Tests
- Failure Analyses
- Consulting

CURRENT ORNL MATERIALS SUPPORT FOR CHEMICAL PROCESSES INCLUDES

- Coal Gasification and Liquefaction
- Methane Reforming
- Molten Carbonates for Waste Incineration
- Pulp and Paper Processes
- Filtration of Hot Gases

THERMOGRAVIMETRIC LABORATORY

Up to four independent, simultaneous experiments can be conducted with each thermogravimetric system consisting of a sensitive, continuously recording microbalance for accurately measuring specimen weight; a controlled temperature furnace; an environmental control subsystem consisting of gas supply, chemistry, and metering equipment; and a computer controlled data acquisition

MICROSCOPY SYSTEM FOR IN-SITU EROSION-CORROSION STUDIES

The system is a scanning electron microscope (SEM) that has been extensively modified to permit in-situ study of a material's surface while it is undergoing attack. Erosion of a sample in the microscope is accomplished by bombarding the viewing surface with tungsten carbide spheres at a controlled velocity and trajectory. Corrosive conditions are produced by using a heated sample holder and a gas control system that directs a controlled amount of a corrosive gas onto the sample surface.

ELECTROCHEMICAL TESTING EQUIPMENT

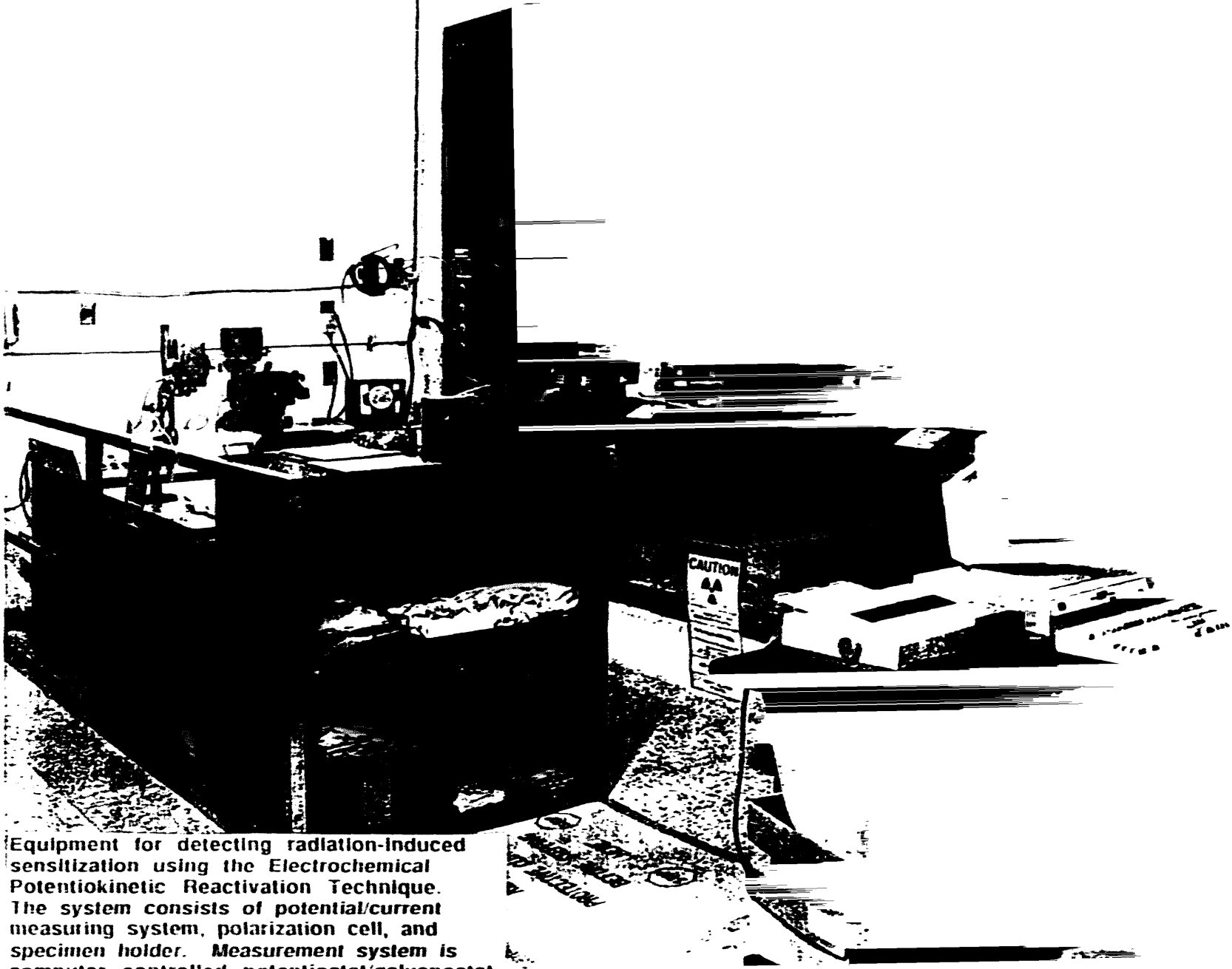

Equipment for detecting radiation-induced sensitization using the Electrochemical Potentiokinetic Reactivation Technique. The system consists of potential/current measuring system, polarization cell, and specimen holder. Measurement system is

CYN-4517

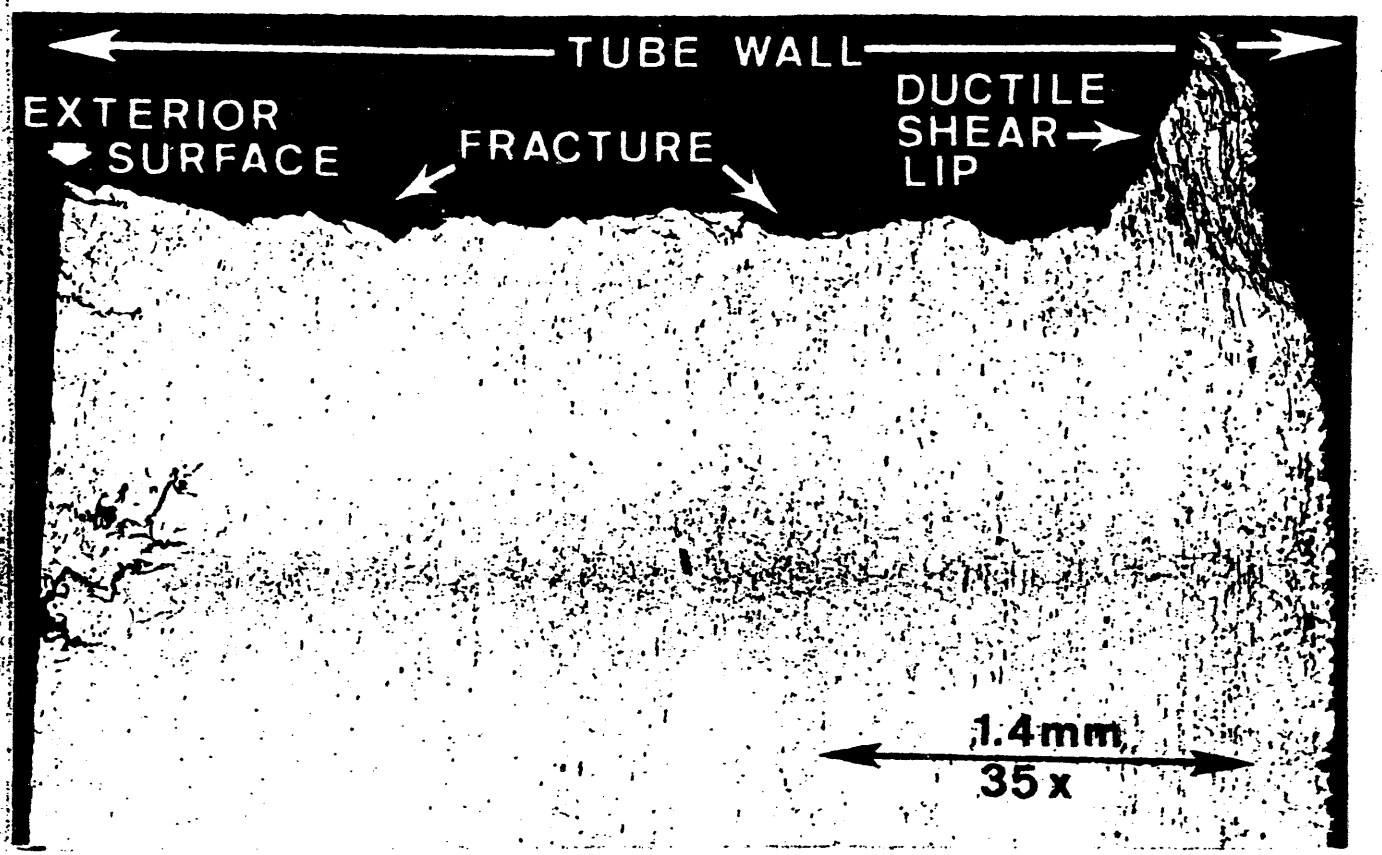

TUBE WALL, SHOWING THAT CRACKING ORIGINATED IN EXTERIOR SURFACE.

A ductile shear lip developed as the fracture neared the inner surface.

Note secondary transgranular cracking originating at exterior surface.

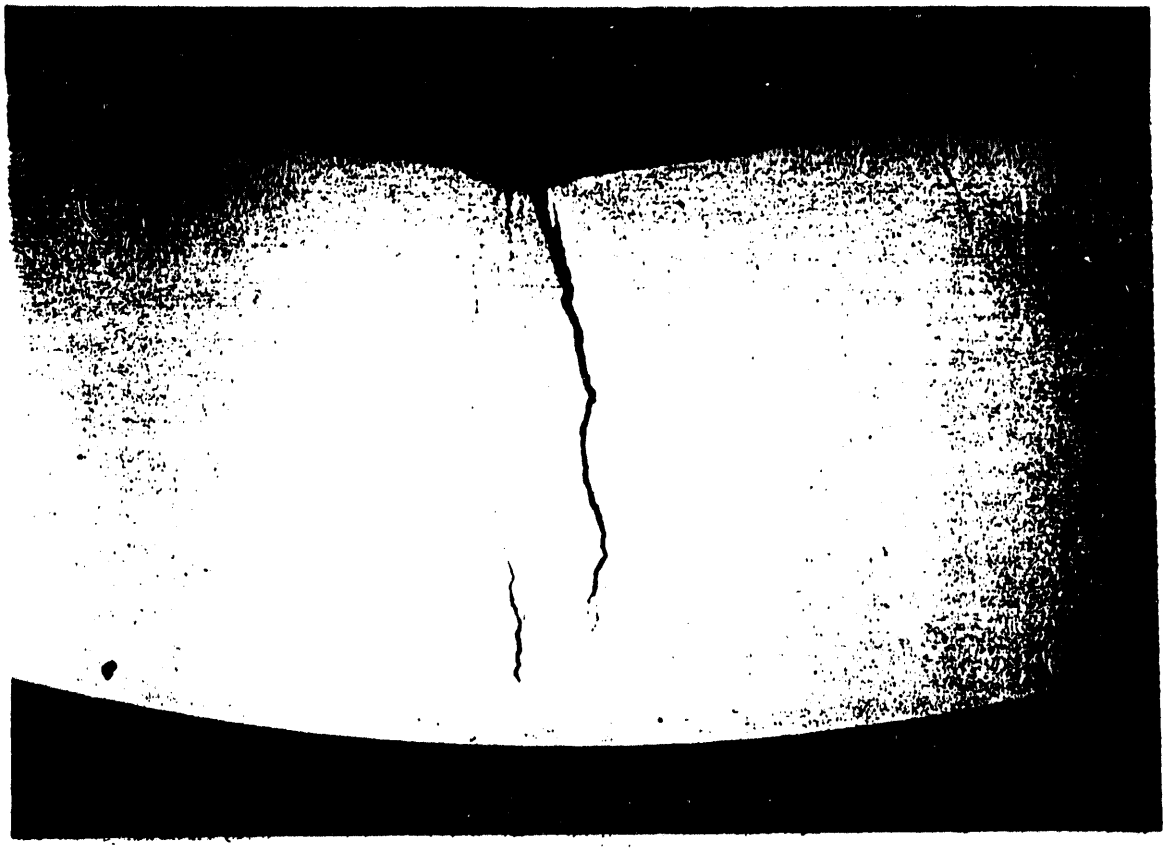

TRANSGRANULAR CHLORIDE STRESS CORROSION CRACKING OCCURRED IN TYPE 316 VENT LINE BETWEEN PREHEATER AND DISSOLVER

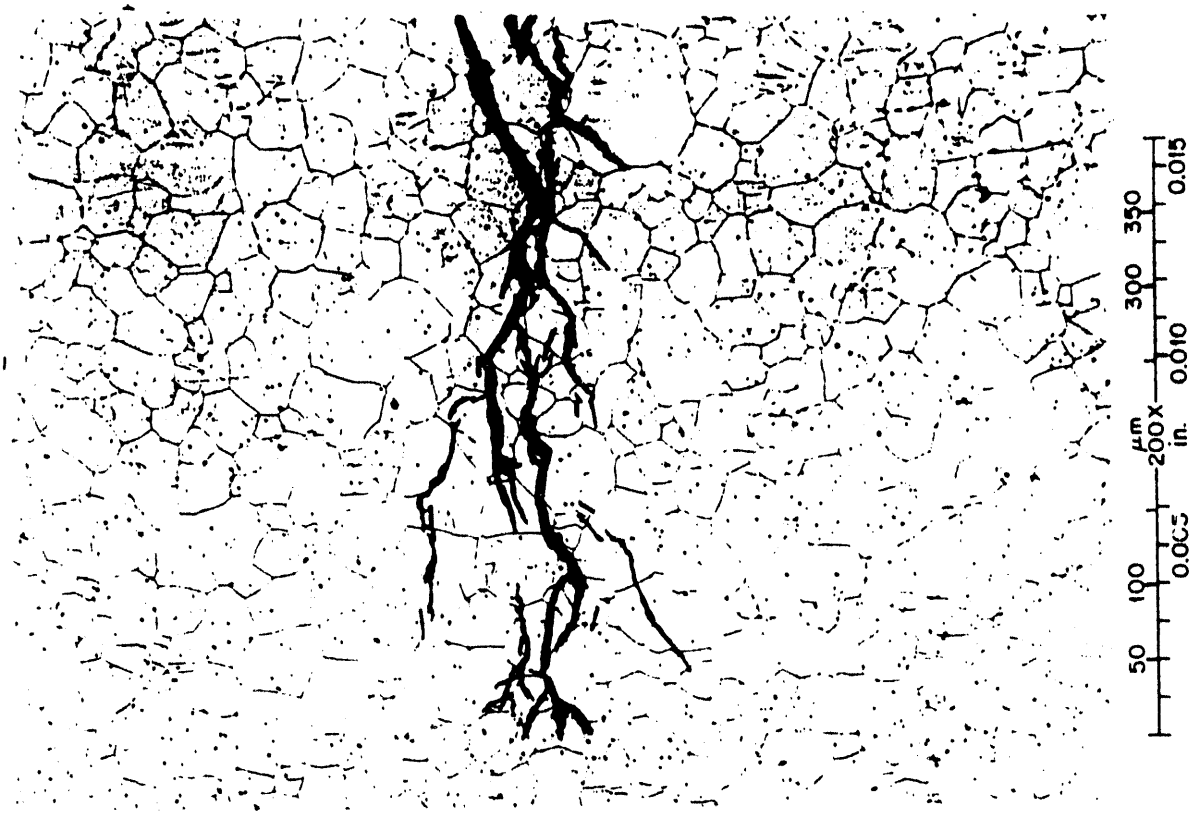

YP16613

MICROSTRUCTURAL EXAMINATION SHOWED CONTINUOUS, ADHERENT LAYERS

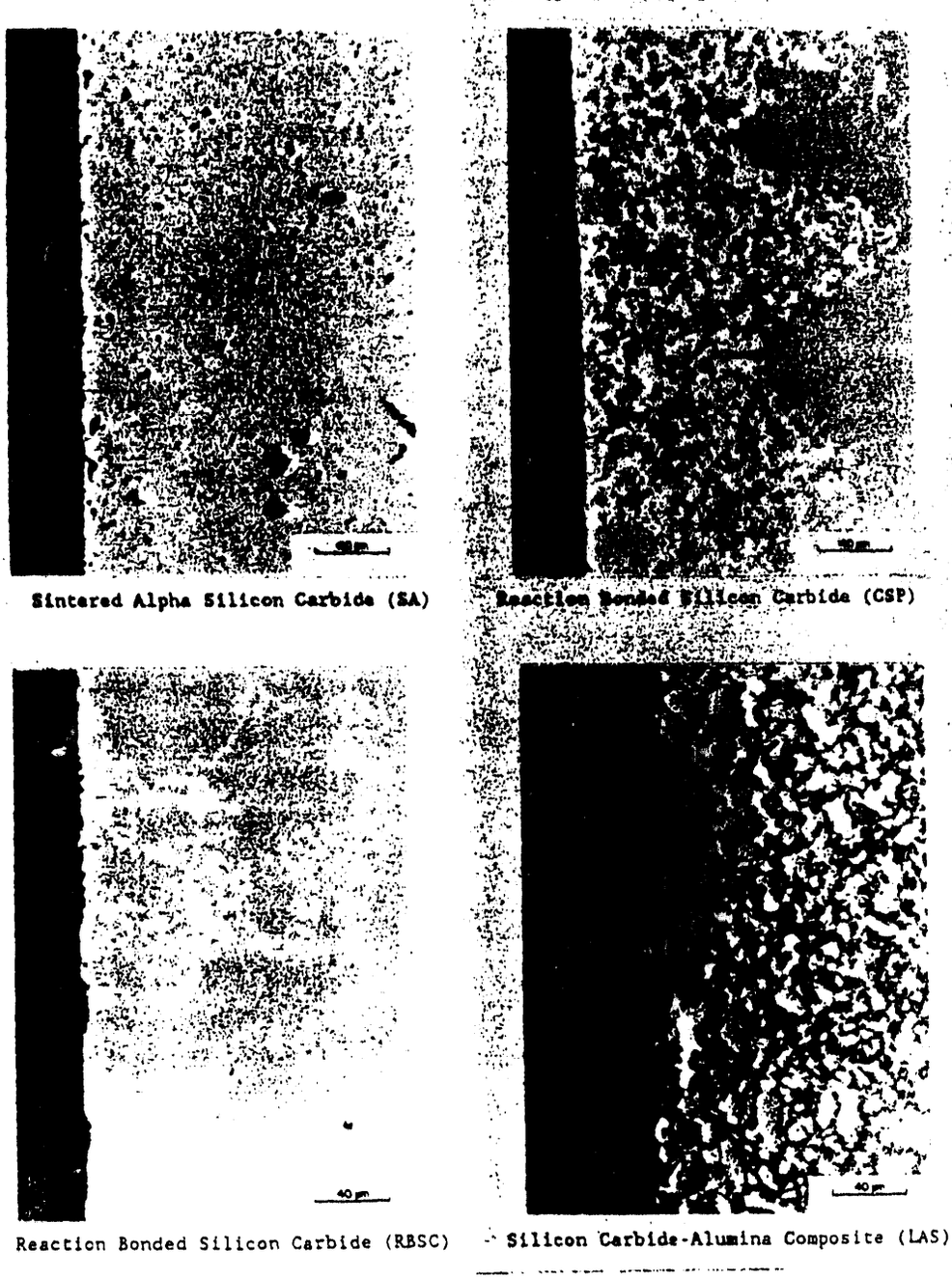

Micrographs of samples exposed at 1260°C for 500 h with 1.0 atm total pressure and 0.30 atm steam partial pressure showing continuous, adherent layers.

MICROSTRUCTURES OF SAMPLES EXPOSED AT 925°C SHOWED EFFECT OF STEAM PARTIAL PRESSURE

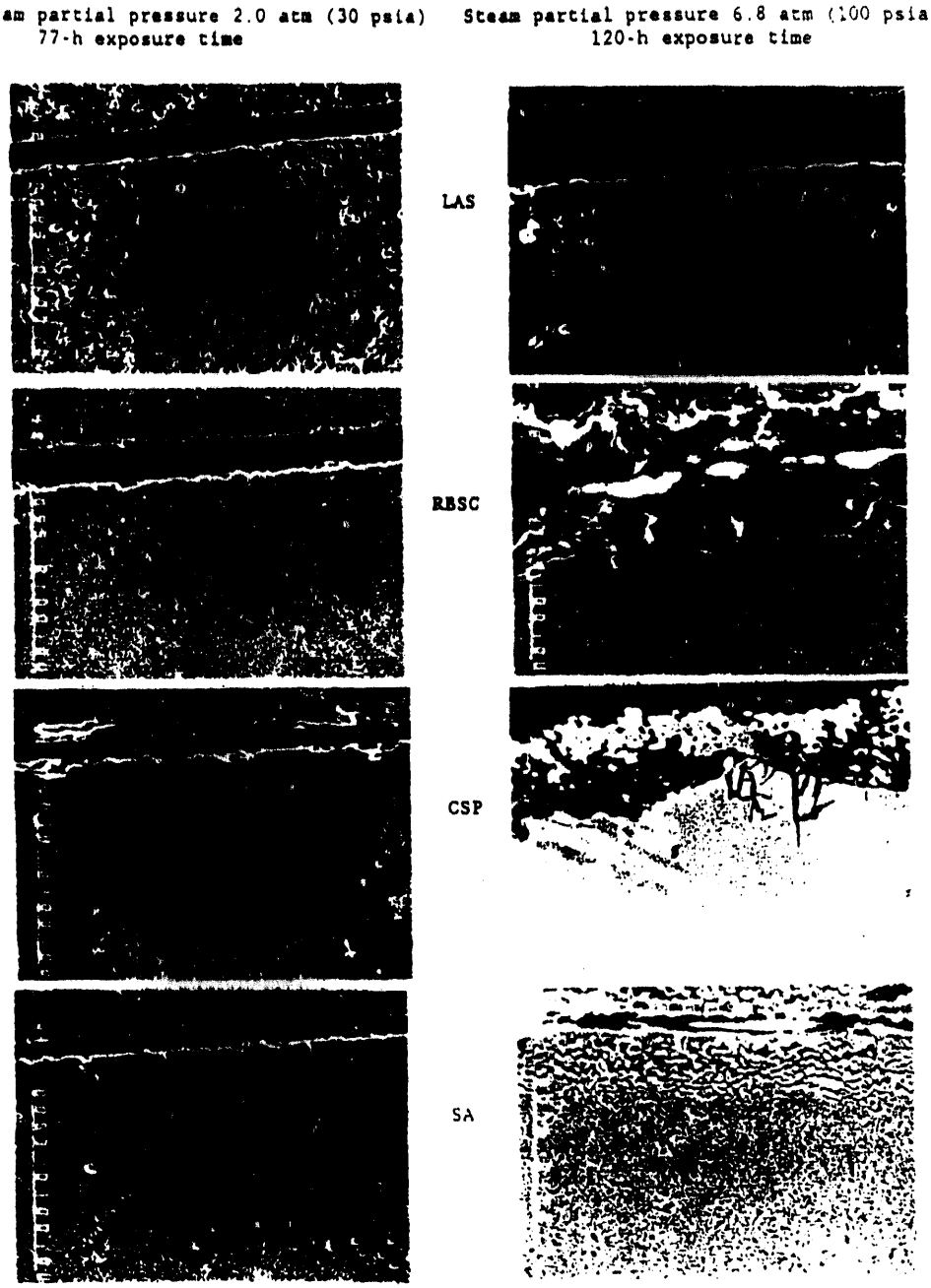

Micrographs of candidate reformer tube materials after exposure for about 100 h at 925°C to simulated steam-methane reformer atmospheres.

ORNL SAMPLES BEING EXPOSED IN WILSONVILLE FRACTIONATION COLUMN INCLUDE THESE U-BEND AND COUPON RACKS.

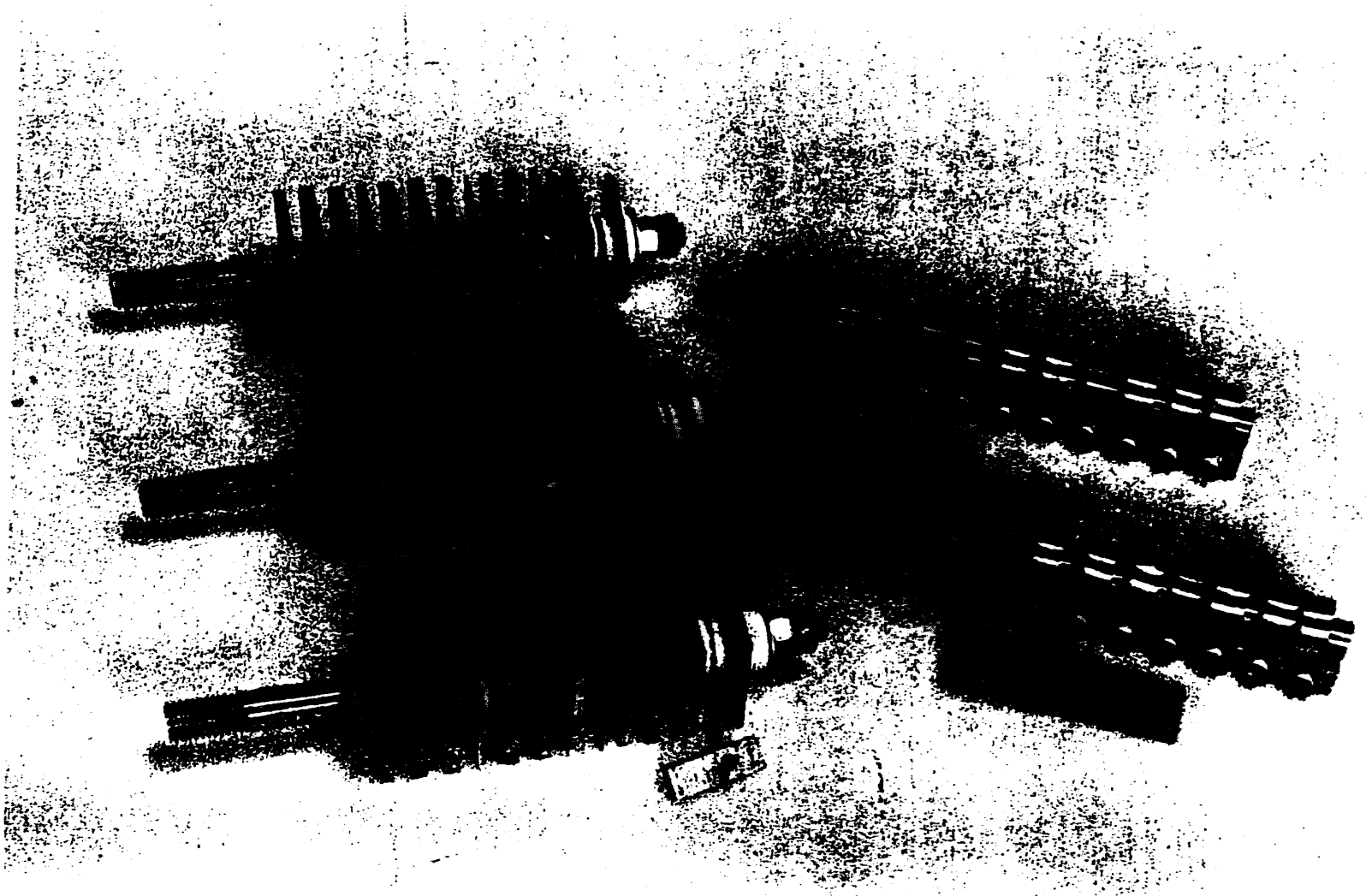

SUMMARY

- Research In ORNL's CS&T Group Is Directed To Determining The Compatibility Of Materials

- A Wide Range Of Experimental Facilities Is Available In The CS&T Group

- Members Of The CS&T Group Have Considerable Experience In Evaluating The Performance Of Materials In Chemical Processing Systems

DOE/NREL/ORNL WORKSHOP LOW COST MATERIALS OF CONSTRUCTION FOR BIOLOGICAL PROCESSES
MAY 13, 1993

Surface Analysis of Corrosion Pits Initiated at MnS Inclusions in 304 Stainless Steel

Richard C. Alkire
Department of Chemical Engineering Materials Research Laboratory
University of Illinois at Urbana-Champaign, Illinois 61801

ABSTRACT

Formation of pits near MnS inclusions on 304 stainless steel in NaCl (0.1 and 0.3*M*) and $Na_2S_2O_3$ (0 and 2 m*M*) solutions was investigated by a combination of surface analyses (Auger electron spectroscopy, scanning electron microscopy, and energy dispersive x-ray analyses) and electrochemical methods. Microlithography techniques were developed to monitor a single corrosion pit initiated at a single preselected inclusion. Pits were observed to form primarily at MnS inclusions. It was found that chemical dissolution of MnS occurred at the rest potential. Sulfur species were found to spread onto the adjacent passive surface over an area having a diameter about four times the size of the inclusion. Subsequent dissolution of metal was observed to occur only at MnS inclusions larger than about 1μm. The surface of the microcavity adjacent to the inclusion was found to be enriched in S and, in later stages of dissolution, by Cr. These observations indicated that S-species play a key role in the processes that lead to pit initiation in this system.

In situ atomic force microscopy was used in conjunction with microlithography and scanning Auger electron spectroscopy to monitor localized corrosion near iron-rich inclusions in Al-6061-T6 immersed in 0.6 M NaCl and also sulfur-rich inclusions in 304 stainless steel (SS-304) in 0.5 M NaCl. The local rate of aluminum corrosion was found to depend on the shape of the nearby iron-rich inclusion. at the corrosion potential, trenches were observed to form in the aluminum host matrix adjacent to the inclusions,a nd the corrosion sites gradually evolved into circular shapes owing to dissolution. During the dissolution process, the width of the dissolution area was an order of magnitude greater than the depth. Application of a 400 Mv cathodic overpotential prevented corrosion initiation,while application of a 500 mV cathodic overpotential greatly accelerated the dissolution rate in comparison with that at the rest potential. On SS-304, exposure to 0.5 M NaCl was accompanied by formation of deposits, which decorated the inclusion surface as well as the surrounding area up to four times the radius of the original inclusion.

Reprinted from JOURNAL OF THE ELECTROCHEMICAL SOCIETY
Vol. 139, No. 6, June 1992
Printed in U.S.A.

Surface Analysis of Corrosion Pits Initiated at MnS Inclusions in 304 Stainless Steel

Ruoru Ke* and Richard Alkire**

Department of Chemical Engineering and Materials Research Laboratory, University of Illinois at Urbana-Champaign, Illinois 61801

ABSTRACT

Formation of pits near MnS inclusions on 304 stainless steel in NaCl (0.1 and 0.3*M*) and $Na_2S_2O_3$ (0 and 2 m*M*) solutions was investigated by a combination of surface analyses (Auger electron spectroscopy, scanning electron microscopy, and energy dispersive x-ray analyses) and electrochemical methods. Microlithography techniques were developed to monitor a single corrosion pit initiated at a single preselected inclusion. Pits were observed to form primarily at MnS inclusions. It was found that chemical dissolution of MnS occurred at the rest potential. Sulfur species were found to spread onto the adjacent passive surface over an area having a diameter about four times the size of the inclusion. Subsequent dissolution of metal was observed to occur only at MnS inclusions larger than about 1 μm. The surface of the microcavity adjacent to the inclusion was found to be enriched in S and, in later stages of dissolution, by Cr. These observations indicated that S-species play a key role in the processes that lead to pit initiation in this system.

The deleterious effect of sulfide inclusions on the resistance of stainless steel toward pitting and crevice corrosion has been recognized for many years (1-4). Certain fundamental questions remained unanswered, however, concerning events involved in early stages of such attack. In the present investigation, the sequence of events during initiation of pitting in Cl^--containing solution at site of MnS inclusion on 304 stainless steel (ss) was examined by a combination of surface analysis and electrochemical methods.

Commercial stainless steels contain a variety of sulfide inclusions that are generally recognized to serve as pit nucleation sites (5-7).

Mechanisms by which nucleation occurs on stainless steel in chloride solutions have included chloride ad-

* Electrochemical Society Student Member.
* Electrochemical Society Active Member.

sorption (8), crevice formation at the edge of dissolving inclusions (9), and the concerted depassivating action of chloride and thiosulfate (10-12). Investigations of local surface chemistry in the vicinity pits and inclusions on 316 SS in acidic NaCl revealed that dissolution of the inclusion was accompanied by release of sulfur species which contaminated the surrounding metal including the passive film (13).

Thus the view has emerged that dissolution products lead to deposition of sulfur and/or sulfur-containing species on regions surrounding inclusions play a central role in subsequent breakdown of the passive oxide film. To further clarify the mechanisms by which pits initially begin to form, and to organize these concepts eventually into the framework of a mathematical model for the initiation of pitting, additional quantitative information is needed.

In the present study, formation of pits near MnS inclusions on 304 SS in NaCl (0.1 and 0.3*M*) and $Na_2S_2O_3$ (0 and 2 m*M*) solutions was investigated by a combination of surface analysis and electrochemical methods. Microlithography techniques were developed to register the specimens so as to observe preselected MnS inclusions before and after exposure to corrosive conditions. In addition, techniques were developed to monitor a single pit initiated at a single preselected inclusion.

Experimental

Three types of specimens of commercial 304 SS were examined: (i) unmasked specimens provided information on the composition of inclusions prior to exposure to corrosive conditions; (ii) specimens that were unmasked or partially masked provided information on a large collection of inclusions exposed to corrosive conditions; and (iii) specimens that were masked everywhere except for a single inclusion provided detailed local information.

Specimens were cut from rod stock in the form of disks (14.8 mm diam), and polished down to 0.05 μm alumina finish. In a Class 100 clean room, cleaned specimens were prebaked (180°C, 20 min), spin-coated at 3000 rpm with a positive photoresist (Microposit 1450J, Shipley), and soft-baked (90°C, 20 min). To expose a group of inclusions, a chrome-plated glass photomask was used to make a grid on the region of interest. The grid was 1100 × 1100 μm, divided in 121 square regions 100 μm on a side. By using this grid as a reference register, an inclusion of interest could be identified before and after exposure to corrosive solutions. For specimens that were masked except for a single inclusion, a second chrome-plated glass photomask was utilized, having a single square opening (50 × 50 μm). The overlay of these two photomasks made possible the exposure of a single-square region containing a single inclusion.

After exposure (2001 Kaspar Inst. Model 762 UV light, Optical Associates), the exposed region was developed (Microposit, Shipley), spray rinsed with deionized water, jet dried with filtered nitrogen, then postbaked in fresh air (120°C, 25 min) and stored in a desiccator until use. These procedures gave a photoresist that was approximately 2 μm thick.

Specimens were mounted facing upwards in an unstirred Plexiglas cell. A saturated calomel electrode (SCE) was used as a reference electrode; the counterelectrode was a Pt foil. Electrochemical experiments were carried out under potential control (PAR, Model 273). Cyclic staircase voltammetry (CV) and chronoamperometry (CA) were used. *In situ* microscopic observation (Nikon, 200 times) was made during pit initiation and growth. Solutions of various concentrations and mixtures of electrolytes were prepared with deionized water and analytical grade NaCl and $Na_2S_2O_3$ reagents.

Quantitative energy dispersive x-ray (EDX) analyses were carried out (JEOL 35C) to provide general information on the composition of steel and inclusions. The surface topography and chemistry of inclusions, pits and surrounding areas were observed by scanning Auger microscope (SAM) (PHI 660), scanning electron microscopy (SEM), and EDX (HITACHI S-800 fitted with Link AN 10,000) before and after exposures of samples to corrosion conditions. To obtain Auger data, a 10 kV accelerating beam voltage and 10 nA specimen current were found to give good signals and spatial resolution for most conditions. The stage tilt-angle was usually 30°. The spatial resolution was ≈0.13 μm. The atomic concentration (ac) calculation was based on the peak-to-peak height in the differential spectrum. The elements C, O, S, Cl, Cr, Mn, Fe, Ni, and Cu were monitored at kinetic energy 271, 510, 151, 181, 529, 541, 703, 848, and 920 eV, respectively. EDX measurements (HITACHI S-800 SEM fitted with Link AN 10,000) were carried out under an accelerating beam voltage of 20 kV and a working distance of 15 mm. Stereo images were obtained with an angle difference of 8°, topography was determined by computer analysis.

Results and Discussion

Results are presented below in a sequence which includes (i), observations on individual inclusions prior to exposure to corrosive conditions, (ii), specimens which had a large number of inclusions, some of which led to pitting corrosion, and (iii), specimens that were masked so as to only expose a single MnS inclusion to corrosive conditions.

Observation prior to exposure to corrosive conditions.—Quantitative EDX analyses on individual inclusions indicated that three general categories were found: (i) oxides of various elements, primarily Cr_2O_3 and MnO with some Al_2O_3; (ii) manganese sulfide, MnS; and (iii) mixed oxide-sulfide inclusions. The size of MnS inclusions was observed to be less than 2 μm. By counting the bright spots on EDX sulfur maps of a number of areas chosen at random, the number density of MnS inclusions on the surface was estimated to be $(3 \pm 1) \times 10^4/cm^2$.

Corrosion specimens having a large number of inclusions.—In the experiments described in this section, a number of inclusions were exposed to solution on a single specimen, but the specimen was masked with a photoresist grid so that any particular inclusion could be selected for surface analysis and, following exposure to corrosive solution, be identified again for postexposure surface analysis. Results are reported below for exposure to two 0.1*M* NaCl solutions, one of which contained 2 m*M* sodium thiosulfate.

0.1M NaCl solution.—The purpose of electrochemical pretreatment was to create corrosion pits under controlled conditions for subsequent surface analysis. Specimens were exposed to cathodic reduction (1 mA/cm^2) for 10 min and then held at the rest potential for 15 min. The current was then recorded while the potential was scanned (1 mV/s) from the rest potential to a desired anodic potential and held at this value for 75 min. The specimen was removed from the cell, rinsed in the laboratory environment and transferred to the AES chamber.

In an experiment labeled 1P, the potential was scanned to E = 430 mV (SCE). While scanning to this potential many pits were found to initiate. During the constant potential holding period, pits kept growing, the anodic current continued to increase from 0.8 to 4 mA when the experiment was terminated at 75 min. Auger electron spectroscopy (AES) analysis was carried out to obtain the local elemental composition on the pit interior and surrounding surface. A typical result, shown in Fig. 1, illustrates the Auger spectrum recorded from one particular pit interior. Signals from the elements of S, Cl, C, O, Cr, Mn, Fe, Ni, and Cu appear in this spectrum. Similar data from some half dozen pits showed that sulfur was present in all such pits.

Local surface compositions measured at a pit (radius of about 0.75 μm) and various points on the surrounding area were measured by AES and results are given in Table I. A dimensionless distance R was defined as the distance from analysis point to the center of pit divided by the radius of the pit. In a similar manner a dimensionless concentration was defined for elements S and Fe as the concentration at the analysis point divided by the concentration in the pit interior. These results will be discussed below along with those presented in the next paragraph.

For experiment 2P, during the potential scan to 400 mV (SCE) the anodic current started rising, and pits appeared.

J. Electrochem. Soc., Vol. 139, No. 6, June 1992 © The Electrochemical Society, Inc.

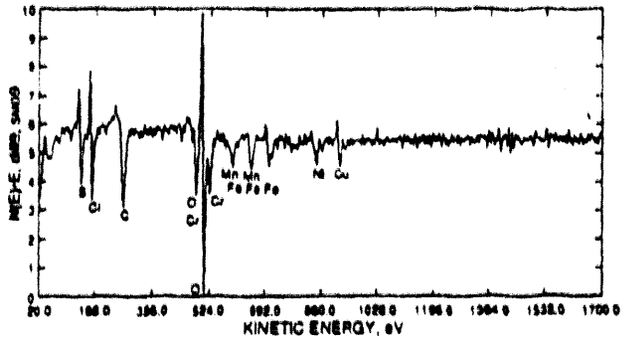

Fig. 1. AES spectrum recorded from one particular pit interior. 1.0 eV/step; 15 ms/step; acquisition time = 4.2 min.

The sample was held at this potential for 75 min during which the current remained at 5 μA, and the initiated pits did not grow. Composition on the interior of a pit with a radius of about 0.75 μm is given in Table I. The distribution of S and Fe for this pit is shown in Table II.

Pits 1P and 2P were initiated under different electrochemical conditions but had similar dimension. In both, it is clearly evident that the sulfur concentration was higher at the site of the pits, and decreased with distance from the sites. In the relatively more gentle corrosive conditions of experiment 2P, less sulfur was present, and it was located within one radius of the corrosion sit. For the more severe condition (1P) more sulfur was present. For both pits the Fe concentration increased with distance from the pit. It was also noted that the level of both Cl and Cr within the pit on sample 1P was higher than on sample 2P.

0.1M NaCl and 2 mM $Na_2S_2O_3$ solution.—Based on the results obtained in the previous section, additional experiments were carried out on the sites of selected inclusion groups before and after electrochemical exposure in 0.1 *M* NaCl + 2 m*M* $Na_2S_2O_3$ solution.

After pre-exposure AES and EDX measurements, Sample No. 4 was placed in solution held at the rest potential for 30 min, at which point the potential was changed to 400 mV (SCE) and the anodic current was recorded as a function of time (CA). The experiment was terminated at 17 s by which time the current had increased to 0.2 mA. Following AES analyses of the selected inclusions the sample was re-exposed to the solution for another 600 s at the same potential (400 mV). The same inclusions were then re-examined by AES and EDX. Results are shown in Fig. 2. It is clearly seen that as exposure occurred the sulfur was observed on the area surrounding the inclusions as well as on the inclusions. Moreover, sulfur intensity contrast between inclusions and steel matrix decreased markedly over time. It is thus evident that sulfur, released by corrosive attack of sulfide, spread to the surrounding surface near the inclusion group. The topography of this inclusion group suggested that the site of corrosion attack was already established after the first exposure to solution: a microcrevice between the periphery of the MnS remnant and the steel matrix. The topography of individual inclusions will be discussed further in what follows. EDX maps of elements S, Mn, Fe, and Cr were recorded after the second exposure for this inclusion group. It was found that the signal of these elements changed markedly between inclusion and steel matrix, indicating that the MnS inclusion was only partly dissolved. Following the second exposure, the AES spectra and S map (Fig. 2 iii) showed a strong S signal not only at the site of inclusions but also on the surrounding area. By comparison, EDX data indicated high S intensity at the site of inclusion but not on the surrounding region. Because the AES technique probes regions that are closer to the surface than those probed by the EDX, it was concluded that the sulfur was spread as a thin layer on the top surface.

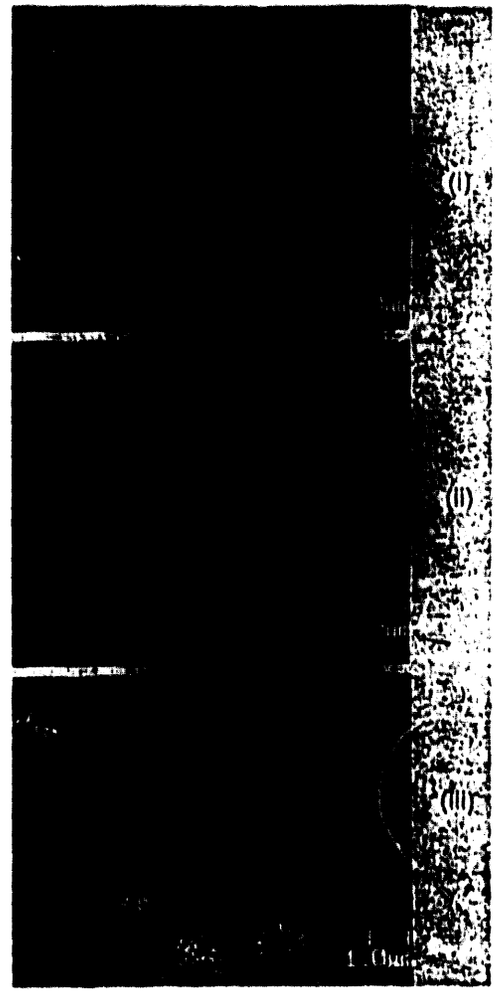

Fig. 2. Sulfur Auger maps on the inclusions in Grid X4Y1, of Sample No. 4: (*i*) before exposure; (*ii*) after the first exposure, in 0.1M NaCl + 2 mM $Na_2S_2O_3$, 400 mV (SCE) for 17 s; (*iii*) after the second exposure for 600 s.

Table I. Elemental distribution on Sample 1P and 2P, 0.1*M* NaCl, $r_o \sim 0.75$ μm.

At%	C	O	S	Fe	Cr	Ni	Mn	Cl	Cu
Sample 1P									
Average, 80 times	34.61	32.91	0.74	12.00	2.70	4.33	0.80	5.73	6.29
$R = 0 - 1$	34.90	25.21	5.26	6.12	4.42	4.68	4.60	6.15	7.66
1.53	39.09	28.94	2.30	10.87	6.54	5.15	0.30	3.71	3.09
1.82	40.87	26.68	1.59	10.21	6.48	4.87	0.38	4.13	5.09
2.65	41.15	25.89	1.43	11.93	5.54	4.99	0.48	4.66	3.90
Sample 2P									
$R = 0 - 1$	35.53	34.52	1.59	19.33	0.97	2.48	0.14	1.41	4.03

Table II. Ratio between concentration in pit interior and other locations surrounding pit 0.1*M* NaCl, $r_o \sim 0.75$ μm.

$R = \frac{r}{r_o}$	1.00	1.17	1.33	1.53	1.67	1.82	2.00	2.33	2.65	3.00
θ_s 1P	1.00	—	—	0.42	—	0.30	—	—	0.26	—
θ_s 2P	1.00	0.82	0.49	0.16	0.06	0.06	0.03	0.03	0.03	0.02
θ_{r_o} 1P	1.00	—	—	1.27	—	1.22	—	—	1.41	—
θ_{r_o} 2P	1.00	1.24	1.49	1.71	1.78	1.82	1.89	1.91	1.89	1.80

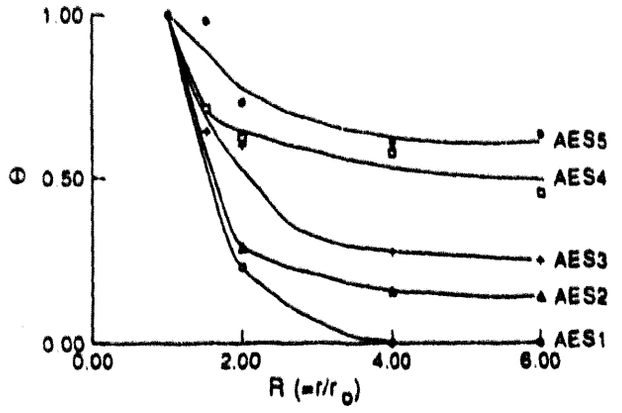

Fig. 3. Sulfur intensity ratio, as the function of exposure time and dimensionless distance R, 0.1M NaCl + 2 mM $Na_2S_2O_3$ solution.

from 1.01 to 0.43, respectively. Such changes suggest that the sulfur compound formed by sulfide dissolution diffused away from the inclusions to the surroundings but the manganese remained at the original site. However, the corrosive attack initiated on the inclusions during the first exposure did not develop further during reimmersion; that is, during the exposures, pits initiated and grew elsewhere on the sample surface.

To explore further the results suggested by Sample No. 4, and to find out how the element distribution changed as the function of exposure time, a series of experiments was arranged for the Sample No. 48 as follows: AES 1 analysis before immersion; immerse at rest potential for 40 min, AES 2; immerse at 400 mV for 18 s, AES 3; immerse at 400 mV for 18 s, AES 4; immerse at 400 mV for 200 s, AES 5. Two inclusions and several pits were selected for monitoring through the exposure sequence. The S intensity ratio Θ ($=I_r/I_{Ins}$) was obtained as the function of exposure time and dimensionless distance R ($=r/r_o$). The results from one such inclusion are shown in Fig. 3. It may be seen that, before the specimen was exposed to the corrosive solution, the S signal appeared at the site of the inclusion as well as at nearby regions. The S signal on the host matrix may be (i) real owing to the sample pretreatment (since specimens had been baked several times and exposed to Cl^--containing sensitizer in the positive photoresist), or (ii) apparent because of limitation on the resolution of the electron beam (e.g., at the accelerating voltage of 10 kV and beam current of 10 nA, the electron beam size was about 0.13 μm, and most inclusions were 1-2 μm in size). When this specimen was immersed in solution at the rest potential, MnS dissolution took place to more or less extent on various inclusions. It may be recognized that during the sequence of exposures at the applied potential of 400 mV, MnS dissolution continued and the sulfur dissolution product spread to the surrounding surface so that sulfur on the sample surface became increasingly more uniformly dispersed. Although the absolute values of the ratio Θ varied from site to site, the tendency was the same for all observed inclusions and pits. It can be recognized in Fig. 3 that when $R > 4$, the sulfur intensity ratio achieved constant level and did not decrease further with increased distance from the individual inclusion or pit.

The mechanism by which the sulfur species is transported from the inclusion to the surrounding area is not clear. Among possible candidates would be transport by diffusion through the solution, by surface diffusion of adsorbed species, and by movement within the solid surface oxide film.

Although the progress of MnS inclusion dissolution could be seen in Sample No. 48 with each successive exposure, a corrosion pit did not initiate at this preselected inclusion. Pits did not necessarily initiate at all sulfide inclusions on a sample surface. Certain inclusions were evidently more effective in nucleating pits than others. In the presence of these sulfidic inclusions, pits that have already formed may prevent further outbreak of new pits in surrounding areas having less effective inclusions as has been noted previously (14). In addition multiple clusters of inclusions may affect each other owing to their size and relative position. Compared with other inclusions, it may be that those inclusions selected for analysis were illuminated by the electron beam which may modify the surface properties in a way that influenced th ir subsequent corrosion behavior.

Corrosion specimen having a single inclusion.—In order to understand the behavior of individual MnS inclusions during the pitting process, observations were made on single inclusions at which a single pit initiated.

Electrochemistry of single pits.—Individual pits were initiated at preselected sulfide inclusions having a size of 1-1.5 μm, and were observed in three solutions and at various applied potentials. The composition of the solutions was: 0.1M NaCl, 0.1M NaCl + 2 mM $Na_2S_2O_3$, and 0.3M NaCl + 2 mM $Na_2S_2O_3$. The specimen was first held at the rest potential for about 20 min after which the desired potential was applied and the current was recorded as a function of time. Experiments were terminated in some cases when the in situ microscopic observation showed that a single pit had initiated, and in other cases when the current increased to a preselected value.

In each case the electrochemical results showed the pitting rate increased when the applied potential increased. An increase of concentration of Cl^- from 0.1 to 0.3M, and the addition of 2 mM $Na_2S_2O_3$ to NaCl solutions both served to increase the pitting rate at all potentials.

Surface chemistry of single pits.—To obtain surface composition of the samples covered with photoresist, a stainless steel, or gold sheet was placed over the sample to shield the surface except for a small opening at the center through which the electron beam reached the surface.

Effect of extent of dissolution.—A series of chronoamperometry experiments was carried out in 0.1M NaCl solution at 370 or 400 mV (SCE), and at various total charge values (1, 2, and 4 μC) to obtain a sequence of stages of pitting. Specimens were then analyzed by AES, SEM, and EDX techniques.

Figure 4 shows SEM images of three corrosion pits which initiated adjacent to a MnS inclusion. In Fig. 4a (Sample No. 67), pit growth (at 370 mV) was stopped at a very early stage (1 μC). The majority of the inclusion (medium grey region above and left of center) had not yet dissolved. Along the upper side of the inclusion, the passive film had not yet broken (light grey region above and left of inclusion). The microcavity adjacent to the inclusion appeared as black region on the image (below and right of the inclusion). The maximum depth of the microcavity was found by SEM stereo observation along two trace lines illustrated in Fig. 4a to be 1.5μm.

In Fig. 4b (Sample No. 65), the growth (at 400 mV) was terminated at 2 μC. The dissolution of MnS was more complete compared with that in Fig. 4a; the MnS remnant appears as the medium grey portion. As seen in the stereo scans in Fig. 4b, the maximum depth of the pit was approximately 4 μm and the diameter was about 5.5 μm.

Figure 4c shows a pit which was grown at 400 mV and terminated at 4 μC (Sample No. 68). The majority of MnS inclusion had dissolved; only a small remnant may be seen at the top of the cavity. The diameter of this pit was roughly 7 μm, and the maximum depth was 5.0 μm. Based on these dimensions, the volume of the pit in Fig. 4c, was estimated by considering the pit shape to be a spherical section, and was found to be 160 μ^3. The volume which corresponds to 4 μC of anodic dissolution of Fe to the ferrous state was calculated by Faraday's law to be 150 μ^3, in rough agreement with the experimentally observed value.

Local AES analyses were also carried out at about a dozen locations to determine the element distribution within the pit and the surrounding region. The local sulfur concentration obtained in this manner is shown as a function of distance from the center of the pits in Fig. 5. In general, the sulfur concentration increased significantly as pitting developed, both within the pit and on the surrounding passive film.

J. Electrochem. Soc., Vol. 139, No. 6, June 1992 © The Electrochemical Society, Inc. 1577

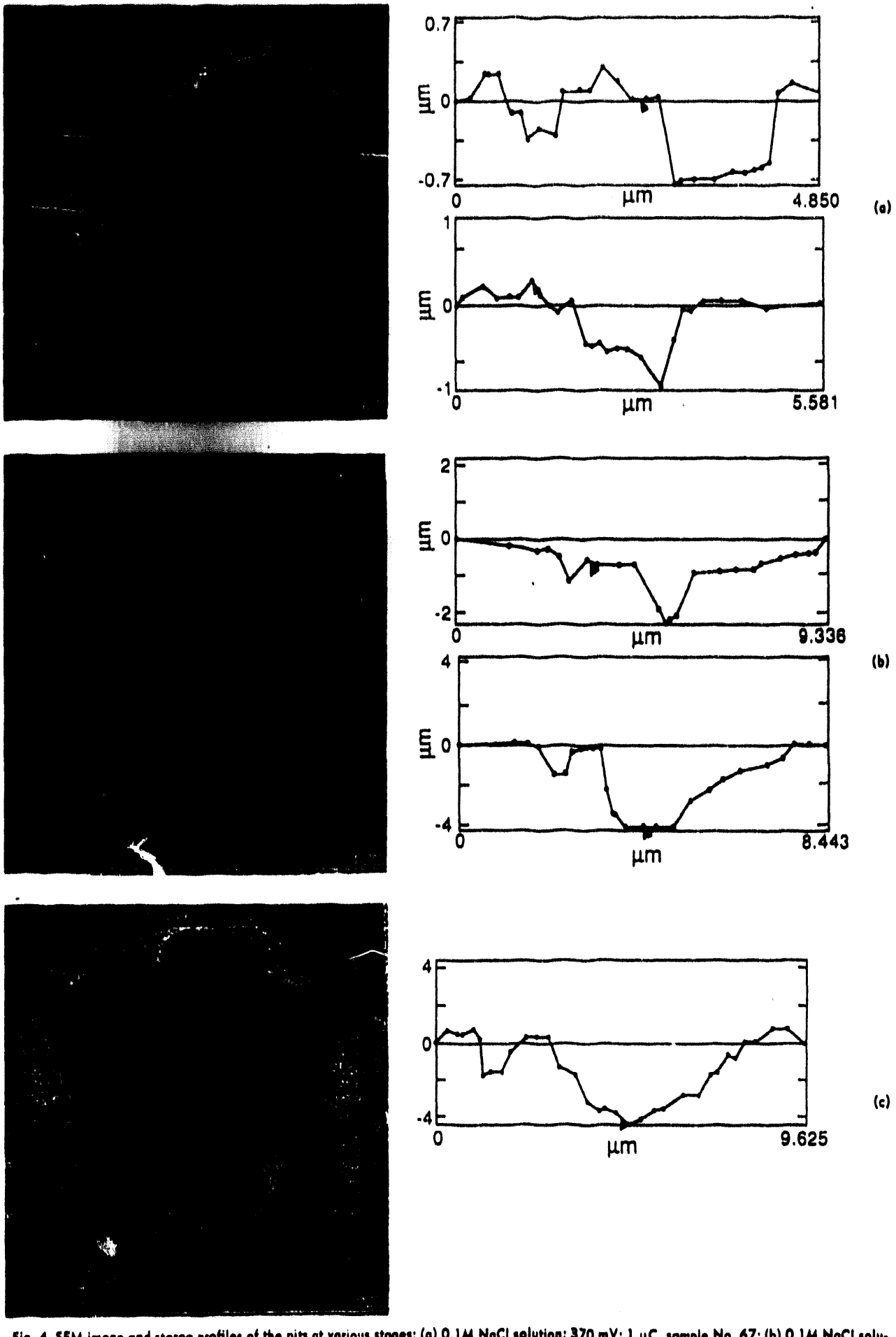

Fig. 4. SEM image and stereo profiles of the pits at various stages: (a) 0.1M NaCl solution; 370 mV; 1 μC, sample No. 67; (b) 0.1M NaCl solution; 400 mV; 2 μC; Sample No. 65, (c) 0.1M NaCl solution; 400 mV; 4 μC Sample No. 68.

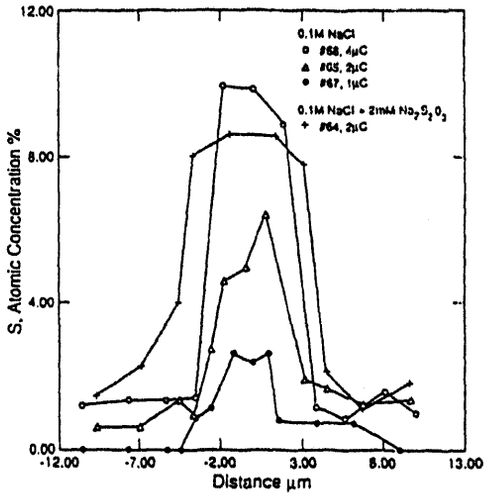

Fig. 5. Sulfur surface concentration as a functoin of distance from the center of pits.

It was found from these point analyses that the Cr concentration in the Pit No. 67 (1 μC) was lower than that of the surrounding surface. However, the Cr concentration level inside Pit No. 65 (2 μC) was higher than the average level of the surrounding area; furthermore, in Pit No. 68 (4 μC) Cr enrichment was observed not only at the pit site but also on the surrounding surface. These data supported the view that chromium dissolved from the bare steel exposed by partial dissolution of the inclusion, and that the Cr dissolution product hydrolyzed and remained as solid deposit at the region closest to the inclusion. As the corrosion proceeded, Cr enirchment presumably occurred both by hydrolysis deposition and also by selective dissolution of iron from the passive film. This interpretation is consistent with observations reported above on multiple pits in 0.1*M* NaCl and 0.1*M* NaCl + 2 m*M* $Na_2S_2O_3$ solutions. For example, for Pit No. 67, where the corrosion process was stopped at very early stage, enrichment of Cr was not observed on the inclusion or near-pit region, in accord with the situation of Pit No. 4 after the first exposure. In Pit No. 4, Cr enrichment was observed only after the second exposure, when the MnS inclusion dissolution took place, followed by the dissolution of metal and hydrolysis of Cr. The Auger results also showed that Mn appeared on the pit wall during pit initiation.

Effect of thiosulfate addition.—The measurement of element distributions of a pit initiated in 0.1*M* NaCl + 2 m*M* $Na_2S_2O_3$ solution at 400 mV was carried out (No. 64) to determine the effect of addition of thiosulfate ions on surface composition and film depassivation during pitting. Results were compared with No. 65 which was obtained in 0.1*M* NaCl solution at same potential and discussed previously in conjunction with Fig. 5. Sample No. 64, which was terminated at 2 μC, is shown in Fig. 6, together with stereo profiles and AES scans. From the observed mean diameter (7.5 μm) and maximum depth (3.3 μm), a volume of 92 μm^3 was estimated; some of this volume was occupied by what remained of the inclusion. The dissolution of 2 μC of Fe to Fe^{+2} would correspond to a volume change of 75 μm^3 which was consistent with the observed value. Also seen in the SEM image of Fig. 6 is the presence of a thin ruptured passive film at the edge of pit; the film is slightly brighter than the pit cavity or surrounding steel. It may be recognized from the stereo profile that the height of the film was nearly the same as the surrounding area. Beneath the ruptured film, the metal adjacent to the MnS inclusion dissolved and left a part of the film suspended in midair.

Auger line scans of elements S, O, Fe, and Cl were recorded along lines 1 and 2 shown on Fig. 6. Line 1 did not pass through the remains of the MnS inclusion. Line 2 passed through a portion of the ruptured passive film as well as the remains of the inclusion. Auger data were represented in (P-B)/B form in order to eliminate topographic

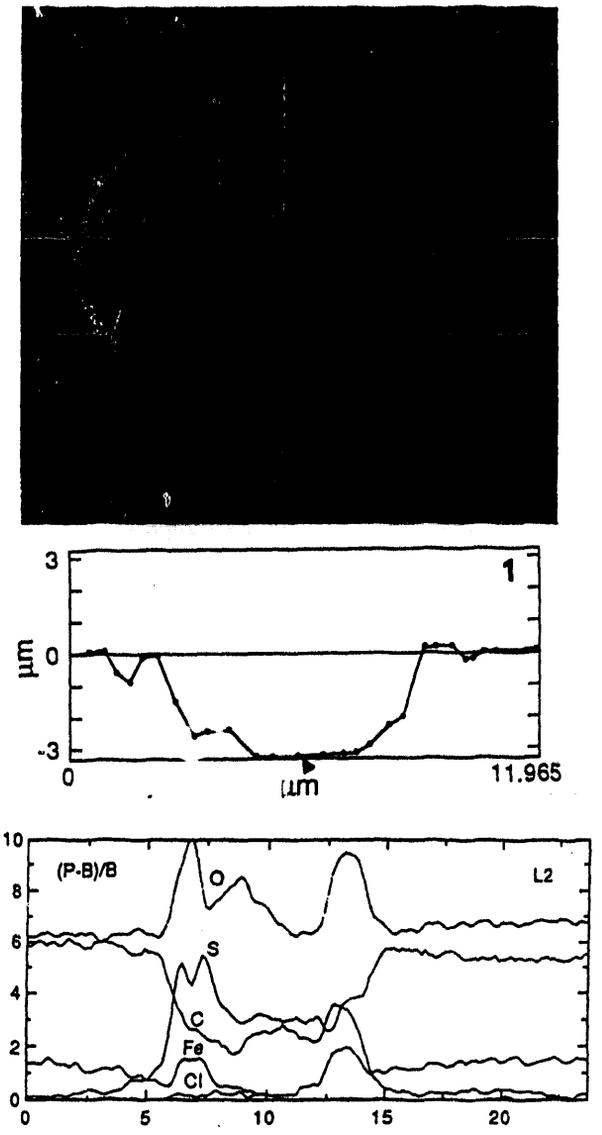

Fig. 6. SEM image (top) and stereo profile (middle) and AES line scans (bottom) of the pit on Sample No. 64. 0.1M NaCl + 2 mM $Na_2S_2O_3$ solution; 400 mV; 2 μC.

differences. The element distribution shown in these two line scans was quite similar: sulfur intensities were highest inside the pit and on the ruptured film; some sulfur spread to the surface surrounding the pit. The oxygen surface concentration in the pit was slightly higher than the average level outside the pit. Iron intensities appeared to be slightly higher on the surrounding steel surface. Both O and Fe Auger signals formed two peak regions where the line scans passed through the remnant of the ruptured film. It may also be seen in Fig. 6 that there was a slight chloride uptake within the pit site.

It is particularly interesting to notice that Line 2 (upper line) passed across the curled up under side of the film (on the left); in this region the S signal intensity exhibited a small valley on the plateau. This may indicate that sulfur concentration was higher on the outer surface of the passive film. Such observation would suggest that S transport away from the inclusion occurred by diffusion along the outer surface, not by movement within the film. More data are needed before firm conclusions could be drawn on the mode of S transport.

A series of AES point analysis was carried out along Line 1 to quantitatively confirm the information obtained from line scan. Results agreed closely with the line scan of Fig. 6. The distribution of sulfur concentration for this sample (No. 64) is also shown in Fig. 5, together with data obtained from $Na_2S_2O_3$-free solution. It is evident from

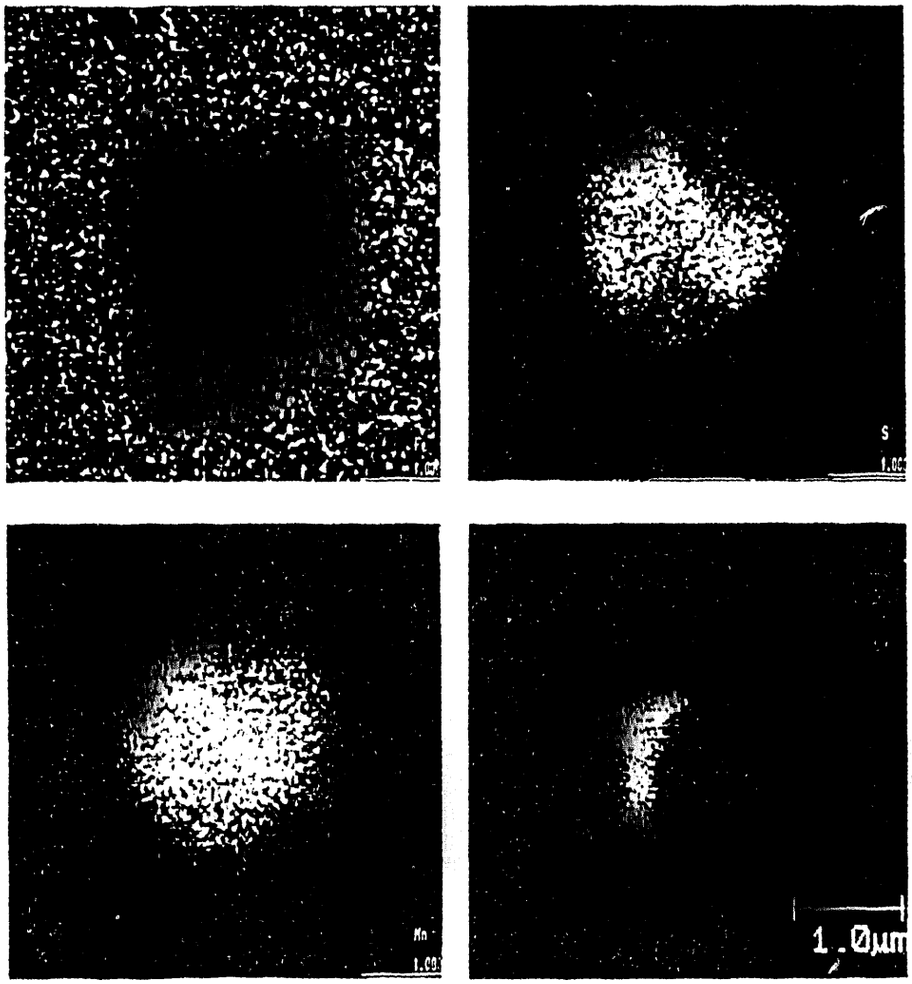

Fig. 7. A MnS inclusion which did not initiate a pit after the repeated immersions on Sample No. 69. EDX Fe, Mn, S maps and AES S map, before exposure.

comparison with No. 65 that the surface sulfur concentration was affected by the addition of 2 m*M* thiosulfate ions. The presence of thiosulfate in the solution significantly enhanced the sulfur concentration on the surface in the region of the pit, as well as on the surface at a distance from pit, and thereby sped up the process of pit initiation.

Figure 7 shows EDX maps for Fe, Mn, and S (Sample No. 69) which clearly indicate the presence of an inclusion region with which is about 2 µm in diameter. However, the AES sulfur map (Fig. 7, lower right corner) shows only a small portion of this inclusion was visible at the surface. This sample had been immersed into 0.1*M* NaCl solution at rest potential for 30 min, then held at 400 mV for 40 min, much longer than the induction times recorded from No. 65 and No. 68. No pit formation was evident from subsequent *in situ* microscopy. The sample was re-immersed and held at 400 and 450 mV. Eventually the photoresist broke and a pit initiated elsewhere on the specimen but no pit formed at the inclusion of interest. Again, local AES analysis was carried out to determine the elemental distribution in the vicinity. It was found at the site of the inclusion of interest, that the Cr peak was not detected. The MnS inclusion was partly dissolved during the repeated exposures and sulfur had spread to the adjacent surface. However, the surface of the exposed portion that remained after the first immersion was evidently too small to give a critical intensity to the corrosion process and, as a consequence, this particular inclusion did not initiate a pit.

Conclusions and Summary

Initiation of pitting corrosion at the site of MnS inclusions on 304 SS in neutral Cl^--containing solutions was studied by a combination of AES, SEM, EDX, and electrochemical techniques. Methods were invented for initiating pits on preselected MnS inclusions. Corrosion behavior and surface composition was observed before and after electrochemical exposure to the solution. These quantitative measurements of local surface chemistry helped clarify the role of inclusions in stimulating pitting corrosion.

Observations were carried out both for multiple pits and for single pits. By using photomasks, MnS inclusions were chosen and located with an optical microscope and analyzed by SAM, then pits were initiated at the sites of such inclusions by an electrochemical method. The progress of dissolution of MnS inclusion and the early stages of pitting were thus quantitatively investigated.

AES and EDX measurements were used to obtain the surface/bulk composition on inclusions/pits and surrounding areas for specimens exposed to 0.1*M* NaCl solution as well as 0.1*M* NaCl + 2 m*M* $Na_2S_2O_3$ solution. The results indicated that the dissolution of MnS inclusions and the spread of product to surrounding area begins to take place at the rest potential. At more anodic potentials, the process proceeds more rapidly. The redeposition of dissolution product gave an increase of sulfur concentration on the surface of both inclusion and vicinity. It was found from measurements on a number of inclusions and pits that the nonuniform distribution of sulfur and iron (Fig. 3) was confined to a region that was approximately four times the nominal radius of the inclusion. Beyond this region, there was a background level of sulfur that depended on the extent of exposure.

To summarize the initiation of pitting corrosion of 304 SS at MnS inclusions in Cl^--containing solution was postulated to occur as follows. Corrosive attack begins with dissolution of MnS inclusions (8, 13) as also supported in the present work from AES, EDX, and SEM images. Dissolution of MnS inclusions produces (11) thiosulfate ions by reaction

$$2MnS + 3H_2O = S_2O_3^{=} + 2Mn^{+\cdot} \quad 6H^+ + 8e^-$$

$$2H^+ + MnS = Mn^{+2} + S + H_2$$

Upon dissolution of the inclusion, a rocavity forms between the inclusion and the adjoining metal and, further, the transport of dissolved sulfur species causes contamination of the surface surrounding the inclusion. Several subsequent events then become possible.

Dissolution of Cr from the bare metal would be accompanied by hydrolysis, causing the local pH to decrease to a critical level at which point the metal in the microcavity might become unstable and dissolve spontaneously (9, 13) whether or not the inclusion continued to dissolve.

The acidic environment would also speed attack of the inclusion as well as the surrounding host metal. By this view, acidification of the microcavity solution occurs only after formation of the microcavity by inclusion dissolution. Chromium enrichment of the surface would take place only after pitting is already developed to a certain extent, as seen in the sample 1P (Table I), the second exposure of Sample No. 4, and on pit on the Sample No. 68.

If, on the surrounding passive film, the concentration of thiosulfate and chloride ions builds up sufficiently to exceed a critical concentration (11, 12), then breakdown of passivity may also occur on the oxide surface adjoining the inclusions.

Pits do not initiate at every inclusion, particularly at smaller inclusions. If the initiation of pitting is caused by establishment of a critical concentration of thiosulfate ions, then it is reasonable to imagine that pits would develop only at MnS inclusions with a size above a critical dimension. For inclusions below this critical size, the rate of production of thiosulfate ions would be less than the rate of transport by diffusion, and the local thiosulfate concentration would not build up above the critical value required for passivity breakdown.

It is generally recognized that hydrodynamic flow suppresses pit initiation. By the view presented here, flow would affect pit initiation by rinsing away dissolution products and thus disrupting the sequence of local chemical events that lead to pit initiation. Convective transport processes near a solid surface are significantly influenced by the presence of surface roughness and microcavities. One may anticipate that clarification of the role of these geometric parameters could thus be gained from hydrodynamic studies.

Acknowledgment

This work was supported by the U.S. Department of Energy under grant No. DEFG02-91 ER 45439 through the Materials Research Laboratory at the University of Illinois at Urbana-Champaign. Photolithography operations were carried out in the clean room of the Microelectronics Laboratory of the University of Illinois. The authors appreciate the assistance of Nancy Finnegan, Irena Dumler, and John Hughes in support of this investigation.

Manuscript submitted July 9, 1991; revised manuscript received Jan. 28, 1992.

The University of Illinois at Urbana-Champaign assisted in meeting the publication costs of this article.

LIST OF SYMBOLS

- I_r sulfur (or iron) intensity at distance r
- I_{Inc} average sulfur (or iron) intensity on inclusion
- I_{pit} average sulfur or iron intensity inside pit
- r distance from center of inclusion or pit to the analysis point
- r_o half-width of inclusion or pit
- R r/r_o, distance ratio, dimensionless
- Θ I_r/I_{Inc} (or I_r/I_{pit}), intensity ratio, dimensionless Θ_s for sulfur, Θ_{Fe} for iron

REFERENCES

1. H. H. Uhlig, *Trans. AIMME*, **140**, 411 (1940).
2. M. A. Streicher, *This Journal*, **103**, 375 (1956).
3. D. Brooksbank and K. W. Andrews, *J. Iron Steel Inns.*, **206**, 595 (1968).
4. Z. Szklarska-Smialowska, *Corrosion*, **28**, 338 (1972).
5. M. Smialowski, Z. Szklarska-Smialowska, A. Szummer, and M. Rychcik, *Corros. Sci.*, **9**, 123 (1969).
6. R. Kiessling, in "Proceedings of International Symposium Sulfide Inclusion in Steel," American Society for Metals, Metals Park, OH (1974).
7. P. Poyet and A. Desestret, *Mem. Sci. Rev. Met.*, **72**, 133 (1975).
8. G. Wranglen, *Corros. Sci.*, **14**, 331 (1974).
9. G. Eklund, *This Journal*, **121**, 467 (1974).
10. R. C. Newman, H. S. Isaacs, and B. Alman, *Corrosion*, **38**(5), 261 (1982).
11. S. E. Lott and R. C. Alkire, *This Journal*, **136**, 973 (1989).
12. R. C. Alkire and S. E. Lott, *ibid.*, **136**, 3256 (1989).
13. J. E. Castle and R. Ke, *Corros. Sci.*, **30**, (4/5), 409 (1990).
14. T. P. Hoar, D. C. Mears, and G. P. Rothwell, *ibid.*, **5**, 279 (1965).

USE OF *IN SITU* ATOMIC FORCE MICROSCOPY TO IMAGE CORROSION AT INCLUSIONS

Rebecca M. Rynders,* Chi-Hum Paik,** Ruoru Ke, and Richard C. Alkire

Department of Chemical Engineering
and
Materials Research Laboratory
University of Illinois at Urbana-Champaign
Urbana, IL 61801

September 12, 1993

*Current Address: Air Products and Chemicals, Inc.; Allentown, PA 18195-1501
**Current Address: Korea Institute of Science and Technology; Seoul 130-650, Korea

ABSTRACT

In situ atomic force microscopy was used in conjunction with microlithography and scanning Auger electron spectroscopy to monitor localized corrosion near iron-rich inclusions in Al-6061-T6 immersed in 0.6 M NaCl and also sulfur-rich inclusions in 304 stainless steel (SS-304) in 0.5 M NaCl. The local rate of aluminum corrosion was found to depend on the shape of the nearby iron-rich inclusion. At the corrosion potential, trenches were observed to form in the aluminum host matrix adjacent to the inclusions, and the corrosion sites gradually evolved into circular shapes owing to dissolution. During the dissolution process, the width of the dissolution area was an order of magnitude greater than the depth. Application of a 400 mV cathodic overpotential prevented corrosion initiation, while application of a 500 mV cathodic overpotential greatly accelerated the dissolution rate in comparison with that at the rest potential. On SS-304, exposure to 0.5 M NaCl was accompanied by formation of deposits, which decorated the inclusion surface as well as the surrounding area up to four times the radius of the original inclusion.

INTRODUCTION

Pitting of metal alloys is known to initiate at a variety of sites, which under certain conditions includes inclusions.[1] Aluminum alloys are susceptible to pitting at iron-rich, intermetallic inclusions,[2] while stainless steel is susceptible to pitting at sulfur-rich inclusions.[3,4,5,6,7] It is thus likely that inclusions of these particular compositions support specific chemical events that accelerate local dissolution of the host matrix. Understanding of such phenomena requires techniques that permit direct measurement of local events near inclusions. The purpose of this work is to report on use of *in situ* atomic force microscopy (AFM) to monitor shape evolution at the nanoscale near individual, well-characterized inclusions during initial stages of dissolution.

Observations of corrosion near inclusions have been made on specific sites randomly selected from among a large number on the specimen surface.[8,9,10] Techniques have included *in situ* opitcal microscopy at low magnification as well as *ex situ* scanning and transmission electron microscopies. Zahavi et. al[8] studied pit initiation at Al_3Fe inclusions using scanning and transmission electron microscopy to determine whether the inclusions dissolved, anodized, or remained unchanged during pitting corrosion. These authors questioned whether the inclusion became dislodged during *ex situ* examination and noted that the resolution of the technique did not give a clear image of pit initiation at the inclusion.

Previous investigations of the surface chemistry at inclusion sites have employed surface analysis techniques, which were applied to the same inclusion before and after exposure to the corrosive environment. With such techniques, it has been demonstrated that

pitting corrosion of stainless steel near MnS inclusions immersed in NaCl solutions initiates by the concerted depassivating effect of chloride and thiosulfate ions, the latter being produced by dissolution of the sulfide inclusion.[6,7,11,12] Fundamental understanding of how chloride and sulfur species interact with the passive film near the inclusion, however, remains unresolved.

Scanning tunneling microscopy (STM) has been used to image certain types of metal dissolution events at the near-atomic scale.[13,14,15,16,17] While the STM technique is convenient for imaging conductive surfaces, most localized corrosion processes involve the presence of nonconductive oxide films and are thus not amenable to imaging by STM. AFM does not have such limitations and appears to hold promise for corrosion studies[18] although there are no known studies on the use of AFM for monitoring localized corrosion. In this work, *in situ* AFM was used in conjunction with microlithography and scanning Auger electron spectroscopy to monitor shape evolution during the initial stages of corrosion in the vicinity of preselected, iron-rich inclusions in Al-6061-T6 immersed in 0.6 M NaCl and sulfur-rich inclusions in SS-304 immersed in 0.5 M NaCl.

EXPERIMENTAL PROCEDURE

Aluminum (Al-6061-T6) and stainless steel (SS-304) alloy specimens were cut from rods (1.5 cm dia) and polished to 0.05 μm alumina finish (Buehler, ECOMET® IV). Using a photolithography method described by Ke and Alkire,[7] a photoresist pattern consisting of an 11 x 11 array of 100 μm square openings was created on the specimen surface. Figure 1 shows a second electron image of the photoresist grid on an aluminum specimen and identifies one particular inclusion that was preselected for detailed study. The patterned sample was examined by Auger electron spectroscopy (Physical Electronics, Model 660) to identify the elemental composition of individual inclusions. It was found necessary to sputter the surfaces of the aluminum alloy with argon ions for 30 minutes at a rate of 6 Å/min to remove the top contamination and the oxide overlayer. For surface composition analysis by Auger electron spectroscopy, a 20 kV accelerating beam voltage was used to examine the aluminum alloy, while a 10 kV accelerating beam voltage was used to examine the stainless steel; in both cases the specimen current was 10 nA. The surface composition of individual iron-rich particles in aluminum and sulfide-rich particles in stainless steel was thus identified, and their positions with respect to the photoresist array pattern were recorded.

A second photoresist mask was then patterned onto the stainless steel specimens, so that only the pre-selected inclusion was left exposed. Figure 2 shows an AFM image of such an opening (2-μm-thick, 50 μm square) in the photoresist mask that covered the photoresist grid on one of the stainless steel samples.

Samples were mounted in the fluid cell on the AFM (Nanoscope II, Digital

Instruments), equipped with a 125 μm scanner, top-view head, a Si_3N_4 tip, and XY translation stage. While viewing the sample surface with a 40X monocular, the photoresist opening that framed the preselected inclusion was aligned under the AFM cantilever via the XY translation stage. Then while imaging the surface in air, the inclusion was located within the AFM scanning region via the XY translation stage and the X and Y offset voltages. Electrolytic solution was then introducted into the fluid cell.

For experiments under potentiostatic control (PAR Model 273), two coiled Pt wires were placed in the inlet and outlet ports to serve as reference and counter electrodes, respectively. The specimen was mounted onto the AFM Invar disk with either silver tape (Structure Probe) and a 3:1 Ga:In eutectic (Johnson Matthey Electronics) or silver epoxy (Transene Silver Bond type 50). Electrical connection to the working electrode was made through the stage head.

NaCl solutions were prepared from deionized water (Barnstead, E-pure) and analytical grade NaCl. Experiments typically lasted between 2 and 24 hours, during which time the solution was replaced every 2 hours to minimize evaporation through the inlet and outlet ports. Images were collected at a scan rate of 5-19 Hz. By using various rotation angles and scan magnifications, it was possible to confirm that the surface morphology observed was not distorted by the tip geometry and that the AFM tip force did not disrupt the dissolution process. Additional experimental details are available elsewhere.[19,20]

RESULTS AND DISCUSSION

Aluminum Alloy Pitting at Iron-Rich Inclusions

The shape evolution of aluminum alloy (Al-6061-T6) around iron-rich inclusions was investigated for three conditions in 0.6 M NaCl. The first system illustrated dissolution around a single inclusion at the corrosion potential. The second system illustrated shape evolution around two closely spaced inclusions at the corrosion potential. The third system demonstrated the effect of cathodic overpotential.

Pit Initiation Around a Single Iron-Rich Inclusion

Figure 3 illustrates a series of *in situ* AFM images recorded over a period of 24 hours during dissolution around the selected inclusion exposed to 0.6 N NaCl. Figure 3(a) shows an image of the initial surface obtained in air prior to exposure to solution. It may be seen that the surface texture of the inclusion was smoother than the surrounding aluminum matrix. A 125 nm deep groove between the inclusion and the matrix may be seen along the left side of the inclusion, while the opposite side of the inclusion was partially buried in the bulk matrix. Because the image did not depend on the AFM scanning direction, it was concluded that the groove was not an artifact of the imaging mechanism. Such grooves were observed at all inclusions and were attributed to the mechanical polishing step.

Figure 3(b) shows the surface after exposure to 0.6 N NaCl for one hour at the corrosion potential. The texture of the inclusion remained smooth, but the surrounding

matrix became rougher. It is also seen that the pre-existing polishing groove did not significantly change shape or size during this period, and that a trench began to form by dissolution of the host metal adjacent to the right side of the inclusion.

Figure 3 (c) shows that after the second hour of exposure to solution, dissolution proceeded in a nonuniform manner around the inclusion. The rectangular features which appeared on the image of the host surface were probably a tip effect. Because the features of interest in this investigation were the inclusion and adjacent dissolution trench, not the surface of the host matrix, the origin of the rectangular features seen in Fig. 3(c) was not pursued further.

Figure 4 illustrates shape evolution profiles that were obtained from section contours along the two lines superimposed on Fig. 3 (a). The letters mark the side that corresponds to the origin in Fig. 4. The curve labels in Fig. 4 correspond to the image labels in Fig. 3, and the vertical dashed lines mark the edges of the original, exposed inclusion. By comparison of curves a and c in Fig. 4 with the corresponding sequence of images in Fig. 3, it may be recognized that, after 2 hours of exposure, the greatest dissolution occurred on the right-hand side of the inclusion where the region of the bulk matrix extends into and is partially surrounded by the inclusion. Less dissolution was observed in regions where the inclusion protruded into the bulk matrix, such as in the lower right part of the image. Discussion of the nonuniform dissolution around the periphery of the inclusion is presented below. By comparison of the z-scale with the x-y scale, it may be recognized that the width of the trench was nearly an order of magnitude greater than its depth.

Figure 3 (d) shows that a circular pit formed around the inclusion after 24 hours

exposure to the solution. Figure 4, curve d shows that dissolution proceeded radially from the inclusion edge and formed a uniform depth around the inclusion.

In the aluminum system, pitting initiates when the passive film breaks down. At the corrosion potential, anodic dissolution of the host metal is accompanied by a corresponding cathodic reaction. Possible cathodic reactions that occur in neutral solutions are the reduction of dissolved oxygen

$$O_2 + 2H_2O + 4e^- \rightarrow 4OH^- \quad (1)$$

and the reduction of water

$$2H_2O + 2e^- \rightarrow H_2 + 2OH^- \quad (2)$$

The iron-rich inclusion, Al_3Fe, in aluminum alloy is known to be a far better cathodic site for oxygen reduction than the surrounding oxide surface.[9] The localization of cathodic reaction at the inclusions would thus cause the local pH to increase as a consequence of Reactions (1) and/or (2). In turn, because the oxide film cannot be sustained in an environment of high pH,[9,10] the passive film on the matrix surrounding the inclusions would break down and dissolution would proceed.

According to this view, the concentration distribution of hydroxide in the vicinity of the inclusion would depend, in part, on the size and shape of the inclusion. For example, in Fig. 3 (c), accumulation of OH^- would be least at the inclusion tip, which extends towards the lower right, where diffusion of OH^- is rapid in all directions. By contrast, accumulation of OH^- would be greatest at the two side pockets on either side of the inclusion peninsula where diffusion is the most restricted.

Pit Initiation Around a Pair of Iron-Rich Inclusions

Figure 5 shows a series of *in situ* AFM images that document pit initiation at a pair of inclusions exposed to 0.6 N NaCl for 12 hours. Figure 5 (a) shows that the surface texture of the inclusions was much smoother than the surrounding matrix and that a 70 nm deep polishing groove existed between each inclusion and the bulk aluminum.

Figure 5 (b) shows that after two hours exposure to solution, a trench developed between the two inclusions. In addition, the inclusions appear to be larger than in Fig. 5 (a), probably owing to dissolution of a smeared surface layer of metal that revealed their true extent. Rectangular features noted in Fig. 3(c) were also seen in this series. After the second hour of exposure, the trench grew and pitting commenced at the exterior edges of the inclusions. Figure 5 (c) shows the pit after three hours exposure. The first trench originated between the inclusions, and not on either side, which is an observation consistent with the suggestion that the initial dissolution rates are dependent on the local accumulation of OH^- generated by cathodic reaction on the inclusion.

After three hours, an air bubble entered the cell from the inlet port and the AFM signal was lost. When the AFM signal was regained, a loosely attached film was observed to cover the surface. The film was swept away by the tip and removed by flushing solution through the cell. Figures 5 (d)-(f) show that after four subsequent hours exposure, the inclusions began to dissolve. Figure 6 provides a shape evolution plot obtained by measuring the cross-section contours at various times along the line shown in Fig. 5(a). Both the AFM images and the shape evolution plot show that dissolution began at the top edges of the inclusions and advanced downward. In particular, by comparing the cross-

section contour at 11.0 and 12.3 hours in Fig. 6, it may be recognized that the relative depth of the pit decreased, which indicated that the pit died but that dissolution of the inclusions continued.

Pit Initiation at an Iron-Rich Inclusion under Cathodic Overpotential

Polarization curves for Al-6061-T6 in 0.6 N NaCl showed that oxygen reduction began just cathodic of the rest potential and became mass transport limited at 25 mV overpotential, and that the onset of hydrogen evolution occurred at 500 mV overpotential. The AFM technique to observe local events around such inclusions while such cathodic potentials were applied.

The aluminum sample was monitored for one hour while placed under 0.6 M NaCl solution and a 400 mV cathodic overpotential. The matrix surrounding the selected iron-rich inclusion showed no signs of dissolution during this time, although rectangular features decorated the surface as indicated previously with the other experiments. After one hour, the scanning region was shifted to examine another inclusion known to be rich in iron. Consistent with monitoring of the first inclusion, the shape did not evolve for the next hour. Figure 7 (a) shows the second inclusion site after three hours exposure to the solution and 400 mV cathodic overpotential. At this time, the cathodic overpotential was increased to 500 mV for 3 minutes then returned to 400 mV. During the 3 minute application at 500 mV, bubbles formed in the cell due to hydrogen evolution and momentarily disrupted the imaging process. Figure 7 (b) was captured during the application of the 500 mv overpotential, and Fig. 7 (c) was captured shortly after the potential was returned to 400

mV. Figure 8 shows the corresponding shape evolution along the centerline length and width of the inclusion (as indicated in Fig. 7 (a)) resulting from application of the 500 mV overpotential. It may be seen that dissolution proceeded around the inclusion to form a circular pit. In Fig. 8(b), curve c, the flat-bottomed feature was an artifact of the AFM tip; the recessed region became too narrow and deep to be measured with the pyramidal tip. We are currently attempting to resolve this limitation with use of more slender tips. After the applied overpotential was returned to 400 mV, the inclusion was monitored for an additional 3 hours, and no further shape change was observed.

We propose the following explanation for the behavior reported in Figs. 5 and 6. At the corrosion potential, i. e., in the absence of an applied overpotential, the oxygen reduction reaction would be localized at the inclusion site. Because the local supply of oxygen to the inclusion site is higher under such conditions, the local pH would be higher, such that the high pH required for film breakdown could be obtained. With an applied cathodic overpotential, oxygen was reduced over the entire surface at the limiting current condition, such that oxygen would become depleted at the surface and the pH required for breakdown would not be achieved. The observation that the cathodic overpotential prevented dissolution around the inclusion, was therefore, actually consistent with the proposed mechanism. At a 500 mV overpotential water reduction would first occur at the inclusion site because it is a better cathodic site. Such a localized increase in pH at the inclusions could then be sufficient to cause the pit initiation as observed in Fig. 7. In addition, the width of the trenches observed was nearly an order of magnitude greater than its depth, which suggests that the transport of OH^- is much greater than the dissolution rate

of the aluminum matrix.

Observations of SS-304 at MnS Inclusions

Figure 9 shows the shape evolution of a MnS inclusion exposed to 0.5 M NaCl solution, which was adjusted to a pH of 4.2 with HCl. Figure 9 (a) shows the surface in air prior to exposure to solution. The inclusion surface was recessed 10 nm below the bulk matrix, probably because the basic developers used in the microlithography processing steps dissolved the inclusion.

Figure 9 (b) and (c) show the surface after exposure to 0.5 M NaCl for 8 and 60 minutes, respectively. The salient feature in these images is the buildup of reaction products on and around the inclusion site. To accelerate this process after one hour immersion, a small anodic potential (50 mV) was applied. Figure 9 (d) shows that after 6 hours of applied potential, the amount of deposited material had increased but had not been distributed over a region farther than four times the radius of the inclusion.

The buildup of reaction products around the inclusion supports previously reported results. In their work, Ke et. al.[7,6] demonstrated the spread of sulfur species onto the passive surface adjacent to a MnS inclusion, while the inclusion site became rich in Mn, Cl, and 0. Based on these previous results, it is possible that the morphological changes observed by *in situ* AFM were the precipitation of sulfide species around the inclusion and oxidation of the manganese species within the inclusion.

In the stainless steel system, pit initiation was never observed at an inclusion while it was being imaged although pits would initiate elsewhere on the same surface. It is

possible that the AFM technique disrupted pit initiation for this system. Investigation of this effect is continuing since such information may provide additional insight into the pitting mechanism of stainless steel as well as methods for prevention of pit formation.

CONCLUSIONS

This work demonstrated that atomic force microscopy is a suitable technique for *in situ* monitoring of shape evolution around a preselected intermetallic inclusion during exposure to corrosive conditions under electrochemical control. In contrast to other techniques, the AFM method provided three-dimensional, real-time information that may be used to follow shape evolution. The use of a photoresist grid permitted single inclusions to be selected *a priori* and characterized by surface analysis techniques and then examined *in situ* during corrosion with use of the AFM. Results presented here have illustrated early stages of pit initiation at an iron-rich inclusion in Al-6061-T6 and corrosive attack at a sulfur-rich inclusion in SS-304.

Pitting in Al-6061-T6: The initial polishing groove observed at all inclusions (Fig. 3, Fig. 5, and Fig. 7) did not provide an initiation site for pitting; in fact, the polishing groove was the last region to corrode. Trenching was initially observed in regions where the ratio of inclusion:host matrix surface area was high, such as concave regions in the oddly shaped inclusion (see Fig. 3) or between two closely spaced inclusions (see Fig. 5). After a trench was formed around the inclusion, dissolution of the aluminum host matrix was uniform and proceeded radially outward from the inclusion edge to form a circular pit. The radial size of the trench was an order of magnitude greater than the trench depth. Two of the three systems presented showed no signs of inclusion dissolution; however, the inclusion pair did dissolve during the pit propagation stage and after pit death. The application of a cathodic overpotential in the oxygen reduction region (400 mV cathodic overpotential) prevented pitting around an iron-rich inclusion; whereas, application of a

cathodic overpotential that marks the onset of water reduction (500 mV cathodic overpotential) accelerated the dissolution process (see Fig. 7). Each of these results supports the view that iron-rich inclusions act as cathodic sites for oxygen reduction to generate a high local pH that initiates pitting corrosion.

Corrosion at a Sulur-Rich Inclusion: The shape evolution of a sulfur-rich inclusion exposed to 0.5 M NaCl adjusted to a pH of 4.2 with HCl was monitored under a 50 mV anodic potential for 6 hours (see Fig. 9). Under these conditions, the inclusion grew and surface roughening was observed around the inclusion site up to a distance of four times the inclusion radius. In conjuction with previous work and it was suggested that the morphological changes observed by *in situ* AFM were attributed to dissolution of the MnS inclusion, resulting in a dissolution/precipitation of sulfide species around the inclusion site and oxidation of the manganese species.

ACKNOWLEDGMENT

This investigation was supported by the U. S. Deparment of Energy Grant No. DEFG02-91ER45439 through the Materials Research Laboratory, University of Illinois at Urbana-Champaign. Nancy Finnegan assisted in the surface analysis of the aluminum samples.

REFERENCES

1. G. C. Wood, W. H. Sutton, J. A. Richardson, T. N. Riley, and A. G. Malherbe, Localized Corrosion, B. F. Brown, J. Kruger, and R. Staehle, eds., NACE-3, Houston, TX p. 526 (1971).

2. K. Sugimoto, Y. Sawada, and S. Morioka, *Trans.Japan Inst. Metals*, **13** (1972).

3. L. Tronstad and J. Sejersted, *J. Iron Steel Inst.*, **127** 425 (1933).

4. Z. Szklarska-Smialowska, *Corrosion*, **28** 338 (1972).

5. G. Wranglen, *Corr. Sci.*, **14** 331 (1974).

6. J. E. Castle and R. Ke, *Corr. Sci.*, **30 (4/5)** 409-428 (1989).

7. R. Ke and R. C. Alkire, *J. Electrochem. Soc.*, **139 (6)** 1573-1580 (1992).

8. J. Zahavi, A. Zangvil, and M. Metzger, *J. Electrochem. Soc.*, **125(3)** 438-444 (1978).

9. K. Nisancioglu, K. Y. Davanger, and O. Strandmyr, *J. Electrochem. Soc.*, **128** 1523-1526 (1981).

10. K. Nisancioglu, *J. Electrochem. Soc.*, **137** 69 (1990).

11. S. Lott and R. C. Alkire, *J. Electrochem. Soc.*, **136 (4)** 973-979 (1989).

12. R. C. Alkire and S. Lott, *J. electrochem. Soc.*, **136(11)** 3256-3262 (1989).

13. F. F. Fan and A. J. Bard, *J. Electrochem. Soc.*, **136** 166-170 (1989).

14. O. Lev, F. F. Fan, and A. J. Bard, *J. Electrochem. Soc.*, **135** 783-784 (1988).

15. I. C. Oppenheim, D. Trevor, C. Chidsey, P. Trevor, and K. Sieradzki, *Science*, **254** 687 (1991).

16. H. W. Pickering, Y. C. Wu, D. S. Gregory, and S. Geh, *Vac. Sci. Technol. B.*, **9** 976-983 (1991).

17. X. Zhang and U. Stimming, *Corr. Sci.*, **30** 951 (1990).

18. B. J. Cruickshank, A. Gewirth, R. M. Rynders, and R. Alkire, *J. Electrochem. Soc.*, **139** 2829-2832 (1992).

19. C. H. Paik, *Ph.D. Thesis, University of Illinois*, 1993.

20. R. M. Rynders, *Ph.D. Thesis, University of Illinois*, 1993.

LIST OF FIGURES

Figure 1. Scanning electron micrograph of the first photoresist layer on Al-6061-T6. The arrow indicates the iron-rich inclusion selected for study and is shown in detail in Fig. 3.

Figure 2. AFM image of the second photoresist layer showing a 50 μm square opening. This specimen was on SS 304.

Figure 3. AFM image (z=250 nm/div) of Al-6061-T6 and an iron-rich inclusion (a) in air and (b) *in situ* after exposure to 0.6 N NaCl at the corrosion potential for 1 h, (c) 2 h, and (d) 24 h.

Figure 4. Shape evolution along section lines shown in Fig. 3(a). Curve labels correspond to image labels in Fig. 3.

Figure 5. AFM image (z=250 nm/div) of Al-6061-T6 and an iron-rich inclusion pair (a) in air, and (b) pit initiation after exposure to 0.6 N NaCl at the corrosion potential for 2 h, (c) 3 h, (d) 6 h, (e) 7 h, and (f) 10 h.

Figure 6. Shape evolution along section lines shown in Fig. 5 (a). The long and short dashed lines mark the edges of the large and small inclusion, respectively.

Figure 7. AFM images of (a) Al-6061-T6 and an iron-rich inclusion exposed to 0.6 N NaCl at 400 mV overpotential for 2 h, then (b) 500 mV overpotential for 3 min and (c) after overpotential was returned to 400 mV.

Figure 8. Shape evolution along section lines in Figure 7 (a). Labels correspond to images in Figure 7 and show evolution from a 3 min 500 mV cathodic overpotential.

Figure 9. AFM images (z=50 nm/div) of sulfur-rich inclusion in SS-304 (a) in air and (b)after exposure to 0.5 M NaCl (pH=4.2) for 8 min, (c) 60 min, and (d) after exposure to 50 mV anodic overpotential for 6 hours.

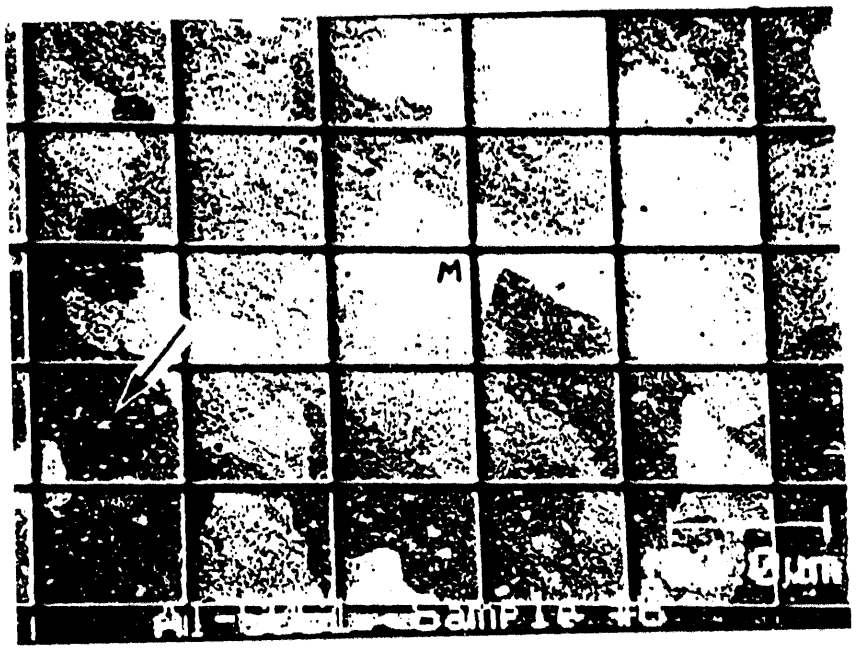

Figure 1

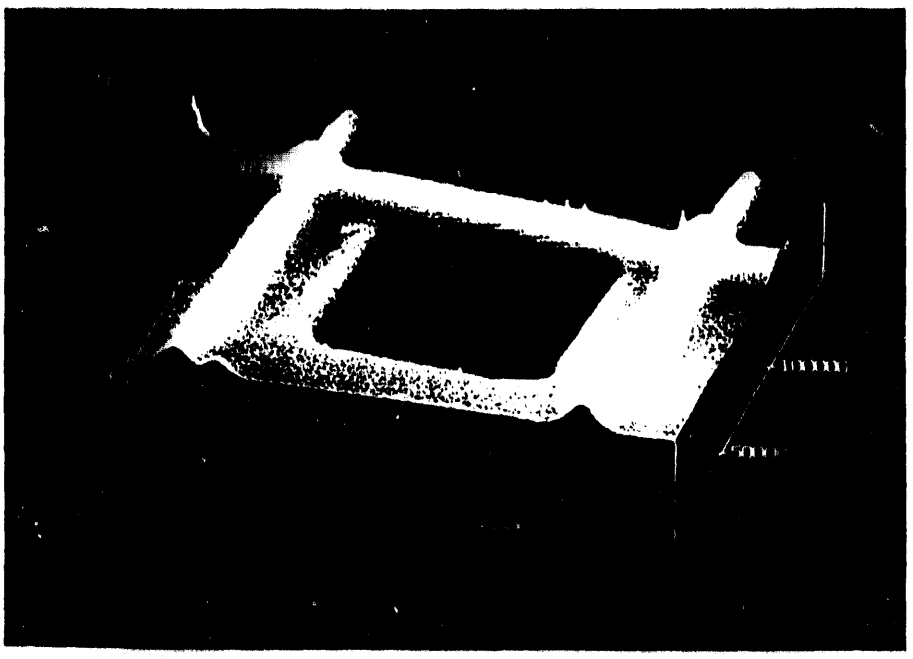

Figure 2

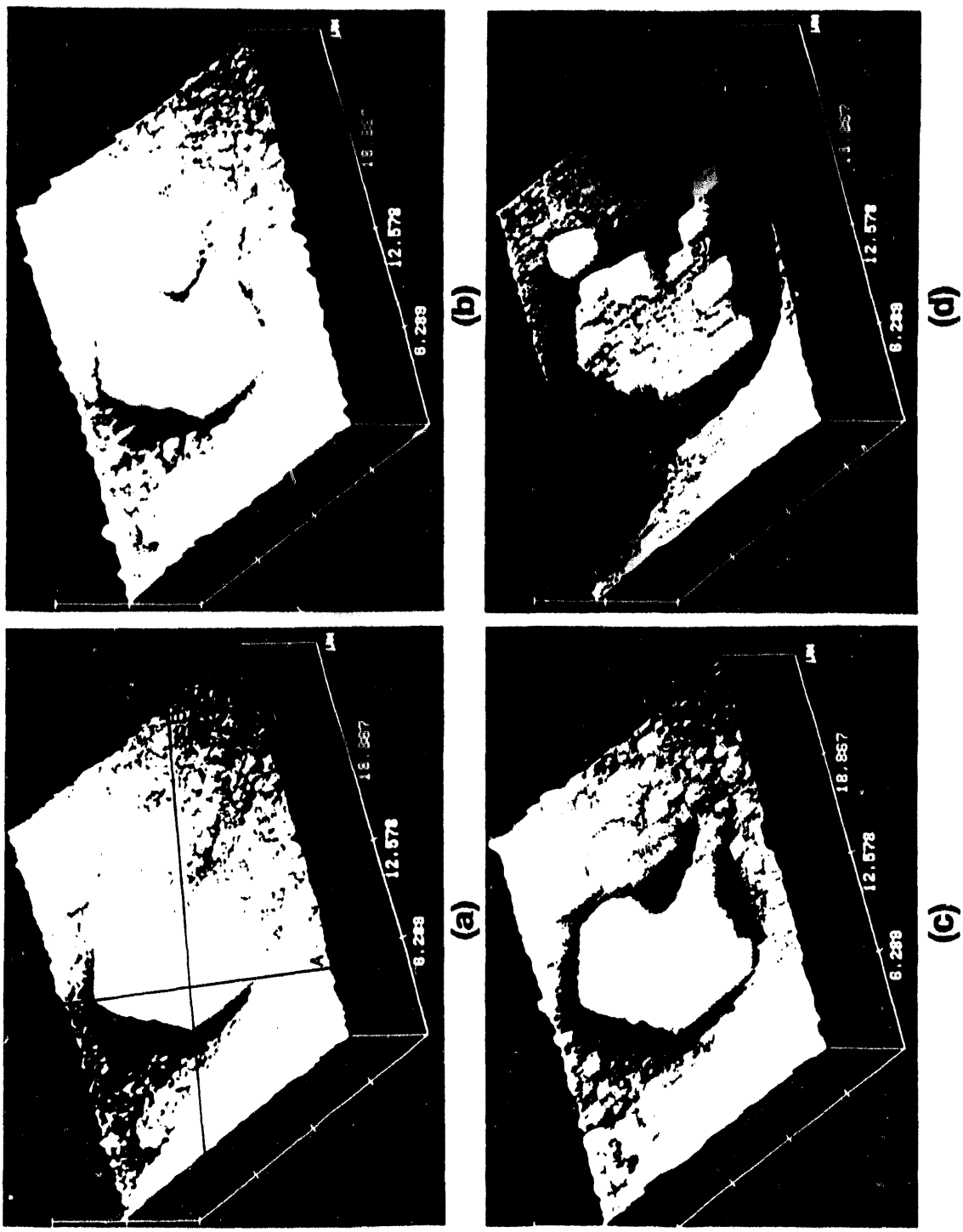

Figure 3

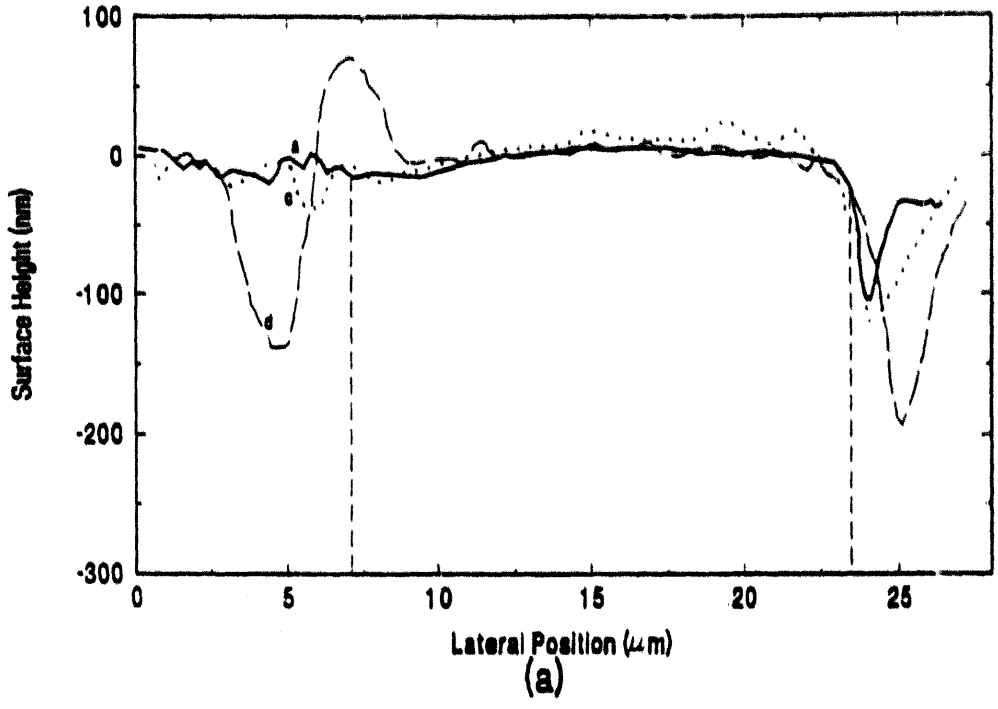
100
0
-100
-200
-300
Surface Height (nm)
0
5
10
15
20
25
Lateral Position (μm)
a
c
d

(a)

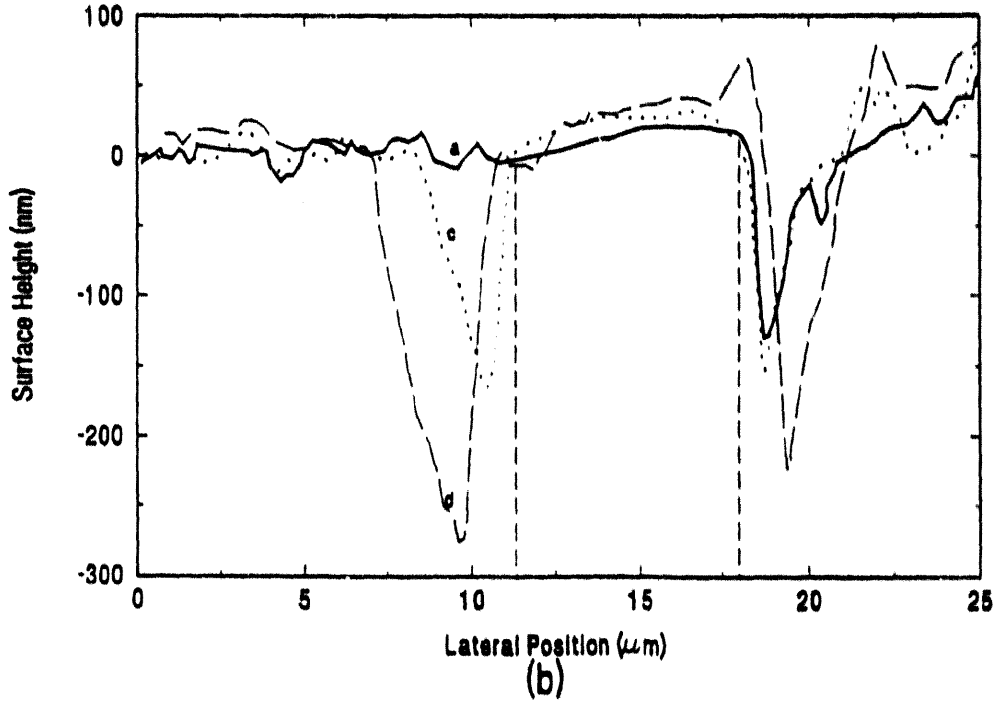
100
0
-100
-200
-300
Surface Height (nm)
0
5
10
15
20
25
Lateral Position (μm)
a
c
d

(b)

Figure 4

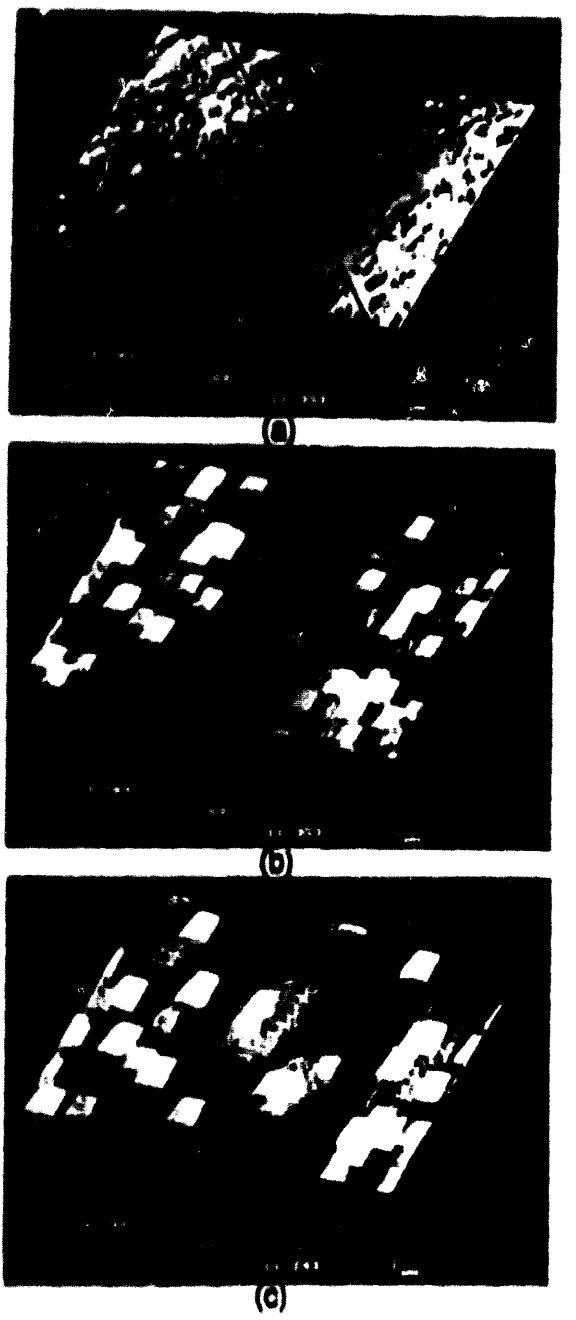

(b)

(c)

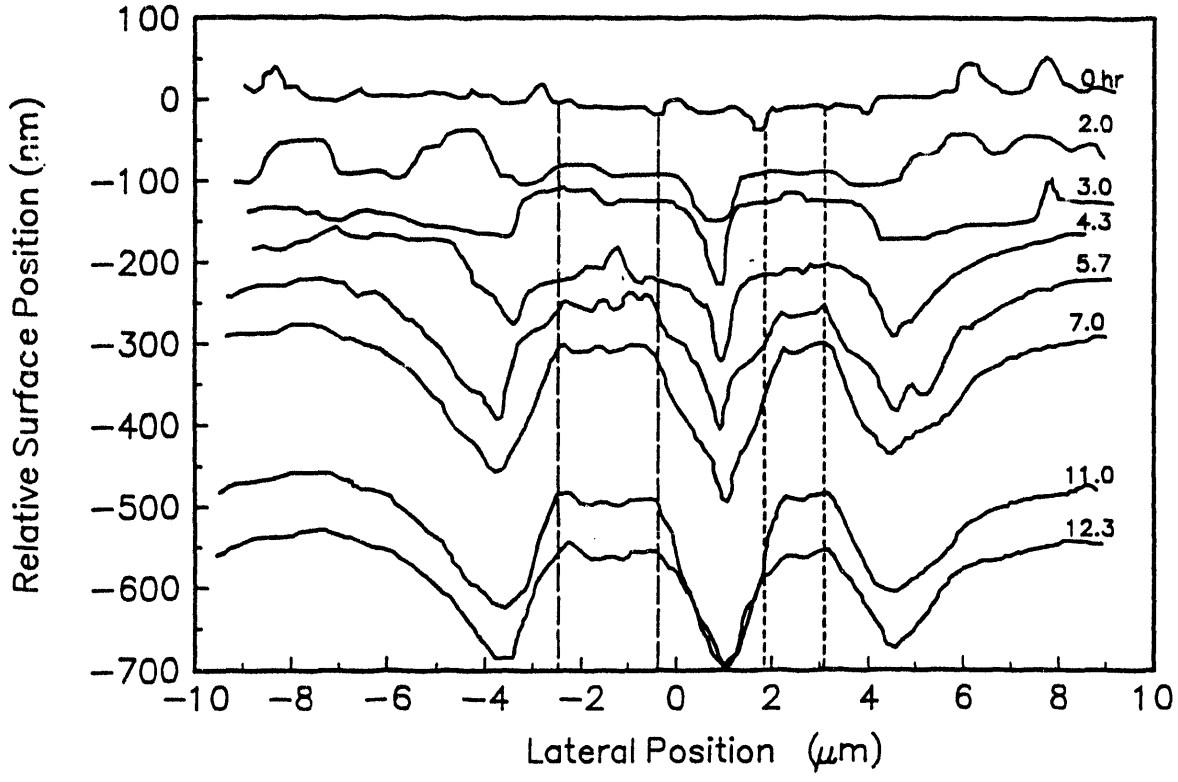
100
0
−100
−200
−300
−400
−500
−600
−700
Relative Surface Position (nm)
−10
−8
−6
−4
−2
0
2
4
6
8
10
Lateral Position (μm)
0 hr
2.0
3.0
4.3
5.7
7.0
11.0
12.3

Figure 6

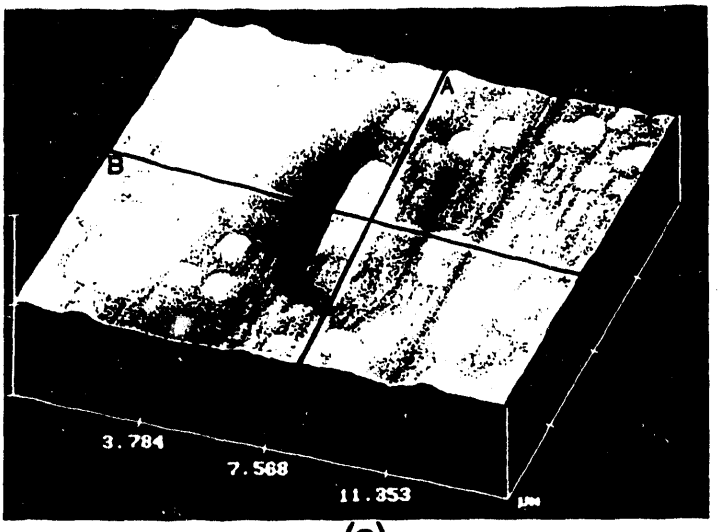

(a)

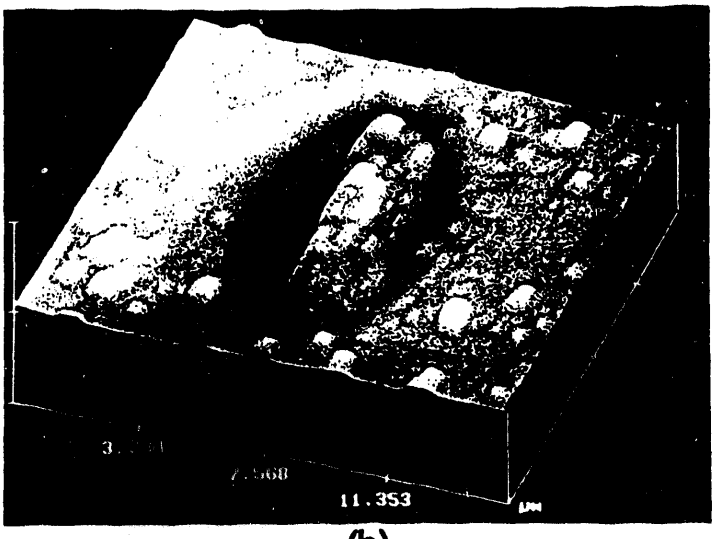

(b)

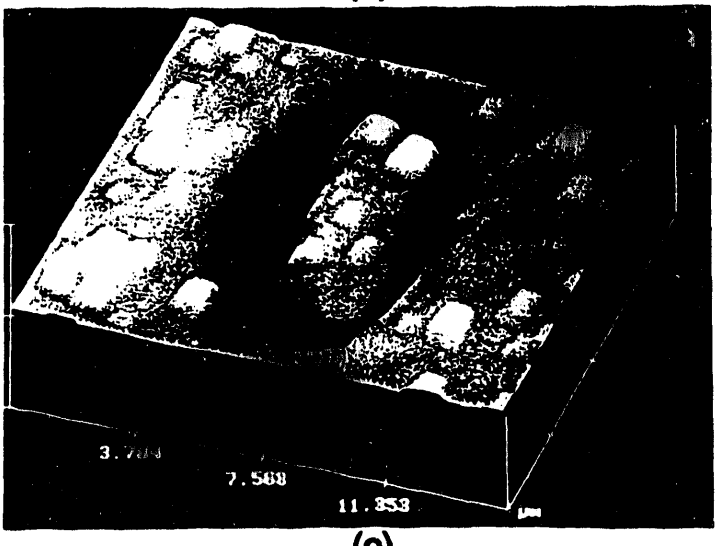

(c)

Figure 7

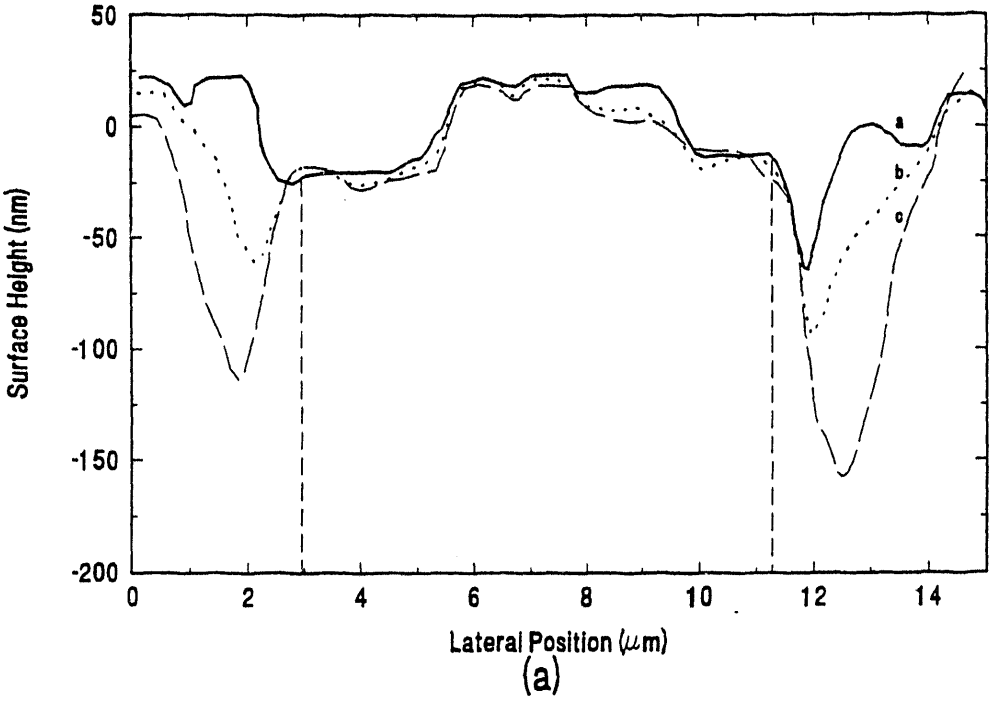
50
0
-50
-100
-150
-200
Surface Height (nm)
0
2
4
6
8
10
12
14
Lateral Position (μm)
a
b
c

(a)

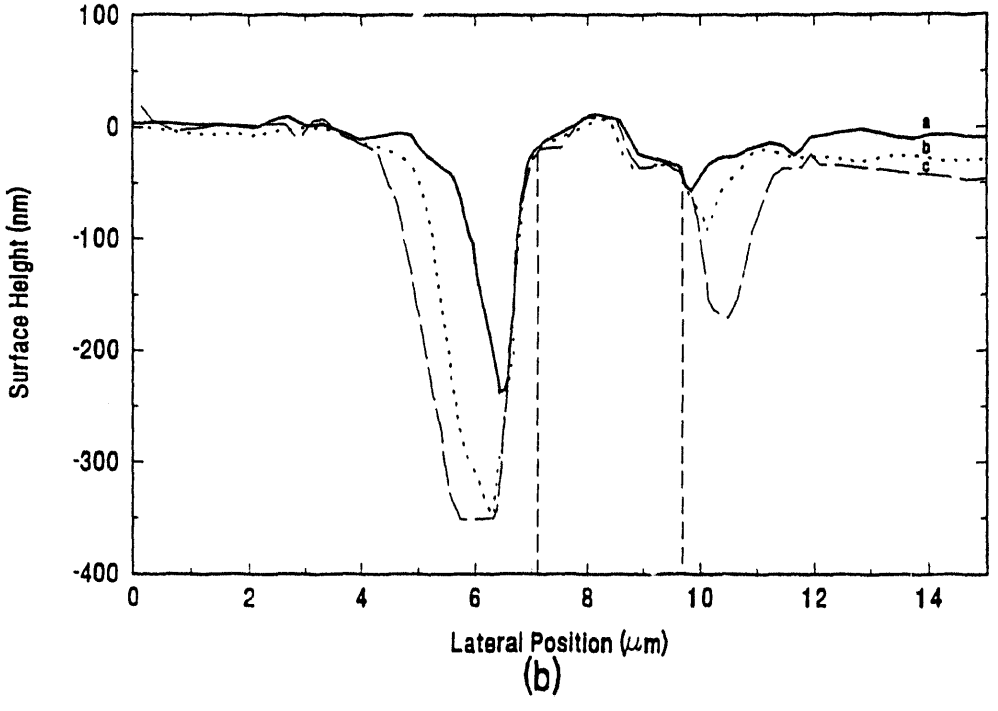
100
0
-100
-200
-300
-400
Surface Height (nm)
0
2
4
6
8
10
12
14
Lateral Position (μm)
a
b
c

(b)

Figure 8

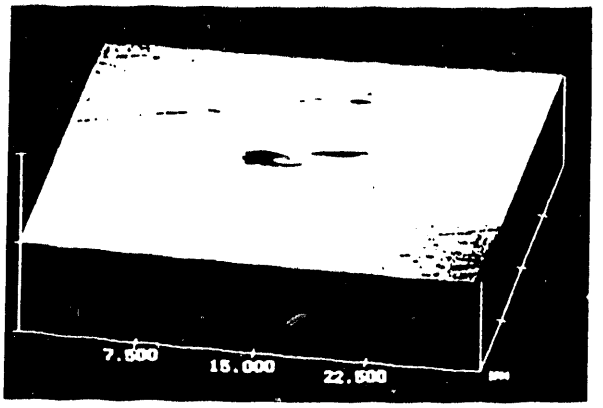

(a)

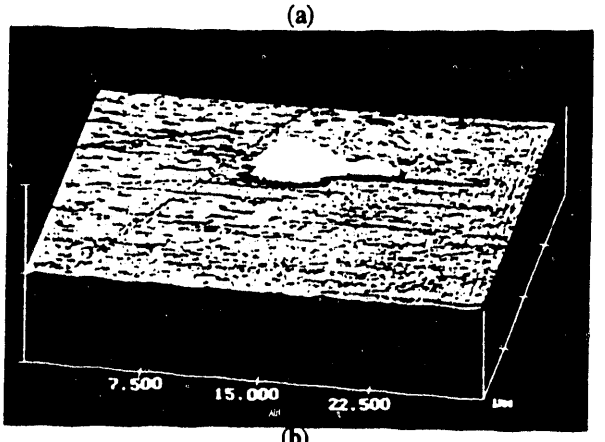

(b)

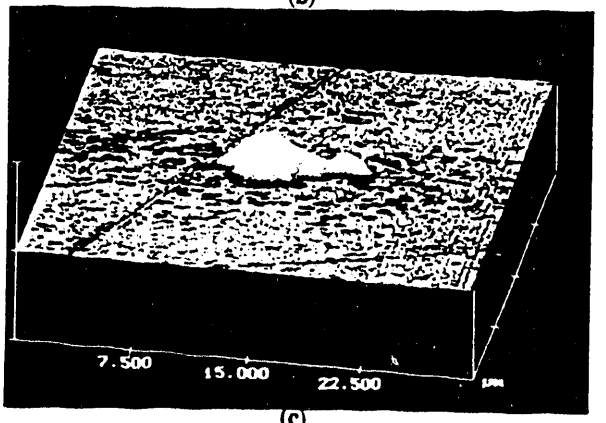

(c)

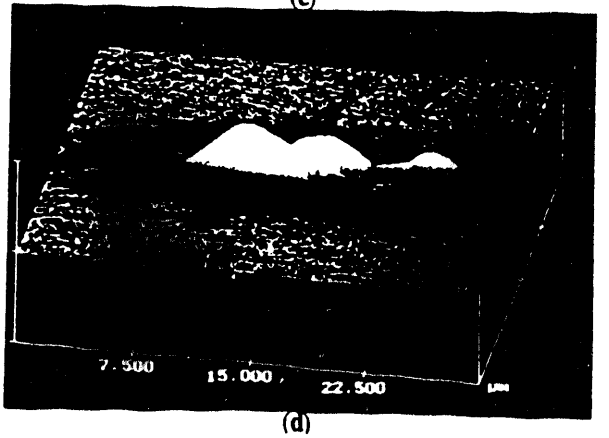

(d)

Figure 9

DOE/NREL/ORNL WORKSHOP LOW COST MATERIALS OF CONSTRUCTION FOR BIOLOGICAL PROCESSES
MAY 13, 1993

High Resolution Molecular Emission Spectroscopy For Material Characterization and Corrosion Studies

Dr. George Andermann
University of Hawaii at Manoa
Dept. of Chemistry
2545 The Mall
Honolulu, HI 96822

ABSTRACT

This report offers an evaluation of the use of molecular X-ray emission spectroscopy (XES) for material characterization in general and for corrosion studies in particular. It is shown that some of the difficulties in corrosion studies dealing with non-destructive sample depth profiling, in order to obtain meaningful evaluation of the nature and extent of corrosion (chemical modification) of metal surfaces, can be handled by the use of molecular XES in combination with various techniques which are inherently available in the XES technology. Since high resolution molecular XES represents a pioneering area of science and technology, and since it is not widely understood, an effort has been made to explain some of the most important features of this area. This is then followed by a report on the application of these techniques for studying air oxidation of various metal surfaces as well as of methanol induced corrosion studies of a more limited number of metal surfaces. Finally a brief report is offered on the U of Hawaii XES instrumentation as well as on the additional analytical capabilities at U of H.

HIGH RESOLUTION MOLECULAR X-RAY EMISSION SPECTROSCOPYY FOR MATERIAL CHARACTERIZATION STUDIES IN GENERAL AND FOR CORROSION STUDIES IN PARTICULAR

by G. Andermann and F. Fujiwara
DEPARTMENT OF CHEMISTRY, UNIVERSITY OF HAWAII AT MANOA

INTRODUCTION

In this presentation we wish to cover several topics, namely, (1) the general analytical difficulties in carrying out meaningful corrosion studies,and the suggestion of using high resolution molecular x-ray emission spectroscopy (XES) for these studies.(2) a brief explanation of the nature of high resolution molecular XES, (3) the application of this technique for thin film analysis, (4) a brief report on our methanol induced corrosion studies using this spectroscopic technique, and (5) a brief description of our XES instrumentation capabilities as well as the description of additional analytical capabilities at the U of Hawaii.

(1) GENERAL COMMENTS ON DIFICULTIES OF CORROSION ANALYSIS

Corrosion of a metal surface represents a highly complicated mechanism. In general the process is quite heterogeneous in the sense of the chemistry involved as well as in terms of the lateral and in depth spatial distribution. Techniques are available to study the morphology of the corrosion problems as well as the changes in the elemental composition of the process both on micrroscpic as well as macroscopic basis.Three analytical problems, however, have not been handled well in the past. These are (a) nondestructive sample depth profiling of the corroded surface, (b) testing of corrosion in situ , and (c) the evaluation of the chemical nature of the corrosion, i.e. the appropriate identification of the chemical species, involved in the corrosion proces.It is our intention to show that the appropriate utilization of high resolution molecuar XES can solve problems (a) through (c). This technique of XES is a highly pioneering one and our group has made major contibutions in this area using unique instrumentation developed at U of H. While the use of low resolution XES is well understood for elemental analyis, there is essentially very little textbook information on molcular high resolution XES, and, therefore the next section deals with this topic.

(2) HIGH RESOLUTION MOLECULAR X-RAY EMISSION SPECTROSCOPY

The field of XES is a historically old one, dating back to 1912. In its original useage the tecnique was used to probe the electronic structures of atoms. After a

few years of research it was realized that each atom had its own characteristic X-ray emission lines. Under relatively low optical resolution the characteristic radiation of an element corresponding to core electron transitions, for example, the Kα line did not show any effect when the element in question was involved in a different chemicial combination, say Cl in chloride vs. chlorine in chlorate. However, by 1919, using high optical resolution, it was found that the characteristic Cl Kα radiation showed a shift in going from chloride to chlorate, thus, establishing XES as the first spectroscopic technique to show a chemical shift, preceding the use of X-ray photoelectron spectroscopy for chemical shift studies by some 40 years. Yet, today it is XPS (x-ray photoelectron spectroscpy) which is being used in a practical way for chemical shift studies rather than XES . In other words, there is commercial instrumentation available for XPS studies but not for XES studies. The answer to this riddle is many-folded. First of all, when using core electron transitions, say K and or L shell excitation,. then with XPS the fundamental information is more reliable than with XES. (2) The observed shifts with XPS are larger than with XES. (3) To-date the time to take an XPS spectrum is at least ten times faster than is the case with XES. However, when it comes to obtain molecular valence electron (chemical bonding) information, which is far more reliable than chemical shift studies using core electrons, then XES has numerous fundamental advantages over XPS, or for that matter over any other electron spectroscopic techniques.(For additional details on this topic see Appendix A and B. A deals with some of the fundamentals and B shows some typical applications) Moreover, since with XES the photon escape depth usually exceeds several thousand angstroms , and with the electron techniques such as XPS and/or Auger the electron escape depth is usually 10 angstroms or less, there are several practical advantages with XES. These are as follows:(a) With electron ejection based techniques it is necessary to have the sample under utrahigh vacuum conditions, whereas with the XES method samples can be studied even in a solution (an extremely important feature in corrosion sudies). (2) Sample preparation with XES is extremely fast (just as fast as in ordinary x-ray fluorescence elemental analysis) as compared with XPS and/ or with Auger. (3) Spectroscopic resolving power of 4,000 to 10,000 is readily attainable with XES, thus, yielding a resolution of 0.1 ev or less, whereas 0.5 ev resolution with XPS is very difficult to achieve. Thus, the only residual practical advantage of say XPS over XES is detector speed. But, this last problem has been adressed successfully by a number of laboratories,and it is in the process of being solved by our own laboratory as well. Thus, it is relatively safe to assert that high resolution molecular XES is on the verge of a historical major breakthrough, which , when it is accomplished, will have the same sort of impact as the well-known NMR(nuclear magnetic resonance) for solving difficult analytical problems, But whereas the utility of NMR has been primarily in the field of organic chemistry, the utility of XES will be in the areas of inorganic app[lications.

(3)THIN FILM ANALYSIS

As already stated above, the photon escape depth in X-ray emission spectroscopy is usually several thousand angstroms (in fact, for large atomic number elements the characteristic K radiation can approach tens of thousands of angstoms). This means that with ordinary methods of electron or photon excitation and using ordinary sample optics (large angles of incidence and exit) XES is primarily an analytical tool for bulk analysis, that is , where the thickness of the sample exceeds thousands of angstroms. In recent years it has been shown by a number of XES workers, including our U of Hawaii group [1] that it is possible to obtain thin film analysis (sample thickness in the range of 1000 angstroms to 10 angstroms) by using a number of different techniquesm such as, grazing angle of exit, grazing angle of incidence, as well as variable low kinetic energy electron excitation. Here at U of H we have emphasized grazing angle of exit as well as low kinteic energy electron excitation. By varying the exit angle using photon excitation, or by varying the kinetic energy of the incoming electrons ,we have demonstrated that XES is a highly useful technique for non-consumptive sample depth profiling in the thickness region of 10 to several thousands of angstroms, thus making XES a powerful tool for corrosion studies. We started to develop the basic technology of this technique in 1982 and by 1985 we began to apply our new methodology of thin film analysis to oxidation problems of transition metal films in magnetic storage materials of interest to IBM. In addition to demon strating the power of XES for thin film studies, we also discovered that XES had the power to study not only the chemical modification (oxidation) of single and multiple layers of thin films, but also the chemical modification at the interfaces of top layers due to the optical (refractive index) effects at these interfaces(2). To the best of our knowledge there are no other non-destructive techniques capable of accomplishing this feat. The significance of this capability for studying corrosion is that if there is a very thin layer(say less than 1 micron of stainless steel coating on a mild steel), then, in principle variable angle XES is capable of studying non destructively any corrosion at this interface. If the stainless steel coating is greater than 1 micron, then the study would have to proceed destructively, but at much larger steps than the 20 angstrom steps normally used with XPS or with Auger. In other words, the corrosion evaluation through a thicker coating is far more practical with XPS than with other techniques.

Historicaly our group has been in the forefront of developing molecular XES for thin film analysis. A brief account of the technology and the application of this technology prior to our studies on methanol induced corosion is given in Appendix C. Finally it should be noted also that, in principle, it is possible to obtain in-situ corrosion studies involving ,say a metal surface immersed in alcohol with XES . Just how this can be done is outlined in Section (5). Note that none of the currently available electron spectroscopic methods can accomplish this feat!

(4) METHANOL INDUCED CORROSION STUDIES

Our studies on methanol induced corrosion were supported by the section of DOE dealing with the alcohol transportation fuel demonstration program super vised by Mr. Russel. The program was started out in January 1991 amd completed in December 1992. The studies were carried out using our high re solution 5 M grating spectrometer (see the next section for details on the inst rument) In what follows below we offer certain pertinent sections of a short communication which is being submitted to Journal of Science and Engineering Corrosion. Additional details are to be found in Appendix D.

Technique to Determine Extent and Kind of Corrosion Using X-Ray Emission Spectroscopy: Application to Methanol Induced Corrosion

F. Fujiwara and G. Andermann
Dept. of Chemistry, University of Hawaii, Honolulu, HI 96822

ABSTRACT

The usefulness of x-ray emission spectroscopy to determine the depth profile, extent and kind of corrosion of metals is presented and is demonstrated for the methanol induced corrosion of mild steel and brass.

Introduction. The current interest in the use of alternate fuels, such as methanol or ethanol, for motor vehicles, presents important problems dealing with the corrosion or oxidation properties of such fuels. In particular, problems such as the following need to be addressed: (1) the corrosiveness of these fuels to different metallic engine and storage components, (2) techniques to compare and minimize such effects, (3) the rate or extent of this oxidation and its chemistry or endproducts and (4) the effects of additives or combustion byproducts on the oxidation properties of these fuels. In this short communication, we only wish to present a few results to demonstrate the usefulness of x-ray emission spectroscopy (XES) techniques to investigate this corrosion process and approach these types of problems. A fuller, more technical exposition of the results from our study will be given in a future paper.

Experiment and Results. We have looked at several metals, viz.,

iron, mild steel (1018), stainless steel 304 and brass, corroded under various conditions. These conditions have included, submersion in methanol, methanol-water and methanol-water-formic acid solutions for several months at room temperature, submersion in water, heating in air and ambient oxidation. For this short communication, only some of the data is presented to illustrate the application of the technique (Figures 1 and 2). The plots shown are those of the intensity ratio, Lß/Lα, against the depth into the sample. As indicated above, each oxidation state of the metal is associated with a particular Lß/Lα intensity ratio and, in general, the ratio increases as the oxidation state increases. Thus, for instance, a rise in the curve as the depth decreases, reflects the increased oxidation of the particular metallic element nearer the surface. The particular values of the intensity ratio reflect the percentage mixture of the different oxidation states involved.

Figure 1 shows the data for mild steel (1018) samples that were: (a) ambiently oxidized, (i.e., polished in air just prior to placement in the spectrometer) ("Amb.Ox."), (b) submerged in a 5% aqueous methanol solution for about 5 to 6 months at room temperature ("5% Aq.") and (c) corroded in 5% aqueous methanol solution electrochemically for a few days at very low potentials to accelerate the corrosion ("EIS"). It can readily be seen from the plots that cases "a" (ambient oxidation) and "b" (5% aqueous methanol submersion) show almost identical small extents of corrosion. In contrast, case "c" (electrochemically corroded) shows noticeably more corrosion, both at the very near surface and at deeper depths.

Figure 2 plots the Lß/Lα intensity ratio versus depth for two brass samples which were: (a) polished in air just prior to placement in the sample chamber of the spectrometer and (b) brass which had been left in the air for a considerable length of time. For both cases, the Lß/Lα intensity ratio for the copper and the zinc are shown. It can be seen that while the copper curves of both samples are almost identical in extent of corrosion, essentially very small and about the same at the very near surface and deeper, the zinc curves show dramatic differences. Case "b" shows much larger oxidation of the zinc, as is expected, since the more reactive zinc is placed in brass for this very purpose, i.e., to corrode in place of the more abundant copper. Note that the zinc for case "a", where exposure to the air was at a minimum, the extent of corrosion is about the same at both near surface and at deeper depths.

Conclusion. We have tried to demonstrate very briefly, the usefulness and potential of XES in the study and evaluation of the corrosion of metals. It was shown how, a depth profile of the oxidation species present can be obtained in a non-destructive manner, which can lead to an evaluation of the extent of corrosion and the type or chemistry of the corrosion. It should be added in passing that chemical modifications other than oxidation can be studied with XES, and its application can be extended to non-metals, as well. Further, it should be possible to do the in situ

monitoring of the corrosion process over a span of time.

REFERENCES

1. G. Andermann and F. Fujiwara, Anal. Chem. 52 (1984) 1711; G. Andermann, F. Fujiwara, T.C. Huang, J.K. Howard and N. Giraud, Adv. in X-Ray Anal. 32 (1989) 261; F. Fujiwara and G. Andermann, Adv. in X-Ray Anal. 35B (1992) 845; E. P. Bertin, Principles of X-Ray Spectrometric Analysis, 2nd. Ed. (New York, N.Y.: Plenum Press, 1979).

2. D. Fischer, J. Appl. Phys. 41 (1965) 3561.

FIGURE 1. Fe Lß/Lα intensity ratios measured at various depths (Angstroms) for mild steel samples corroded under different conditions.

FIGURE 2. Cu Lß/Lα and Zn Lß/Lα intensity ratios for two different brass samples with different extents of oxidation. Sample [1] has larger extent of corrosion.

Figure 1'

MILD STEEL Lb/La vs. DEPTH

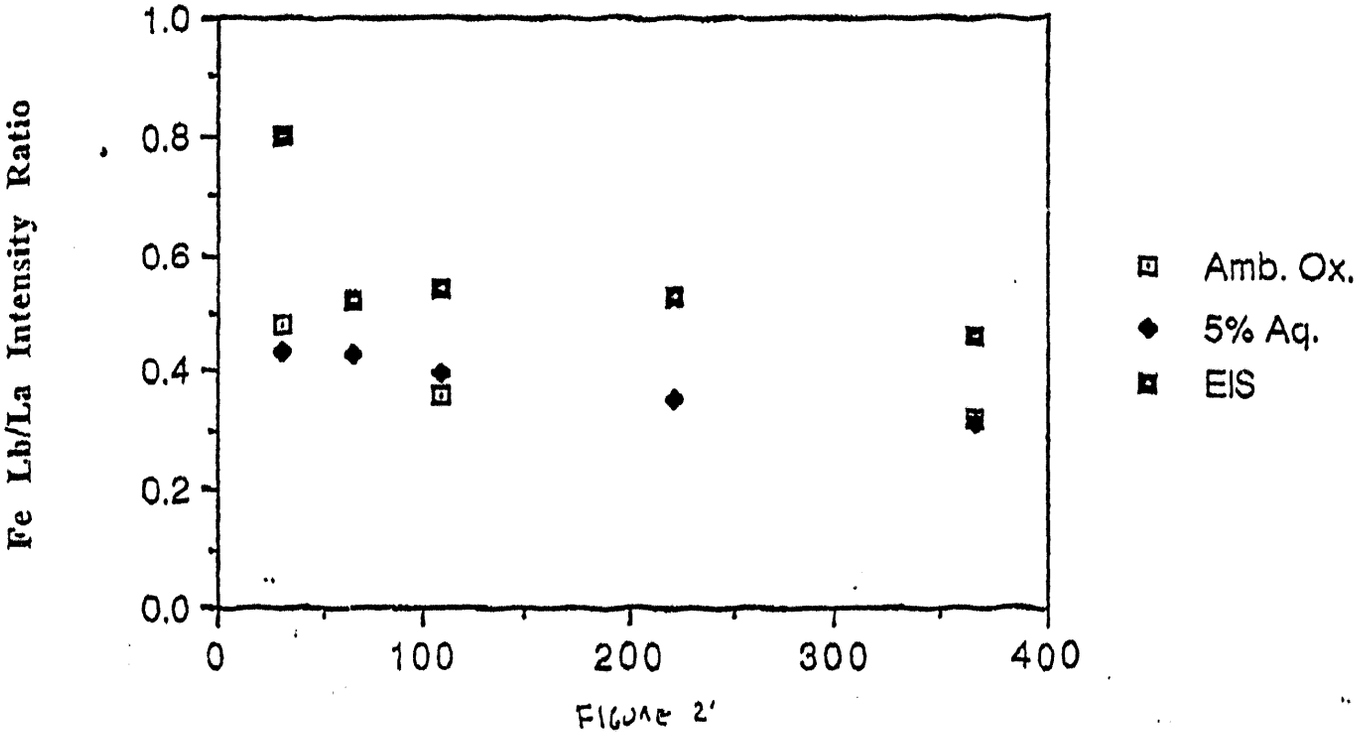

Figure 2'

BRASS Lb/La vs. DEPTH

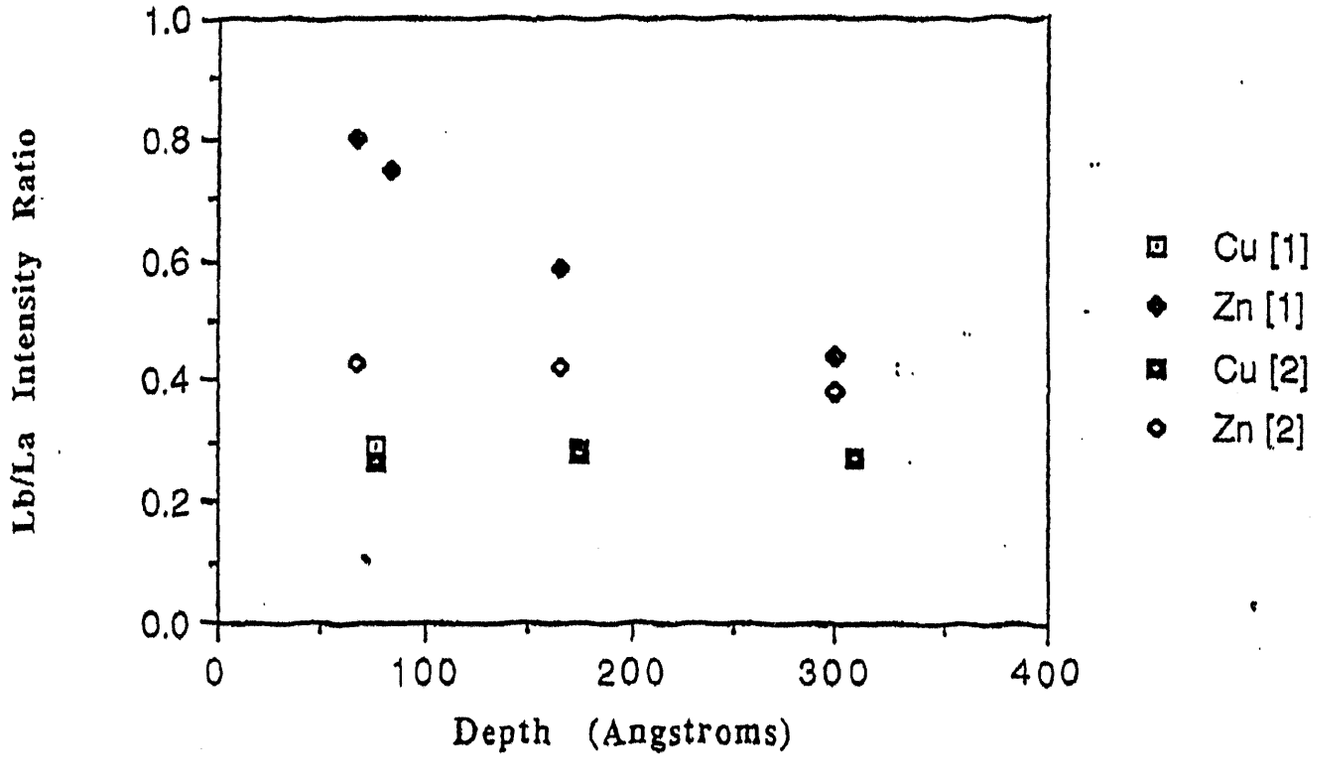

(5) OUR XES INSTRUMENTATION AND OTHER UH CAPABILITIES

Our entry into high resolution XES occurred in 1966 via the develoment of a double crystal spectrometer accessory to a standard Norelco Vacuum emission spectrometer. This project was supported by NSF and the applications covered the evaluation of chemical bonding in dozens of sulfur, chlorine, phosphorus amd silicon bearing compounds. The study involved materials both in the liquid and solid state. This was possible because the K radiations studied were below 10 angstroms in wavelength and the the use of a helium atmsphere permits the use of liquid at these wavelengths. Note that to study valence electron transitions for the transition metals of interest in ethanol induced corrosion will permit the use of air, further facilitating the use of double crystal spectrometry for in-situ study of corrosion. It should also be noted that most of the results discussed in Appendixes A and B were based on the use of these double crystal spectrometer studies.

With NSF support, in 1973 we began the development of a unique high resolution 5 meter spectrometer to cover the region of 10 to 150 angstroms. Note that whereas below 10 angstroms it is possible to sudy corrosion of a metal substrate directly as it is covered by the corroding liquid medium, here above 10 angstroms it is necessary to have the sample in an evacuated sample chamber. Note, however, that the pressure in the sample chamber can be as high as 10^{-3} to 10^{-6} torr, which is relatively easy to achieve as compared to ultrahigh vacuum (10^{-10} torr) required by XPS and Auger techniques.

Figure 1

G. Andermann / Variable grazing exit angle XFS for thin-film analysis

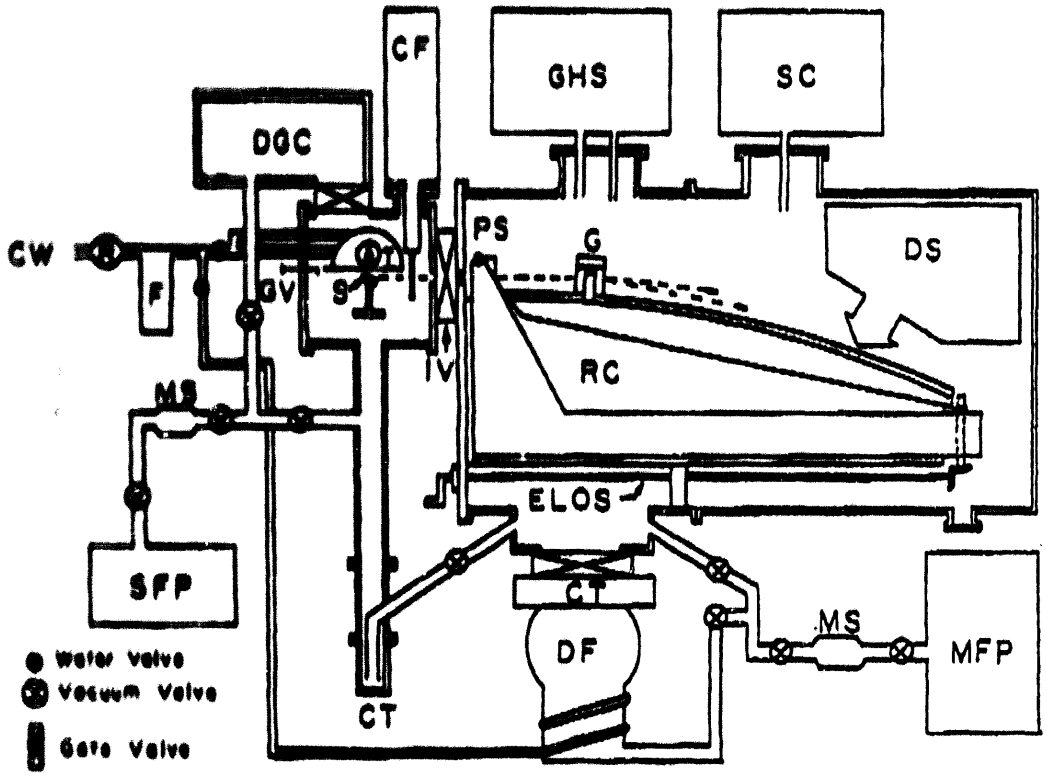

Fig. 9 Mechanical block diagram of the 5 m grating X-ray spectrometer: RC – Rowland circle, G – grating, PS – primary slit, DS – detection system, IV – isolation valve between X-ray tube (T) and sample (S), CF – cold finger, DG – degassing sample chamber, ELOS – external line of sight adjustment, CW – cooling water, R – regular, F – filter, MS – molecular sieve, CT – cold trap, SFP – sample chamber forepump, MFP – main chamber forepump.

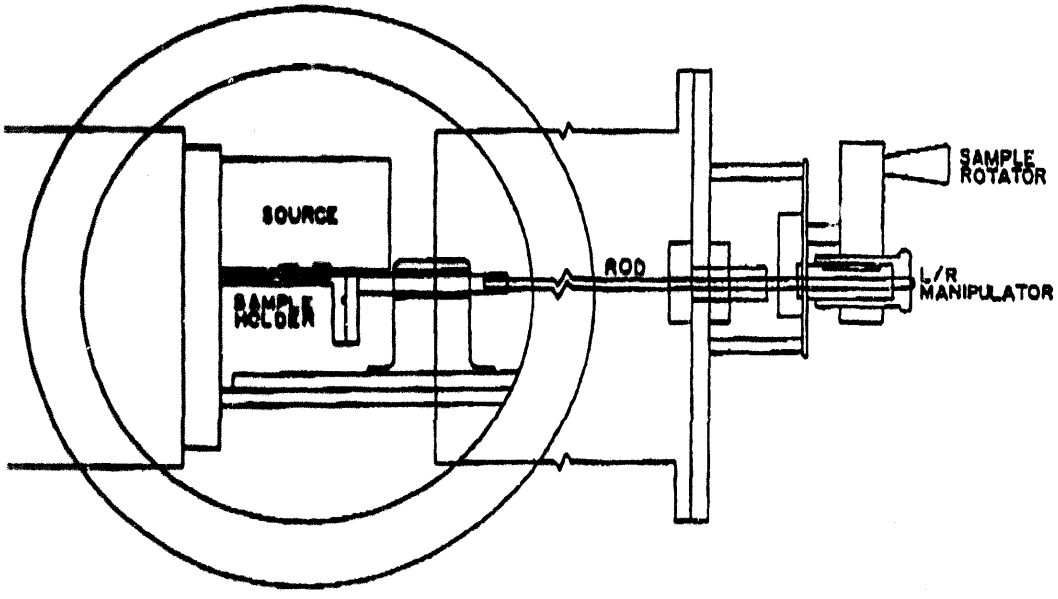

Fig. 10. Rotatable two-position sample holder.

A schematic version of our 5 M grating spectrometer is shown in Figure 1 , Additional details can be found elsewhere (3). The most unique feature of of our instrument is the extremely high optical resolution not found with any other 5 meter spectrometer. It should be noted that we have photographic, scaning photoelectric detection capabilities, and as mentioned before, we are in the midst of the development of a completing position sensing detection system. All of these systems have their special applications, but for the corrosion studies the scaning photoelectric and position sensing detection systems are the preferable ones. These can be intechanged rapidly in a modular manner. The excitaiton of the sample is either by electron or by photon impact. Again these sources are readily interchangeable.

Sample depth profiling is obtained either by variable sample exit angle technology or by variable kinetic electron energy excitation. A review article by Andermann [1] should be consulted for futher details on how sample depth profiling is achievable via sample exit angle variation.

The above instrumentation combination and applications are totally unique and unaivalable elsewhere. However, conventional instrumentation of potential utilization for corosion studies are also available at the U of Hawaii, namely,

(i) Ordinary X-ray fluorescense spectrometry

(ii) Scaning electron microscopy with energy dispersive x-ray spectrometry

(iii) Electron impedance spectrometry

(iv) Scaning tunneling micrscopes

(v) Atomic force microscopes

(vi) Ellipsometers

(vi) Near, mid and far infrared spectometers including reflectometer accessories

(vii) Raman spectrometers with laser microprobe and surface enhancement

(viii) X-ray difractometers

(ix) The usual array of morpholigical and metallurigical instrumentation

Note that our group is either familiar with the use of most of the above instrumentation or it has excellent relationships with personnel who are more familiar than we are.

REFERENCES:

(1) G. Andermann, Surface-Film and Interfacial Analysis Via Variable Grazing Exit Angle X-Ray Fluorescence Spectrometry
(2) G. Andermann, R. Kim and F. Burkard, AIP Conf. POroc. 75 (1981) 309 and references cited therein
(3) G. Andermann, T.C. Huang, J.K. Howard, N.Staud, Characterization of Perm alloy Thin Films Vai Variable Sample EXit Angle Ultrasoft X-Ray Fluorescence Spectrometry, Advances in X-RAy Analysis, Vol 32, 261, 1989

APPENDIX A - FUNDAMENTALS OF MOLECULAR XES

Here we offer a short discussion taken verbatim out of a review article written byAndermann, Applied Surface Science 31 (1988) 1-41. Note that the P, S data were obtained on our double crystal spectrometer, whereas the O and the C data were obtained on our grating spectrometer.

While X-ray spectroscopy (emission and absorption) has been used since 1930 to rationalize the valence electron structure of metals and insulators in terms of solid state band models, the use of molecular models to rationalize the X-ray experimental observations of non-metallics started in the late sixties. A particularly useful review of the use of molecular orbitals in X-ray spectroscopy is due to Urch [42]. A terse account of Urch's explanations, with a somewhat different emphasis and restricting the discussion to XFS, is presented below.

Fig. 27 depicts the energy level diagram of a hypothetical diatomic molecule AB. Shown in this figure are core atomic orbitals ϕ_A, and ϕ_B and the manifold of bonding valence molecular orbitals, ψ_i's as well as the manifold of antibonding orbitals ψ_i^*'s. Also shown in this figure are the typical XP, UP, and ultraviolet absorption (AU) and XF transitions. Even the utilization of the

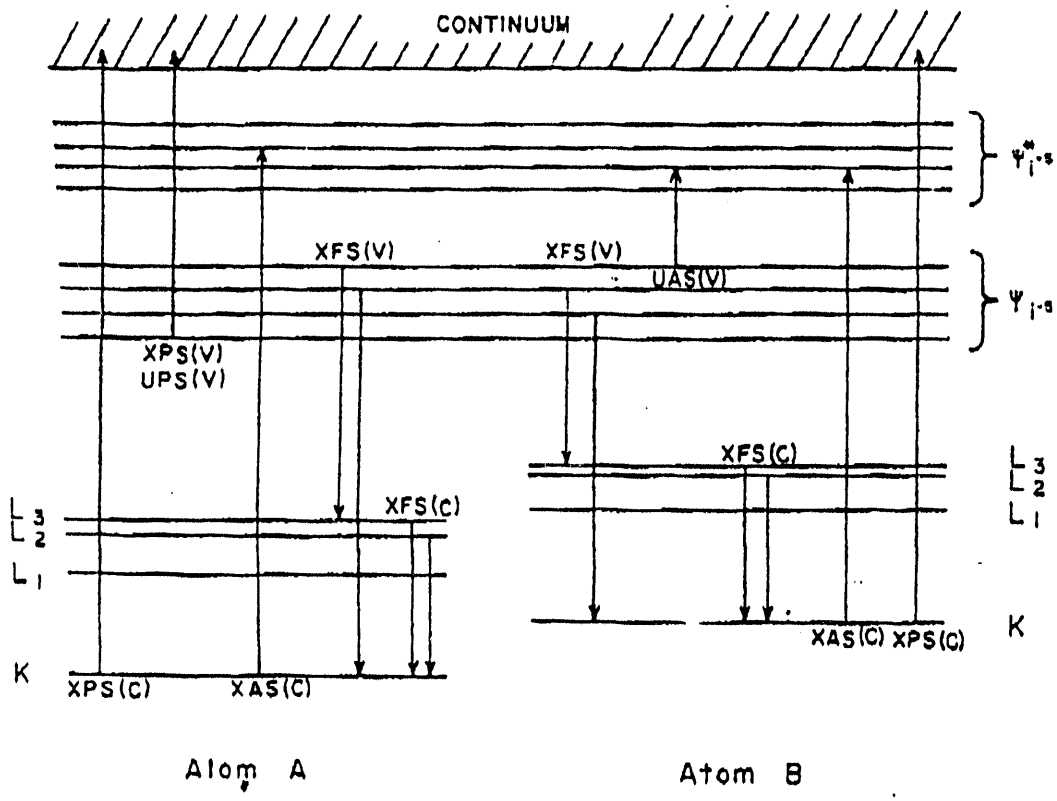

Fig. 27. Highly simplified energy level diagram for a hypothetical diatomic molecule AB showing the various core (C) and valence (V) electron transitions for XFS, XAS, XPS, and UAS.

simplest frozen orbital one electron transition model, namely, that the initial excited state is adequately described by $\phi_{J,l}^{-1}$, and the final state by ψ_i^{-1}, where ϕ is some core orbital of element J (indexed), and l is usually either s or p, and where $\psi_i = \Sigma c_{ji}\chi_j$ with χ_j representing valence atomic orbitals, already offers the following unique fundamental advantages over the other electronic spectroscopic techniques: the number of opportunities q to sample the filled valence electron structure of a molecular equals $\Sigma 2x + \Sigma y$, where x = number of different heteroatoms each with K and L core vacancy initial states, and y = number of different heteroatoms with K core vacancy initial states only. Thus, for example $q = 4$ for PCl_5 (P-K,L and Cl-K,L emission spectra). This multi-atom probe capability to sample the valence electronic structure of a molecule is completely unique since all other electronic spectroscopic techniques, e.g., XPS, UPS, and UAS provide a single spectrum of the filled valence molecular orbitals. This advantage by XFS becomes increasingly more useful as the size of the molecule and the degree of heteronuclearity increases. Using this inherent power, our group has already demonstrated the following unique analytical probe capabilities with $\psi_{J,s}^{-1}$ as the initial state:

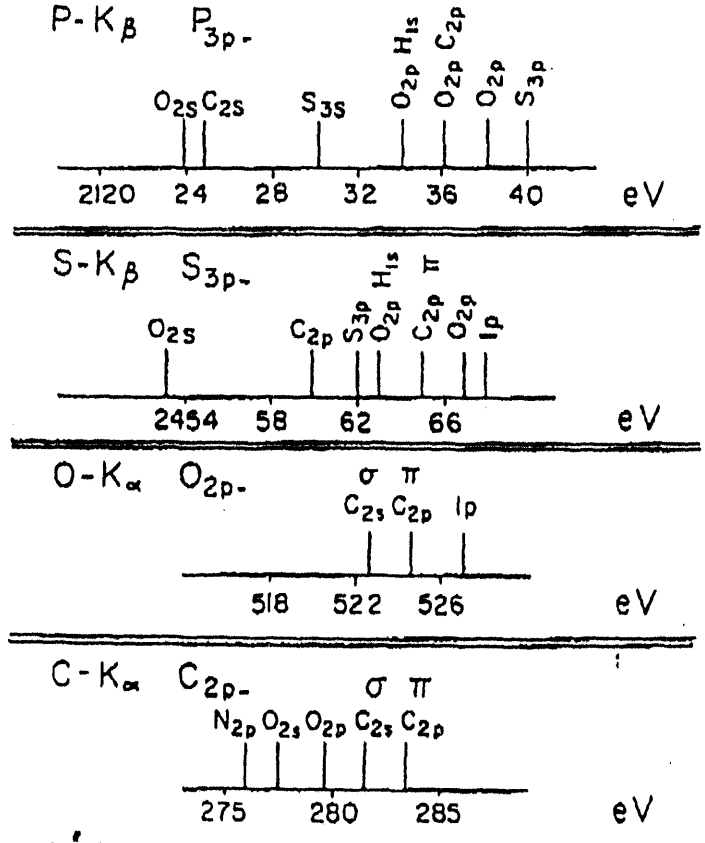

Fig. 28. Tie-dingram for characteristic molecular orbital transitions involving P-Kβ, S-Kβ, O-Kα and C-Kα spectra signifying the ability to use XFS as a ligand identifying "finger-print" analytical tool.

(a) If the charge density is highly localized about element *J*, then XFS may be used to identify ligands attached to *J* [28,43–45,49].
(b) On the other hand, if *J* is a ligand atom, and if *J* is attached to an atom which is involved in a delocalized charge density arrangement (such as a π regime), then XFS can determine how atom *J* feels any perturbation [46–48,50] of the delocalized charge density regime.

The idea of highly localized charge density is particularly useful analytically with XFS. This is illustrated in fig. 28 which shows a partial listing of some of the characteristic transitions our group has observed to date.

APPENDIX B - SOME TYPICAL APLICATIONS

Here we offer a couple of typical spectra obtained on our grating spectrometer. Figure B-1 shows for acetate anion the carbon and oxygen K emission spectra. On the oxygen spectrum we see the 2p lone pair electron band A and the oxygen 2p- carbon 2p bonding oribital band B. For the carbon K spectrum we see strong bands B, C, and D. These correspond to the Carbon 2p- Oxygen 2p, to the Carbon 2p- Carbon 2p, and the Carbon 2p - Carbon 2s molecular orbitals respectively. It should be noted that for ethanol we would see similar types or orbitals but the peaks would have different positions and different intensities.

In Figure B-2 we illustrate how the oxygen K emission spectra vary for Cu(OH) , CuO and Cu O. Accordingly, there are very large differences in the spectra. Knowing the oxygen K emission spectra for these species, then it is possible to see how the oxidation of a copper surface proceeds, i.e. we can see that copper is barely oxidized under ambient conditions(bottom curve), mimics cuprous oxide under first oxidation (first few minutes at high temperature oxidation), but then resembles cupric oxide after third, heavy oxidation. This Figure is also from the same reference as the one given in Appendix A.

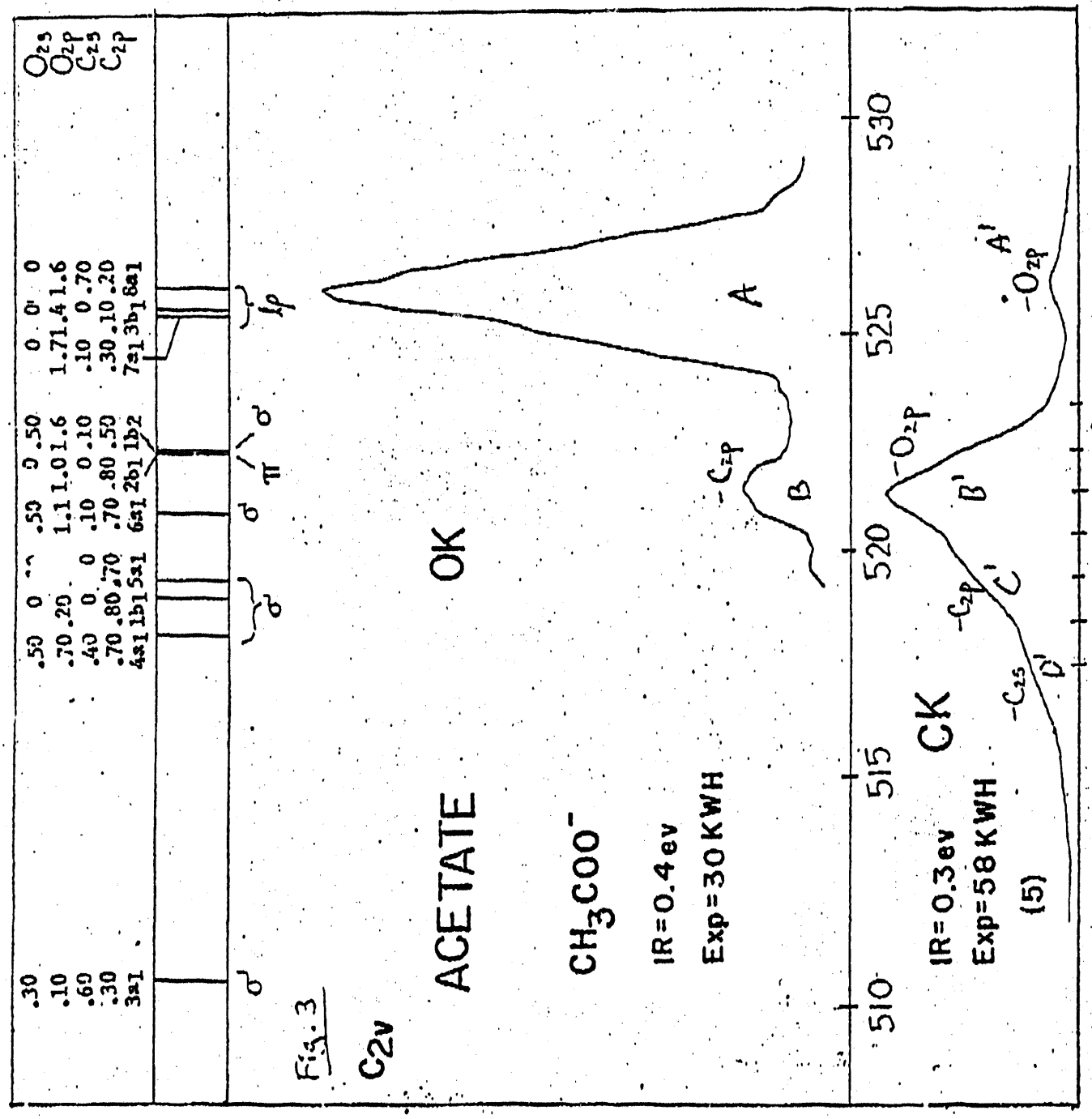
ACETATE
CH_3COO^-
C_{2v}
OK
IR=0.4 ev
Exp=30 KWH
CK
IR=0.3 ev
Exp=58 KWH
(5)
A
B
A'
B'
C'
D'
$-C_{2p}$
$-O_{2p}$
$-C_{2s}$
O_{2s}
O_{2p}
C_{2s}
C_{2p}
INTENSITY
(hv) ev
510
515
520
525
530
275
280

Fig. 3

Fig. B-1

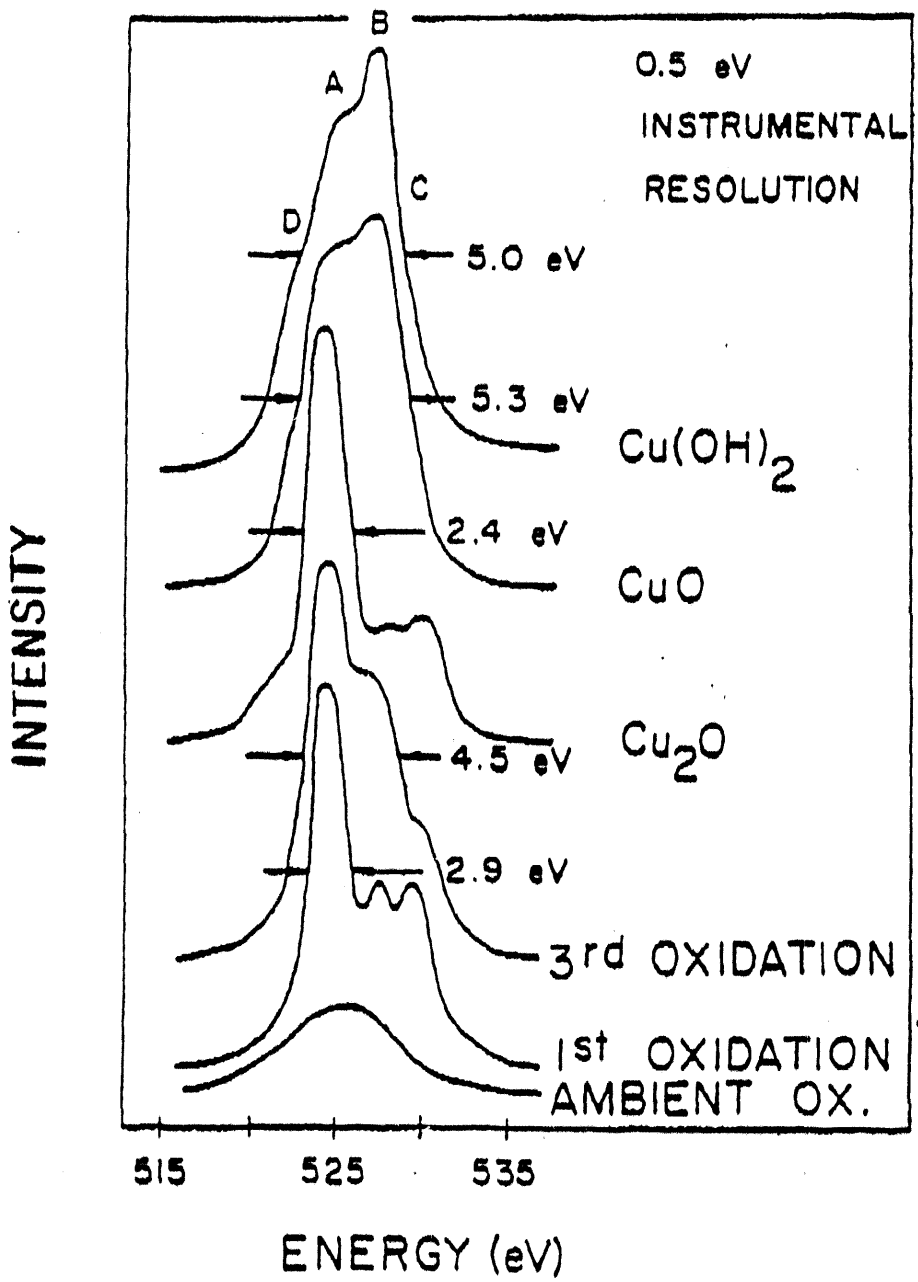

~~Fig. 26~~. O-Kα spectra are shown for pure Cu_2O, CuO, and $Cu(OH)_2$, as well as for some of the surfaces, at various stages of oxidation illustrated in fig. 25.

Figure B-2

APPENDIX C - THIN FILM TECHNOLOGY WITH XES FOR CORROSION STUDIES

The basic idea behind using XES for corrosion studies is relatively straight forward. As shown in Table C-1, it has ben known for some time that the L beta/L alpha inensity ratio for transition metals increases in going from metal to metal oxide. In using variable sample exit technology , that is, in going from about 0,5 degrees to about 20 degrees, as shown in Figure C-1, the spectrometer sees a sample thickness, say about 20 angstroms to about 1000 angstroms respectively. Thus, by plotting the L intensity ratio against exit angle we can obtain an evaluation of oxidation of a surface against sample thickness. A typical set of results is shown in Figure C -2 for nickel surface oxidation using photon excitation. Accordingly, at low exit angles the L intensity ratio shows oxidation even if the oxidation of the surface is minimal.It should be noted that the above plots can be used to get quantitative results (1')

Since 1982 our group has been studying the air oxidation of the following metals: Al, Fe, Ni, Co,and Cr both for bulk metal surfaces as well as for various combination of thin layers of these metals deposited on various substrates. Most of this work was supported by IBM through a Shared University Research Grant program.The work formed the basis of three Master degrees and one PHD thesis.

TABLE C-1

FISCHER'S* Lβ/Lα Data

Metal		Metal Oxide	
Zn	0.33	0.40	ZnO
Cu	0.24	0.27	Cu_2O
		0.38	CuO
Ni	0.24	0.31	NiO
Co	0.22	0.31	Co_3O_4
Fe	0.32	0.56	Fe_2O_3
Mn	0.58	0.72	MnO_2

* 3 KV excitation

D.W. Fischer, J. Appl. Phys. 36, 2048 (1965)

FIGURE C-1
VARIABLE SAMPLE EXIT ANGLE METHOD*

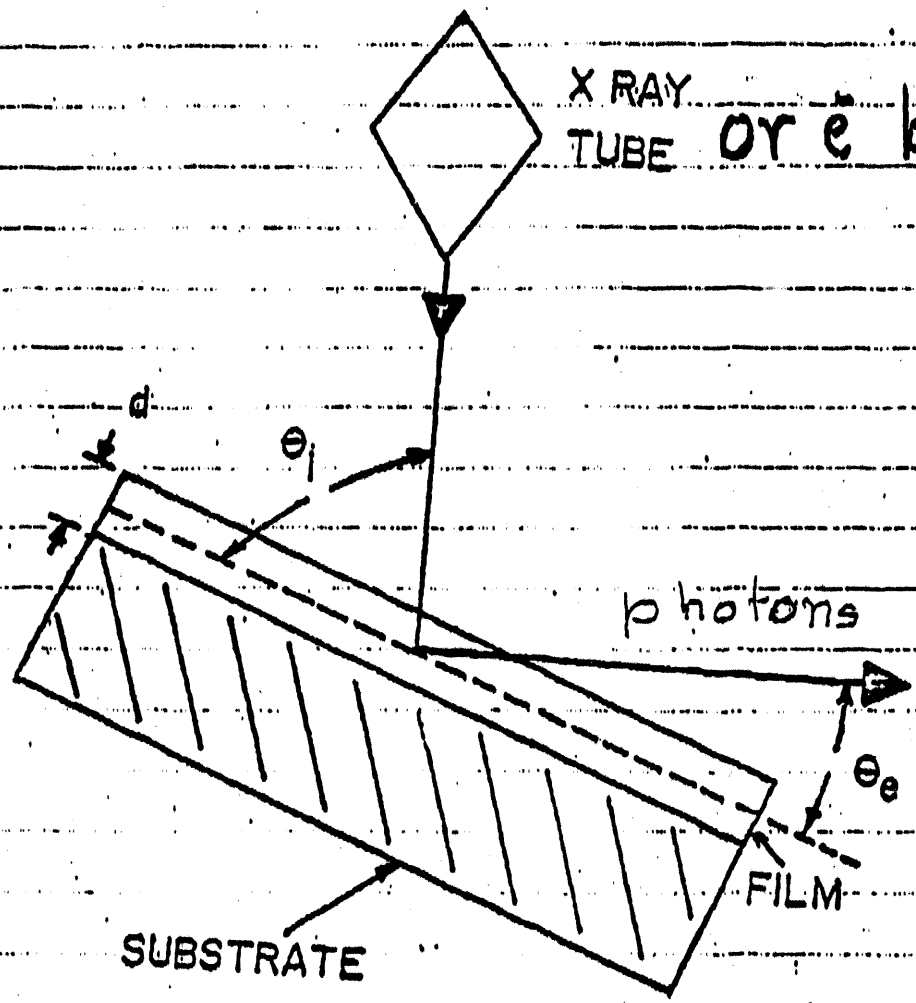

* G. Andermann Appl. Surf. Sci 31, 1-41 (1988)

TECHNOLOGY

-19-

FIGURE C-2

X-Ray Technique May Provide New Way To Study Surfaces, Films

Researchers at University of Hawaii have developed nondestructive approach to obtaining depth profiles of films from 50 to 5000 Å thick

Ward Worthy, C&EN Chicago

Ultrasoft x-ray fluorescence spectroscopy (USXFS) soon may join the list of techniques available for analyses of surfaces and thin films. According to George Andermann, head of the University of Hawaii group that is developing the method, USXFS will provide a new, nondestructive approach to obtaining depth profiles of films from 50 to 5000 Å thick. It promises to be especially useful for dealing with the thin-film problems often encountered in the "real world," he adds.

Principal coworkers on the USXFS project include research associate Francis Fujiwara and graduate students Mark Lawson, Tom Scimeca, and Kevin Kuhn.

Heart of the USXFS system is a 5-meter variable-grazing-incidence-angle grating spectrometer originally built (with National Science Foundation support) for studies of molecular electronic structure. The high-optical-resolution (0.1 eV or better) instrument has been modified to adapt it for surface and thin-film studies—for example, a sample holder was added that is capable of exit angle resolution of 0.05° or better at low exit angles.

Obtaining the needed resolution calls for the use of high-focal-length grating optics (rather than crystal optics), Andermann notes. That makes it essential to use ultrasoft x-rays ($\lambda > 10$ Å), since more energetic x-rays wouldn't be refracted by the grating. However, many of the methods developed for hard ($\lambda < 2$ Å) and soft (2 Å $< \lambda <$ 10 Å) x-ray analysis may be employed. In addition, the Hawaiian chemists are developing a substrate emission technique that promises to be useful for studying the effects of physical and chemical modifications of surfaces.

Explaining the theory behind surface USXFS, Andermann says the key idea is the use of variable-angle sample optics, in particular the use of well-defined exit angles from 20° down to as low as 0.5°. The critical depth, determined by measurements of fluorescence intensity, is a function of the exit angle. That is, as the exit angle becomes smaller, the signal represents a smaller portion of the film's total thickness. By changing the exit angle in small increments, it's possible to monitor changes in intensity at a given wavelength (for elemental analysis) or changes in spectral contours or shifts (for chemical speciation), and thus build up a depth profile of the film being studied.

Andermann notes that characterization of true surfaces—defined to include ultrathin films with thicknesses less than 25 Å—and of surface thin films with thicknesses from 25 to 5000 Å has become an important area of specialization. The problems have been attacked with a number of particle-based techniques, including x-ray photoelectron spectroscopy (XPS), ultraviolet photoelectron spectroscopy (UPS), Auger electron spectroscopy (AES), secondary ion mass spectrometry (SIMS), and ion scattering spectrometry (ISS).

Chemical modifications of thin films change substrate x-ray line ratio

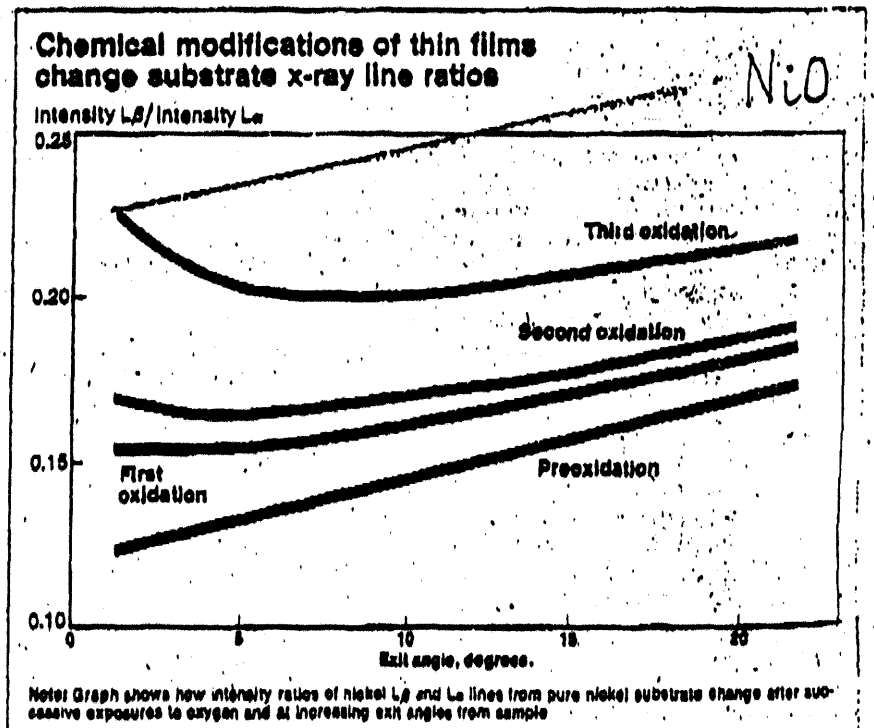

Note: Graph shows how intensity ratios of nickel Lβ and Lα lines from pure nickel substrate change after successive exposures to oxygen and at increasing exit angles from sample

APPENDIX D - ADDITIONAL INFO ON METHANOL INDUCED CORROSION

Using DOE funding Dr. Fujiwara carried out a whole series of experiments to get useful information on methanol induced corrosion of a wide variey of metals, namely, mild steel, pure iron, stainless steel and brass. These materials were exposed to a wide variety of solutions for a wide variety of times. Besides the information already discussed in Section (4), we are forwarding some limited additional information in terms of a series of illustrations (Figures D-1 through 5). There is a wealth of quantitative data incorporated in these figures and the figures are undergoing extensive quantitative evaluation. All of these results will be submitted for publication in the near future.

FIGURE D-1

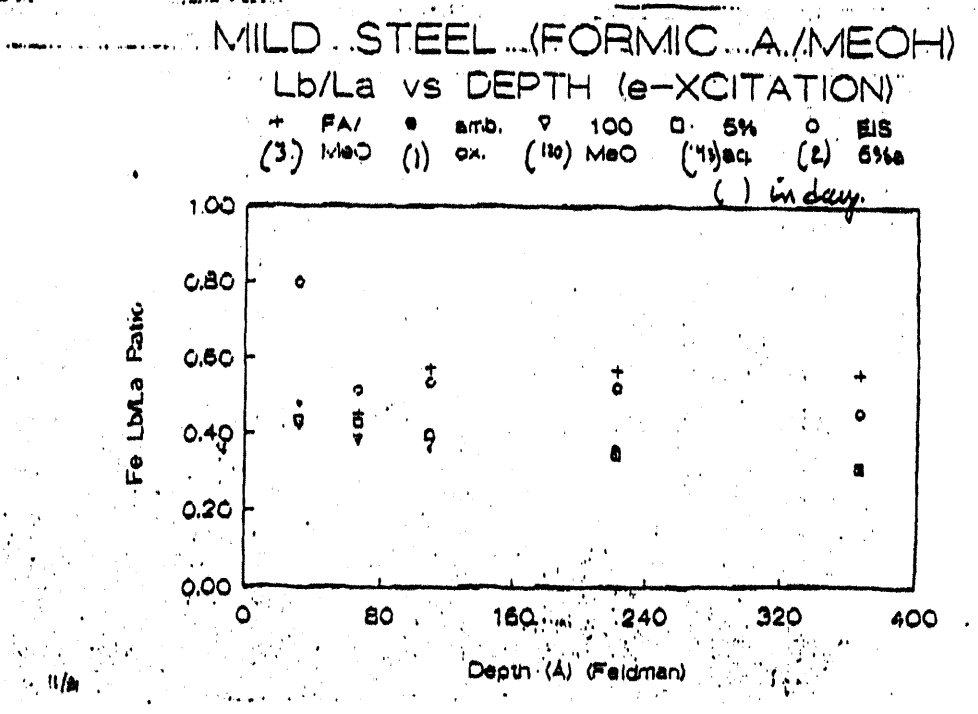

FIGURE D-2

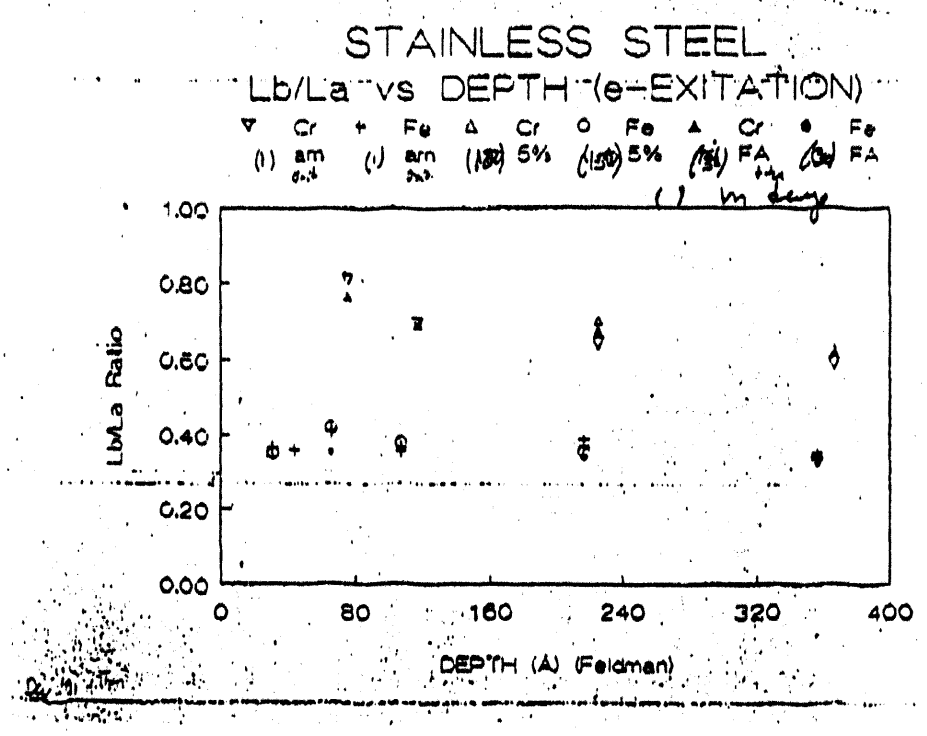

FIGURE D-3

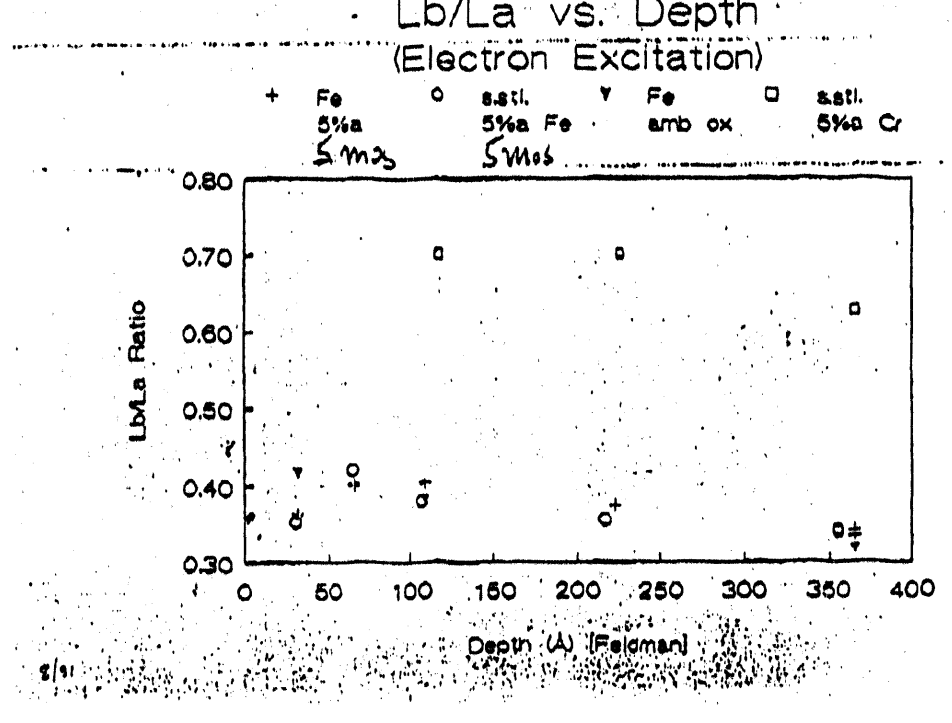

D-4

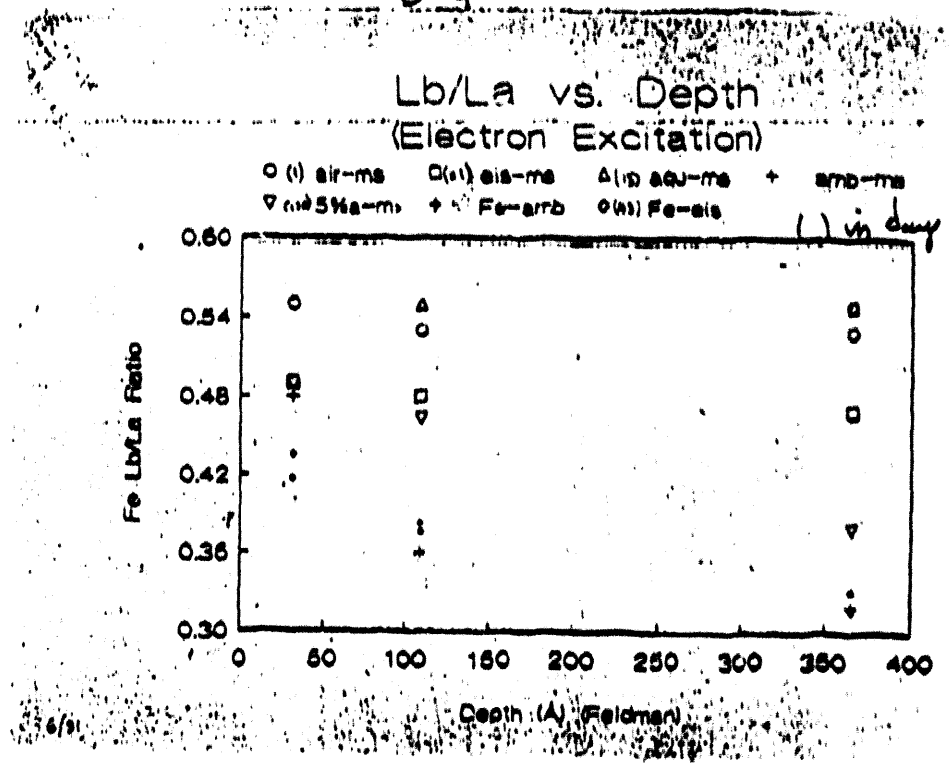
Lb/La vs. Depth
(Electron Excitation)
Fe Lb/La Ratio
0.60
0.54
0.48
0.42
0.36
0.30
0
50
100
150
200
250
300
350
400
Depth (A) (Feldman)

D-5

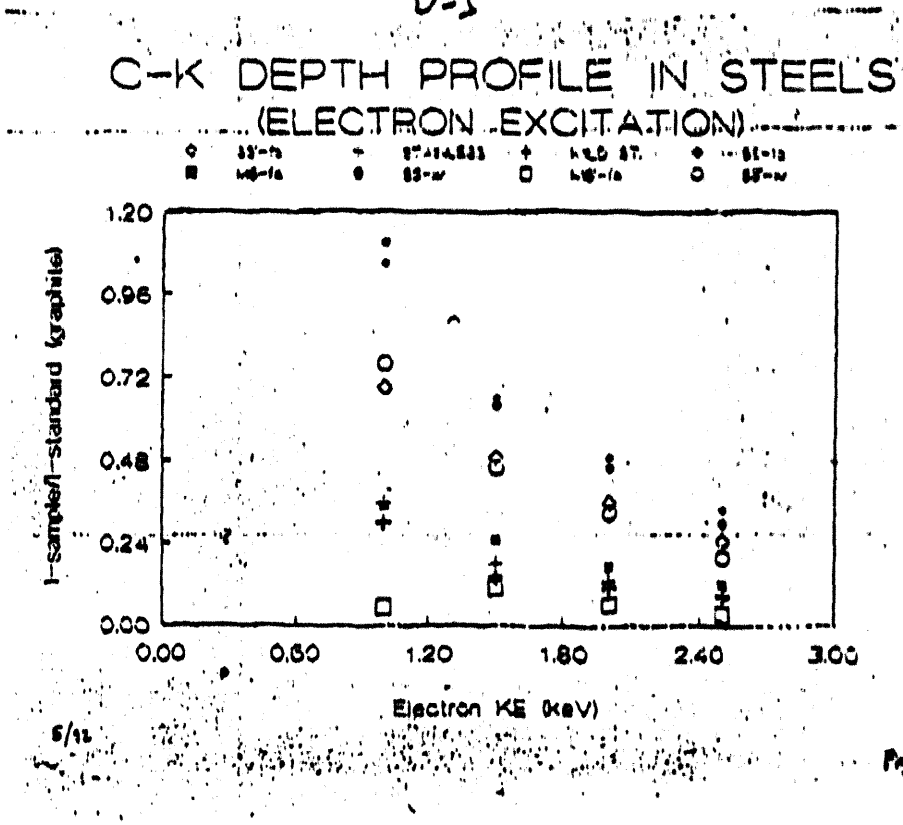
C-K DEPTH PROFILE IN STEELS
(ELECTRON EXCITATION)
I-sample/I-standard (graphite)
1.20
0.96
0.72
0.48
0.24
0.00
0.00
0.60
1.20
1.80
2.40
3.00
Electron KE (keV)

DOE/NREL/ORNL WORKSHOP LOW COST MATERIALS OF CONSTRUCTION FOR BIOLOGICAL PROCESSES
MAY 13, 1993

Electro Chemical Engineering & Manufacturing Co., Background and Capabilities

Dale Heffner
Electro Chemical Engineering & Mfg. Co.
750 Broad St.
Emmaus, PA 18049-0509

ABSTRACT

Information of the background and capabilities of Electro Chemical Engineering & Manufacturing Co. was provided. Acid brick and several types of linings and coatings for steel and concrete were described. A brief discussion of corrosion testing methods was followed by several case studies in which linings technology was applied to solve corrosion problems.

ELECTRO CHEMICAL ENGINEERING & MFG. CO. BACKGROUND AND CAPABILITIES

The original ELECTRO CHEMICAL SUPPLY & ENGINEERING CO. was the first company of its kind in the United States created for the sole purpose of acid and alkali-proof construction and material manufacture. Incorporated in 1912 we have been providing service to the chemical industry for over eighty consecutive years. ELECTRO CHEMICAL personnel were credited with formulating the first silicate and sulphur mortars along with formulation and development of the original DURO fireclay acid-proof brick.

A brief run down of our current capabilities are as follows:

- A complete line of natural and synthetic rubber, PVC, polypropylene, HALAR®, KYNAR®, TEFZEL®, and TEFLON® lining systems for process vessels.

- Custom PVC and polypropylene plastic fabrication of tanks, liners, duct systems, hoods and specialty items.

- Shop applied high temperature, TEFLON®, KYNAR®, TEFZEL®, HALAR®, Bisonite, Plasite, and Heresite coatings.

- Acid-proof brick flooring systems for protection of plant floors which are subjected to corrosive solutions, hard wear, or chemical spills. We also stock standard floor tile, red shale and carbon brick.

- Impervious monolithic corrosion resistant floor toppings exhibiting excellent chemical and physical properties and used when brick and tile installations are not practical. Epoxy, polyester, furan, vinylester and polyurethane toppings are available.

- Corrosion resistant epoxy, neoprene, hypalon, and vinyl industrial paint coatings for protection of structural steel, exteriors of pickling and plating tanks, fume ducts and stacks against corrosive splash, spray or atmosphere.

- Design, build, and certification of complete secondary containment systems.

- Both shop and field experienced technicians to maintain your lined equipment along with shutdown inspection and repair services. Our field technicians normally respond within 24 hours to a repair or service call.

Electro Chemical Engineering & Mfg. Co.
Post Office Box 509, 750 Broad Street
Emmaus, Pennsylvania 18049-0509
Telephone: (215) 965-9061 Fax: (215) 965-2595

Sketch shows a typical steel nozzle lined with membrane and protected from thermal and mechanical damage by installing a stoneware or carbon sleeve. Note that the membrane protects the full face of the flange and indicates recommended recess for sleeve. Detail would apply for any type membrane or brick being used. Service conditions would dictate type of membrane, brick and mortar to be used. Where high temperatures are encountered, additional layers of brick are used and nozzle necks are protected with either a double sleeve or can be brick lined. Also note on picture to the right that a bullseye or compression ring may be installed around pipe sleeves depending on vessel design and construction.

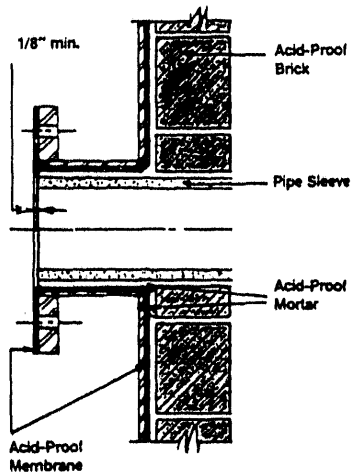

Picture and sketch show a typical acid-proof construction for protecting a concrete lined tank. Sketch is recommended regardless of type of membrane, brick and mortar being used. Service conditions would determine choice and thickness of lining system. Depending on size of concrete tank, it is suggested that the walls be battered and bowed when poured. As a last resort, brick pilasters can be installed to reinforce or strengthen long and deep walls that have been constructed without the batter and bow mentioned earlier. It is good practice to cap the top of any concrete tank wall.

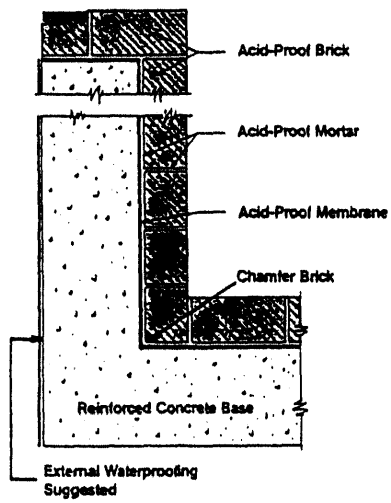

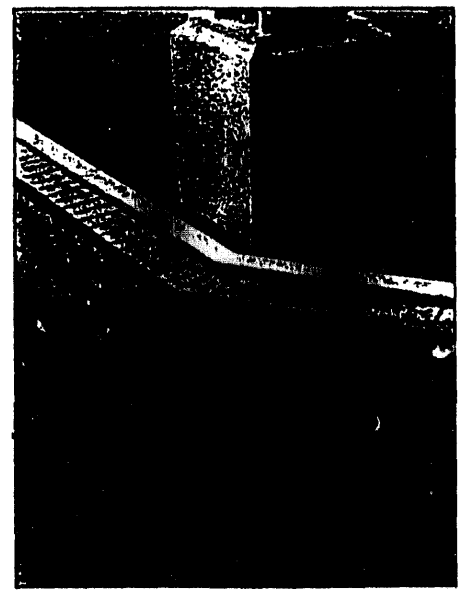

Design and fabrication is very critical to the performance of brick lined steel tanks. Suitable bottom dunnage such as steel I-Beams are suggested to prevent the bottom from oil canning when emptied and filled. To reinforce the side walls, vertical steel stiffeners should be installed on the same centerline as the I-Beams. Steel angles or channels are required to adequately reinforce the tank tops. Type and thickness of membrane, brick and mortar would depend on service conditions. Where mechanical damage could occur, wood bumper boards are recommended to protect the top of the tank.

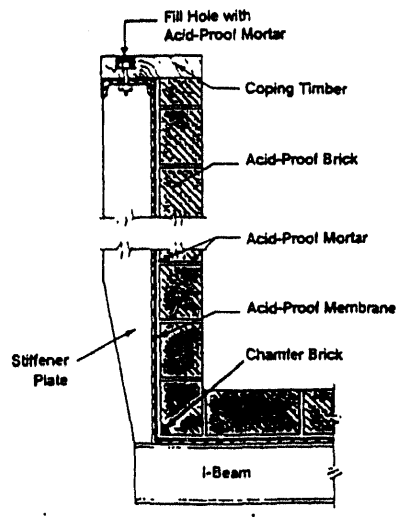

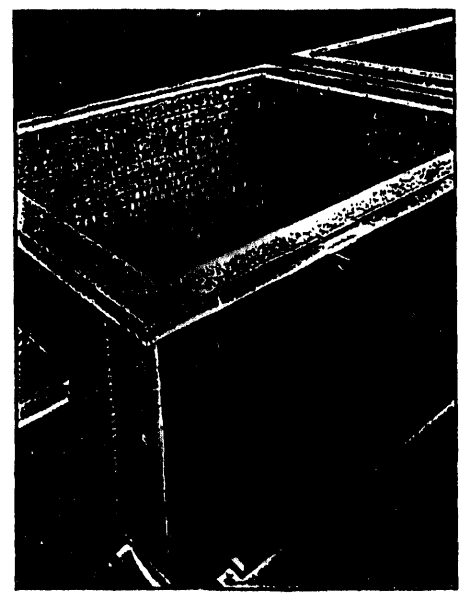

This 100'×50', 9 cell Phosphoric Acid Attack Tank is constructed of concrete and lined with our 3/16" thick EL-CHEM DURO-BOND natural rubber latex and 4-1/2" of carbon brick laid with EL-CHEM #11 carbon filled furan resin mortar. Ceilings are protected with EL-CHEM #103 coal tar epoxy coating. Note that walls of this 27' high attack tank are battered and bowed. Additional carbon brick thickness was installed beneath all agitators to protect the main floor from abrasion.
Flash cooler vessels above attack tank were rubber lined and protected with 4-1/2" carbon brick lining laid using EL-CHEM #11 carbon filled furan resin mortar.

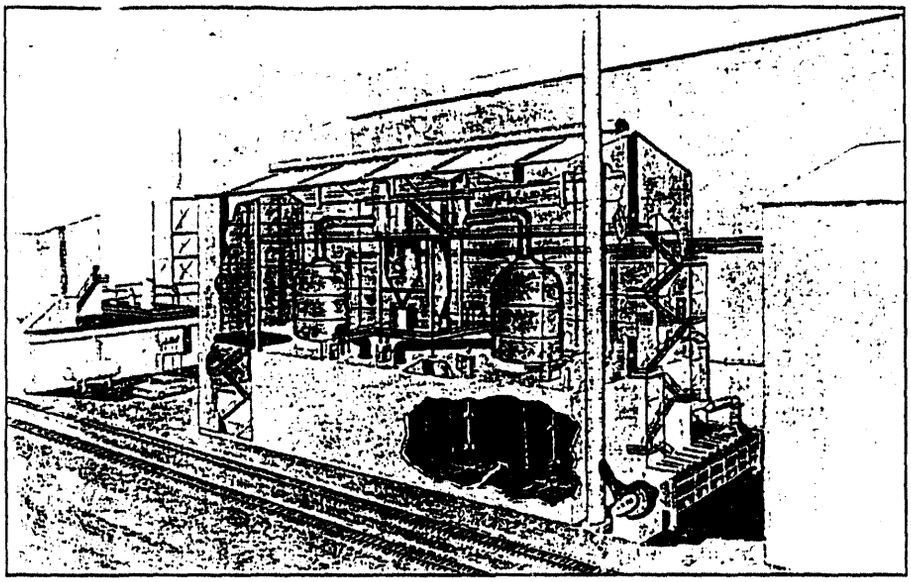

These pictures taken during the construction of a sulfuric acid plant project show the actual installation of the brick support walls in an absorbing and drying tower. These tanks were lined with a chemical resistant mastic and a TEFLON* sheet overlay prior to installing the red shale acid-proof brick lining.

*TM of DuPont Co.

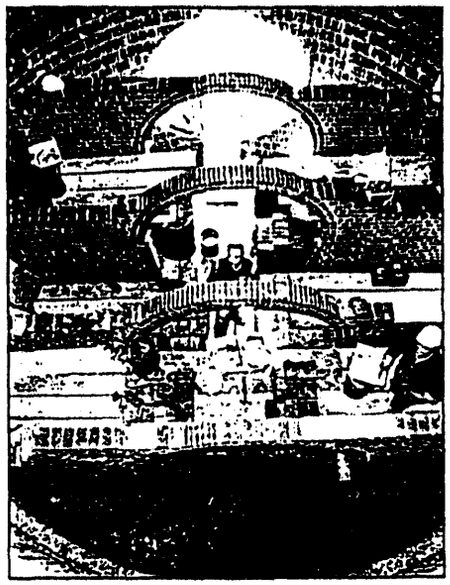

Tank pictured at right was lined with 3/16" thick EL-CHEM DURO-BOND S-103 soft natural rubber sheet and 3-3/4" red shale acid-proof brick. Solid acid-proof brick compressions rings or bullseyes were installed around all outlets located in the vertical shell. Stoneware sleeves were installed in each of the eleven outlets located in the cone bottom of the tank. Note special brick shapes that were installed to support internal piping.

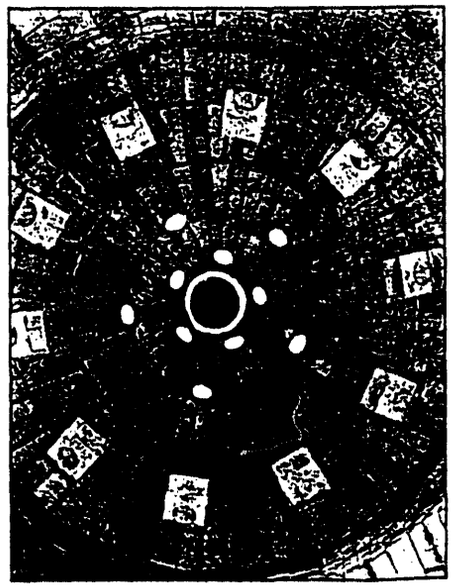

Floors, trenches, pump and equipment pads in this chemical and dyeing operation were protected with KEMSEAL glass cloth reinforced asphalt membrane and red shale acid-proof brick lining. EL-CHEM #555 expansion joints were installed in this construction. EL-CHEM #501 machinery grout was used to set some of the equipment. EL-CHEM epoxy toppings were also used to protect the vertical face of some equipment pads.

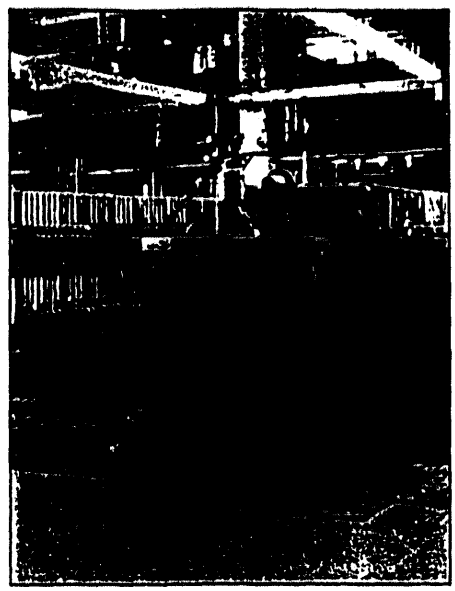

Sketch and picture show an octagon concrete pad that is located in a pretreatment operation that handled acid, alkalies, oxidizers and numerous solvents. Concrete pads and floors were acid washed and overlayed with our EL-CHEM #11 specially formulated furan membrane which is reinforced with EL-CHEM #225 glass cloth. Membrane was then covered with a Hypalon* coating to provide a separatory layer between the furan membrane and acid-proof brick sheathing. Brick lining was installed using vinylester mortar.

*TM of DuPont Co.

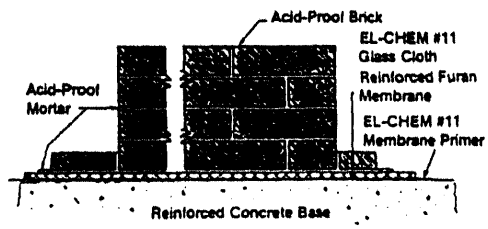

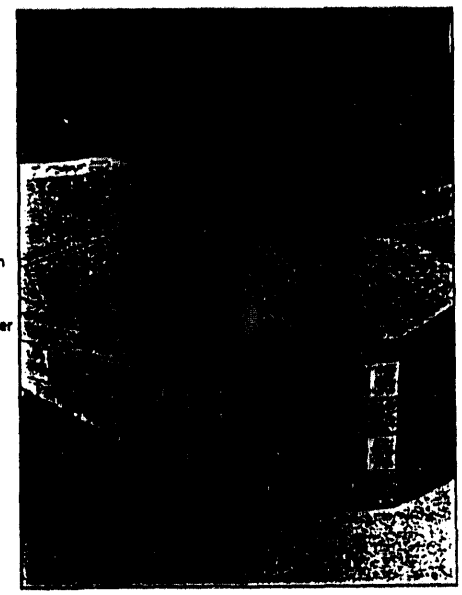

These pictures show the construction phase and completion of a large metering pit. A 3/8" thick KEMSEAL membrane with two layers of EL-CHEM #223 glass cloth is being applied to the walls and floor of the right side pit compartment. The walls of this pit were both battered and bowed. As indicated on the picture, individual compartment walls were also poured with both battered construction, and thrust block notches. Note when brick were installed on compartment partitions how alternating courses are interlocked. EL-CHEM #555 expansion joints were incorporated into this design.

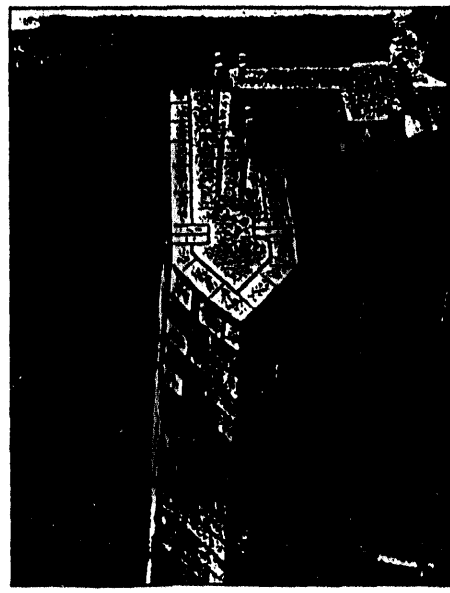

Sketch and picture show a typical acid-proof lining of a concrete drainage trench. Trench is lined with a 1/4" thick KEMSEAL glass cloth reinforced asphalt membrane and a 2-1/4" layer of red shale acid-proof brick. Concrete trench floors should be sloped for drainage purposes at a minimum of 1/4" per foot.
Actual design and thickness of brick lining for trenches is determined by service conditions and size of trench. Picture of trench at far right shows a small portion of a trench from a phosphoric acid plant project which involved nearly a mile of different types and designs of drainage trenches.

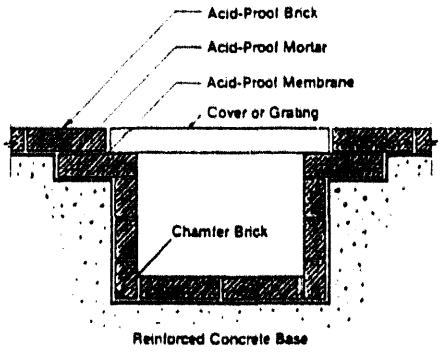

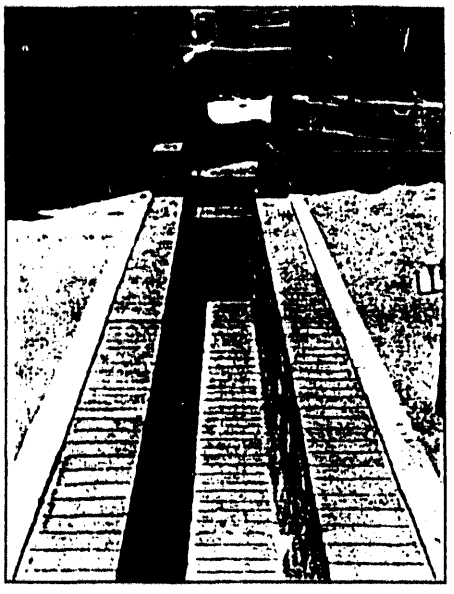

Sketch and picture to the right show a typical floor for a dairy, brewery, pharmaceutical, packing house or other food type floor. Different type bed joint materials are available. The end use is the determining factor for the type tile or floor brick to be used. Tile or floor brick are waxed beforehand to prevent unwanted mortar stains and excess mortar from detracting from the cosmetic appearance of the finished floor.

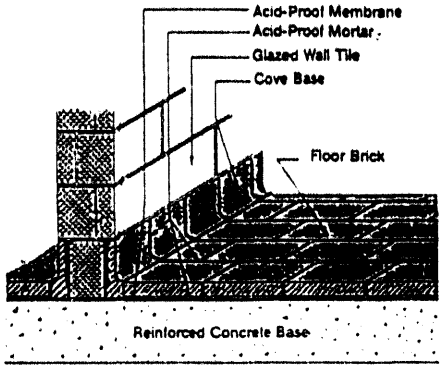

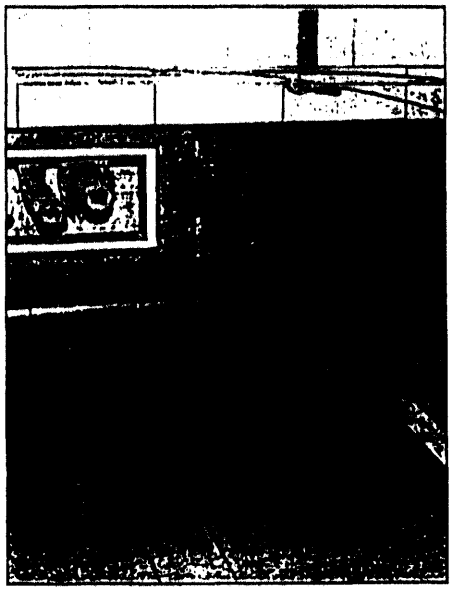

Sketch and picture show similar floors with different type curbs. Both floors were protected with 1/4" thick KEMSEAL glass cloth reinforced asphalt membrane and different thicknesses of red shale floor brick. EL-CHEM #555 expansion joints are visible on the floor, far right, which was part of an uranium recovery project.

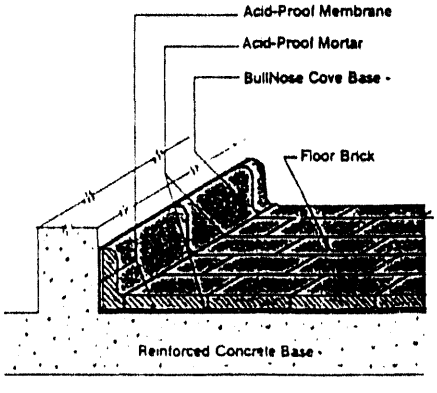

Acid-Proof Brick Types & Sizes

Standard Red Shale Acid Proof Brick

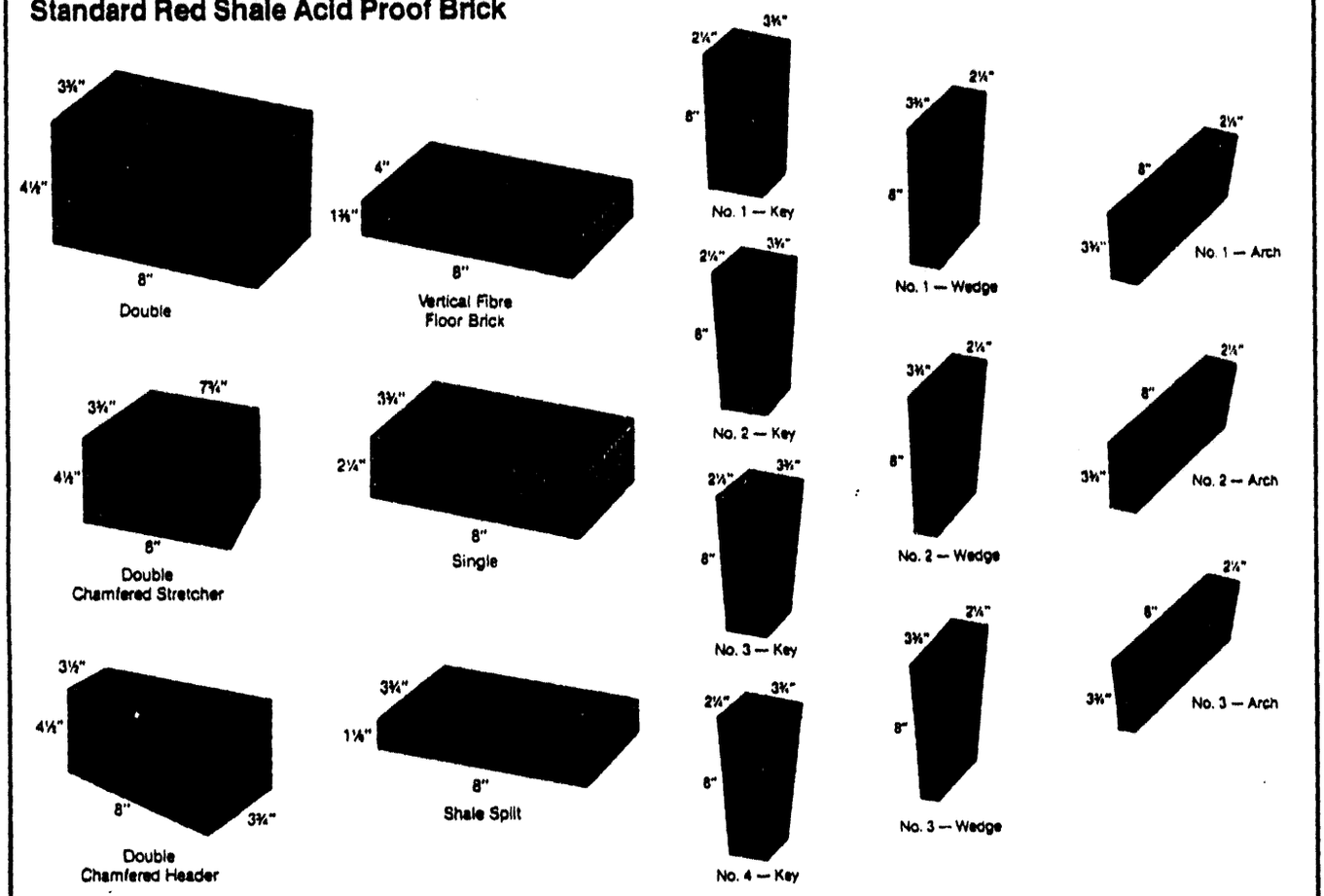

Standard Acid-Proof Fire Clay and Carbon Brick

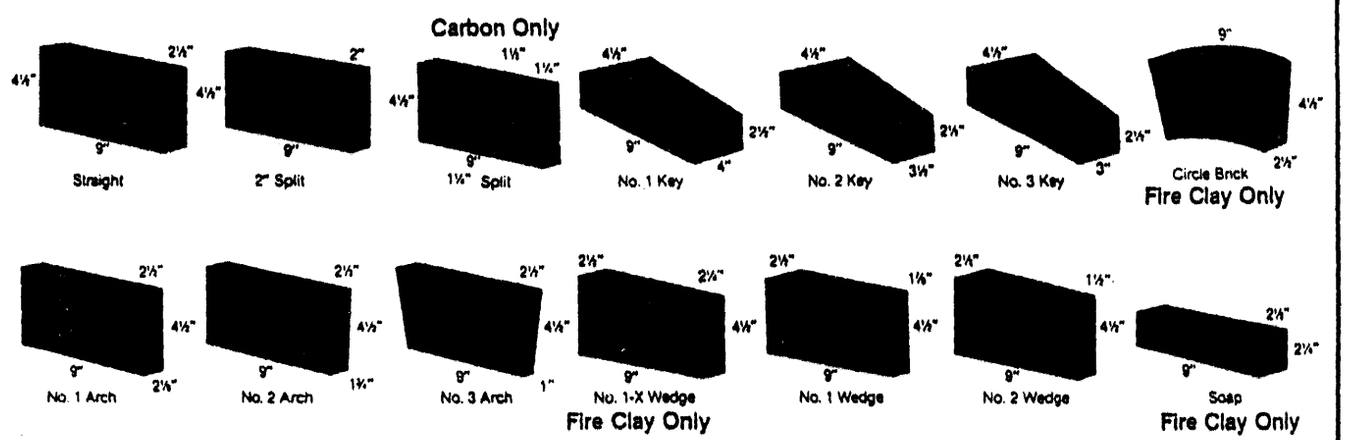

3" Thick Series Is Also Available

Acid-Proof Heavy Duty Floor Brick

Matching Trim Units 1-3/16" or 1-3/8" Thick

Turn-Up Base

#1T Turn Up Base

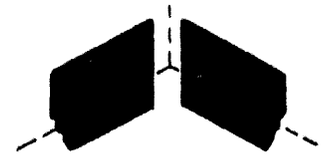

#2T Internal Corner*

*Shipped in pairs (mitred)

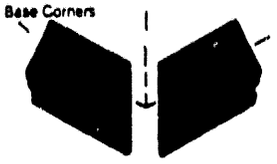

#3T External Corner

Square Top Cove Base

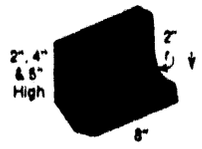

#1 Cove Base

#2 R. or L. Cove Stop

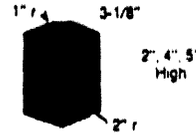

#3 Cove Internal Corner

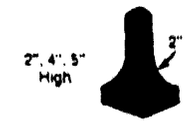

#4 Cove External Corner

Round Top Cove Base

#R1 Cove Base

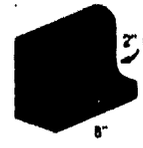

#R2 R. or L. Cove Stop

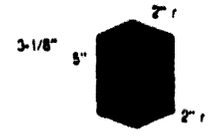

#R3 Cove Internal Corner

#R4 Cove External Corner

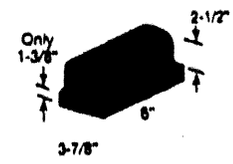

Double Cove Curb

Bull Nose Stretcher and Header

#5 Cove Internal Corner

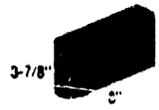

#6 BullNose

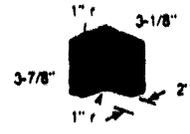

#7 BullNose Internal Round Corner

#8 BullNose Stretcher

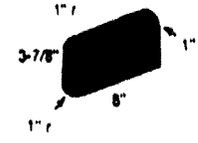

#9 R. or L. BullNose Out Angle

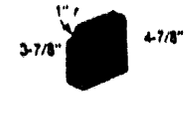

#10 BullNose Internal

Floor Brick 1", 1-3/16" or 1-3/8" Thick

Smooth

Diamond Tread Smooth

Abrasive Surface

1-3/16" or 1-1/8" Thick Vertical Fibre

Conversion Chart

To Convert From	To	Multiply By
Meter	Feet	3.281
Feet	Meter	0.3048
Centimeters	Inches	0.3937
Inches	Centimeters	2.540
Liter	Gallons	0.2642
Gallons	Liters	3.785
Pounds	Grams	453.6
Grams	Ounces	0.03527
Ounces	Grams	28.35
Metric Ton	Pounds	2205
Kilogram	Pounds	2.2046
Cu. Cm.	Cu. Inch	6.102×10^{-2}
Cu. Ft.	Cu. Meters	0.02832
Cu. Inch	Cu. Cm	16.39
Cu. Meters	Cu. Ft.	35.31
Kg/Sq. M.	Pounds/Sq. Ft.	0.2048
Pounds/Sq. Ft.	Kg/Sq. M.	4.8824
Kg/Cu. M.	Pounds/Cu. Ft.	0.06243
Pounds/Cu. Ft.	Kg/Cu. M.	16.02

Brick Estimating Factors

Quantity of brick required for 100 sq. ft.

Size	Thickness	⅛" Joints	¼" Joints
8" x 3¾" x 2¼"	2¼"	458	437
8" x 3¾" x 2¼"	3¾"	747	699
8" x 3¾" x 4½"	4½"	458	437
8" x 3¾" x 4½"	3¾"	384	368
8" x 3¾" x 8"	8"	768	736
9" x 4½" x 2½"	2½"	342	328
9" x 4½" x 2½"	4½"	602	767
9" x 4½" x 2½"	7"	944	895
9" x 4½" x 2½"	9"	1204	1134
9" x 4½" x 3"	3"	342	328
9" x 4½" x 3"	4½"	505	479
9" x 4½" x 3"	7½"	847	807
9" x 4½" x 3"	9"	1010	958
9" x 4½" x 1¼"	1¼	342	328
9" x 4½" x 1½"	1½"	342	328
8" x 3⅞" x 1⅜"	1⅜"	444	424
8" x 4" x 1⅜"	1⅜"	430	411

Thermal Insulation Data

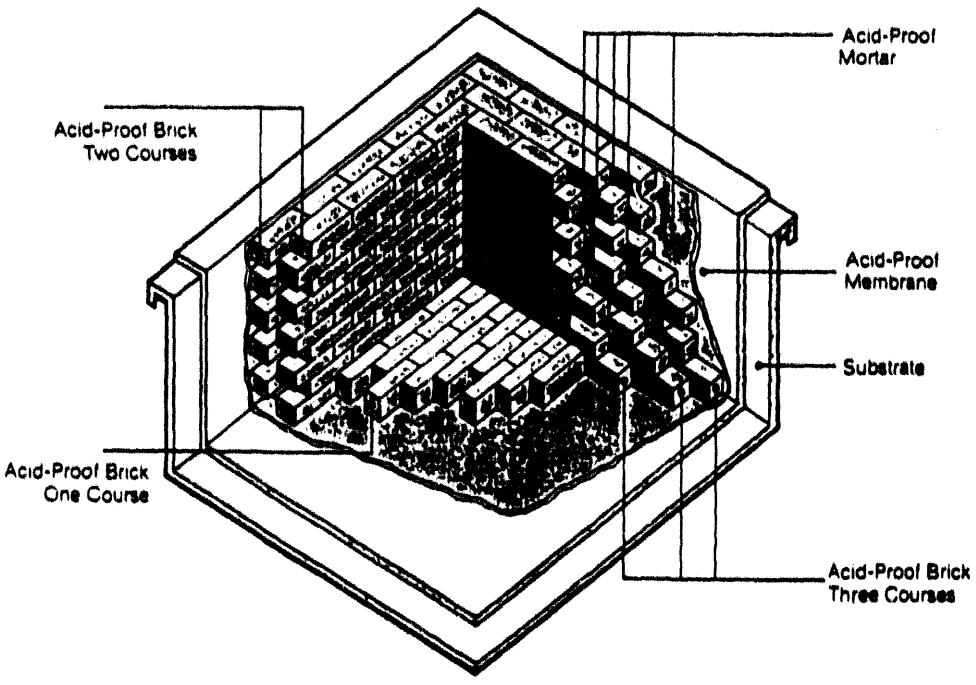

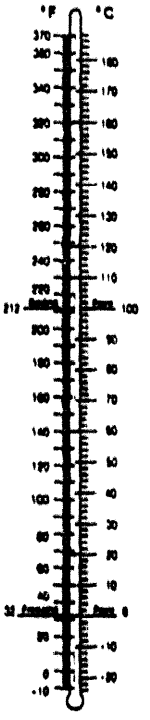

Example of membrane and brick lined tank showing approximate temperature reduction provided by 1, 2 or 3 courses, each 3¾" thick, red shale acid-proof brick lining. Since carbon and fire clay brick have different thermal conductivities, the graphs should not be used to calculate temperature changes for these types of brick.

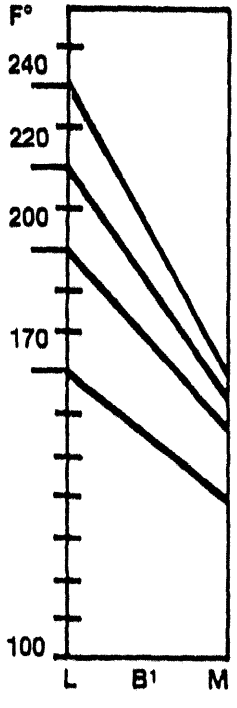

One Course Brick

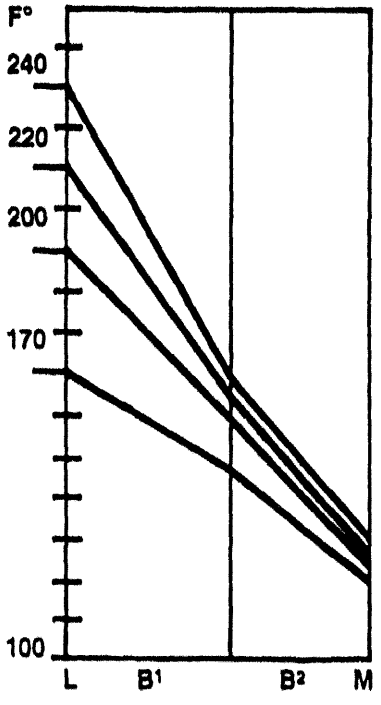

Two Courses Brick

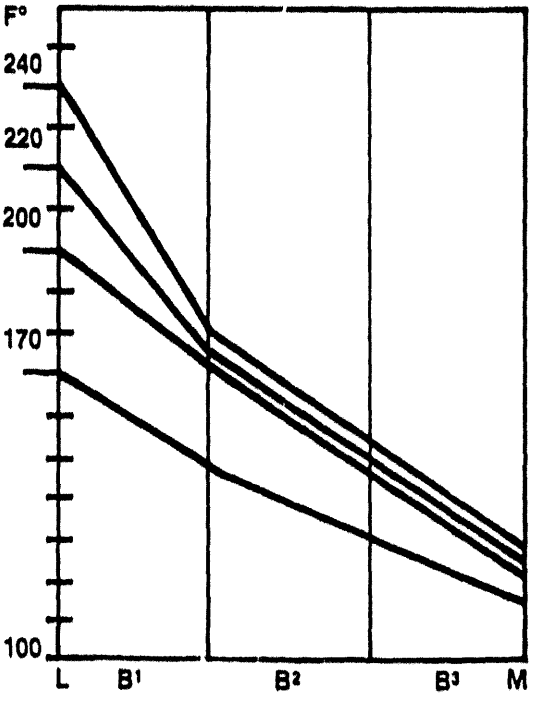

Three Courses Brick

B^1=first layer brick B^2=second layer brick B^3=third layer brick L=liquid M=membrane

CASE HISTORY 01-15-92

Electro CHEM

ENGINEERING & MFG. CO.

oper selection of materials to line concrete drains, trenches, sumps and basins critical to the success of any chemical plants corrosion control and environmental ograms. Tightening regulations on both occupational hazards and on waste id environmental control are creating a need for reliable engineered systems id experienced, well-qualified fabricators to install a complete project with idivided responsibilities.

ie key to finding an economical, long lasting concrete protective liner, suitable r immersion service and able to endure the most corrosive environments is found Acroline® protective liner systems of polyethylene, polypropylene, PVDF id E-CTFE.

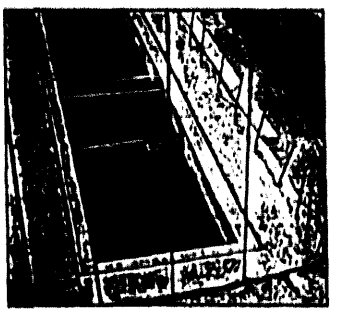

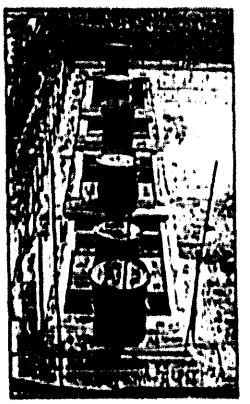

Polypropylene concrete protective sump liner being embedded into concrete.

Unique anchoring system.

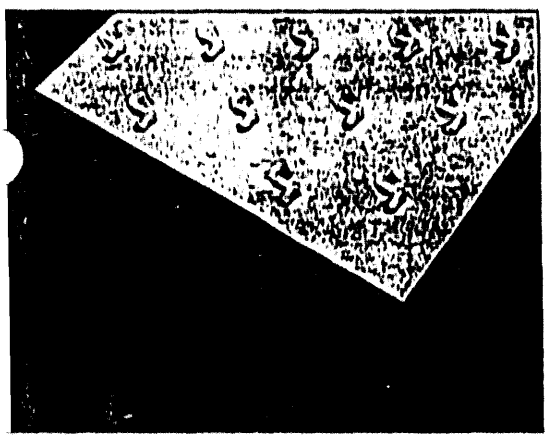

Cross-sectional view of liner joined with monolithic topping.

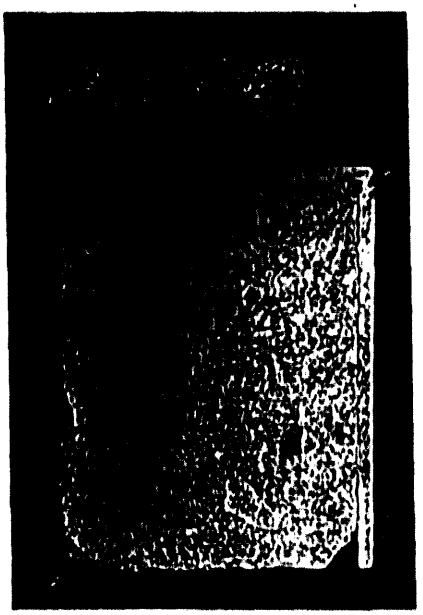

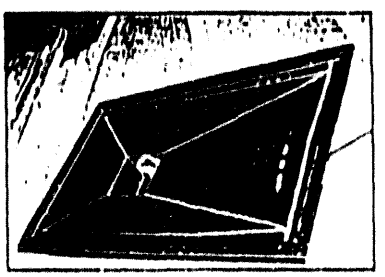

Custom fabricated sump and drain perform dual function as the form for concrete and as a chemical resistant liner.

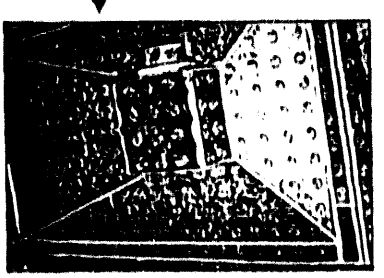

ie Acroline® material can be custom fabricated almost any conceivable shape and size, for wide range of chemical applications. The iique feature of the Acroline® material is at the anchoring points, used to embed the ier directly into the concrete and compensate r thermal cycling, are formed in their final ape during the extrusion process and are not olded or glued in place. The large number anchors, 420 per square meter, guarantees e best possible anchorage between the ncrete and the protective liner.

ELECTRO CHEMICAL ENGINEERING & MFG. CO. INC., is offering a full capability of custom plastic fabrication in all Acroline® materials. ELECTRO CHEMICAL's strength includes the ability to handle turnkey projects (design, fabricate, and install) from the smallest sump to large field installations.

FOR ADDITIONAL INFORMATION CALL:

ELECTRO CHEMICAL ENGINEERING AND MFG. CO.
750 Broad St., P.O. Box 509 Emmaus, PA 18049-0399
(215) 965-9061 Fax: (215) 965-2595

EL-CHEM CONSTRUCTION CO. LTD
937 Cumberland Ave., Box 354, Burlington, Ontario, Canada L7R 3Y3
(416) 634-5586 Fax: (416) 639-8088

CASE HISTORY 12.15.09

ELECTRO CHEM

ENGINEERING & MFG. CO.

After 24 years of continuous service the concrete flooring in a major chemical manufacturer's production area, underneath storage and reaction vessels, had become severely eroded in many areas. The area in addition to being subject to wash water from the equipment also experienced occasional spills of materials with a wide variety of pH ranges.

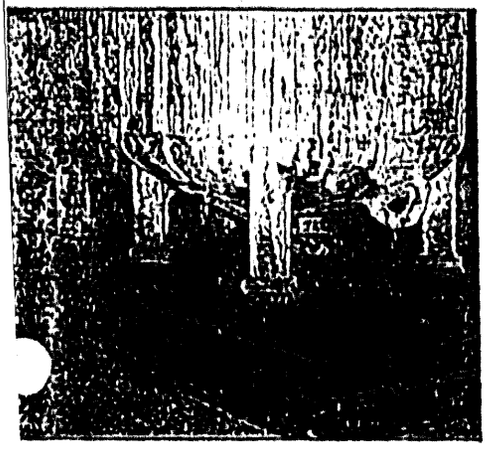

Various coatings were applied to the floor to protect it from the harsh and corrosive products, but with little success. Damage to the coating resulting from spills and washing procedures had created a series of problem areas, which had to be continuously patched. To add to this, when equipment and tanks were washed out, the material being drained created a somewhat hazardous, slippery condition for walking in the area. Maintenance involved in repairing the floor had become increasingly expensive and time-consuming.

Acid-proof chemically resistant brick was used to refurbish the floor area. The first step in the replacement process involved clearing the area and removing the old floor. New concrete was poured and allowed to cure. A coat of EL-CHEM asphalt primer was then applied to the concrete surfaces followed by an EL-CHEM Kemseal Asphalt Membrane. In this system, asphalt impregnated glass cloth is placed over a 1/8" asphalt base and then followed by another layer of 1/8" thick hot asphalt.

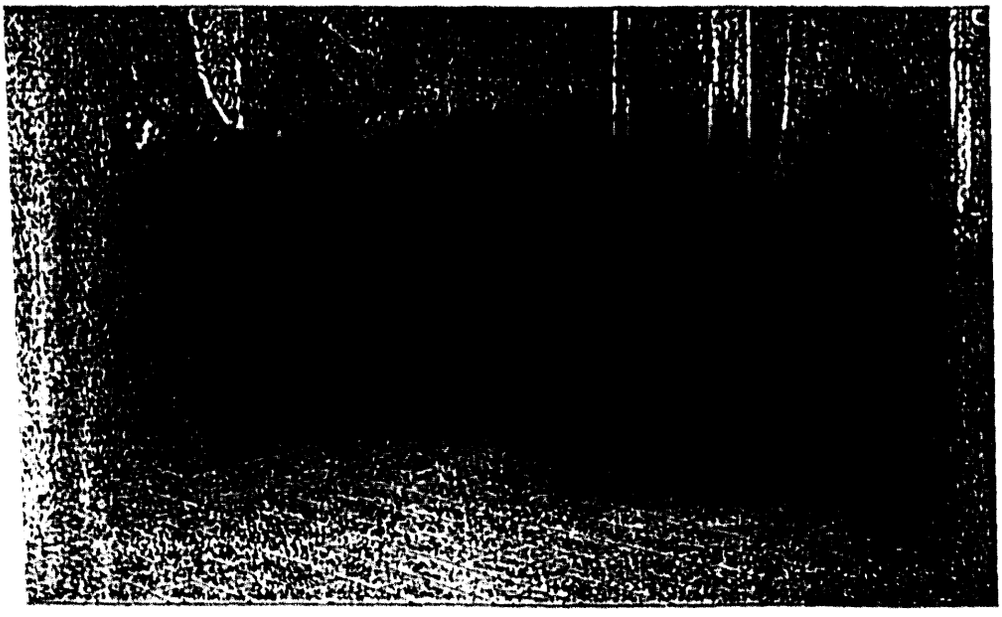

Acid-proof brick was installed by experienced EL-CHEM field crews using EL-CHEM #11 carbon-filled furan mortar. This mortar is inert to all oxidizng acids, except nitric and chromic, all alkalis regardless of concentration, all fats, oils, grease and most organic solvents.

Installation was completed and production was resumed almost immediately after the work had been completed. While safety hazards have been eliminated, the customer has also significantly reduced maintenance headaches. The new flooring is successfully withstanding the corrosive environment. A similarly lined sump, that contains runoff and spills until being pumped out and transferred into the waste treatment system has also proven to be virtually maintenance-free.

FOR ADDITIONAL INFORMATION CALL:

ELECTRO CHEMICAL ENGINEERING AND MFG. CO.
750 Broad St., P.O. Box 509, Emmaus, PA 18049-0399
(215) 965-9061 Fax: (215) 965-2595

EL-CHEM CONSTRUCTION CO. LTD
937 Cumberland Ave., Box 354, Burlington, Ontario, Canada L7R 3Y3
(416) 634-5586 Fax: (416) 639-8088

CASE HISTORY 03.27.90

Electro CHEM ENGINEERING & MFG. CO.

Many different protective linings have been used to try and combat the hot, corrosive, abrasive and erosive conditions found in Flue Gas Desulfurization (FGD) systems used at coal fired power generating plants.

Exposed to service conditions of SO_2 with H_2O vapors and sulfuric acid mist at a normal operating temperature of 165 Deg. F., the 64" x 97" off gas blower housing had been previously lined with various rubber lining systems including a chlorobutyl lining. The fan housing which is tied into the gas recovery system is located outdoors and operates continuously. Service life of the rubber and other elastomeric materials was approximately one (1) year.

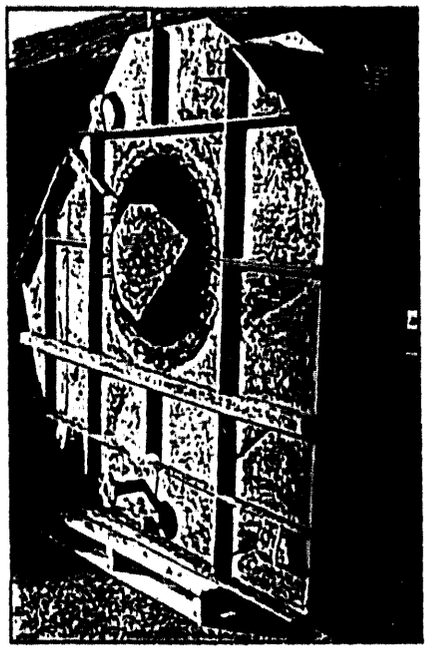

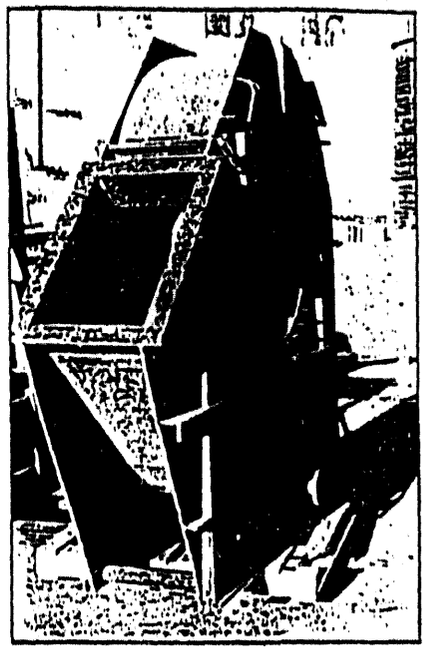

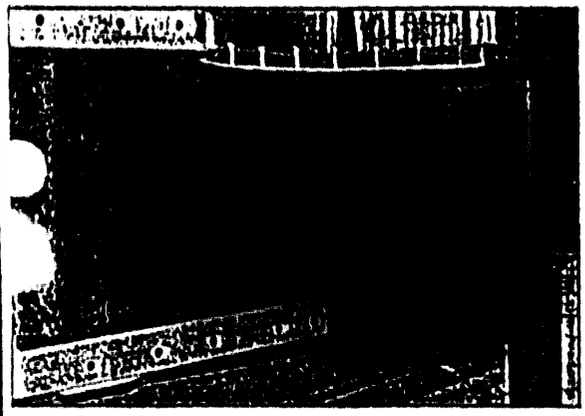

The customer reports that "They have at least doubled and possibly tripled the service life of the blower units".

Electro Chemical stripped the old rubber lining from the internal areas of the fan housing, performed steel repairs and applied a 40 mil EL-CHEM 711 WL Kynar® laminate lining. The protective liner is formed from multiple spray applied layers of Kynar® dispersion and one or more layers of woven cloth reinforcing.

The resultant 711 WL Kynar® laminate lining is mechanically strong, is serviceable over a broad temperature range (– 80 Deg. through 275 Deg. F.), and shows superior resistance to the corrosive chemical environment encountered in the FGD units.

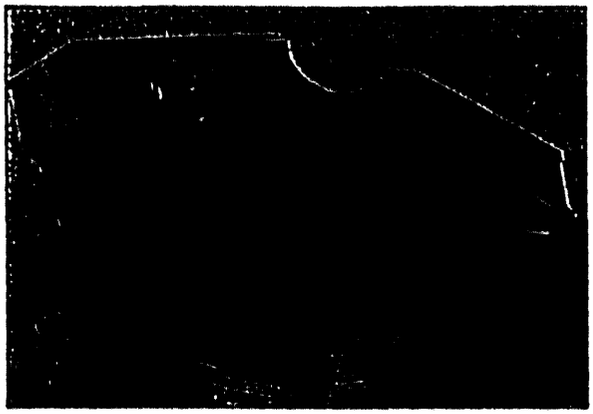

FOR ADDITIONAL INFORMATION CALL:

ELECTRO CHEMICAL ENGINEERING AND MFG. CO.
750 Broad St., P.O. Box 509, Emmaus, PA 18049-0399
(215) 965-9061 Fax: (215) 965-2595

EL-CHEM CONSTRUCTION CO. LTD
937 Cumberland Ave., Box 354, Burlington, Ontario, Canada L7R 3Y3
(416) 634-5586 Fax: (416) 639-8088

CASE HISTORY 05.01.90

Electro CHEM

ENGINEERING & MFG. CO.

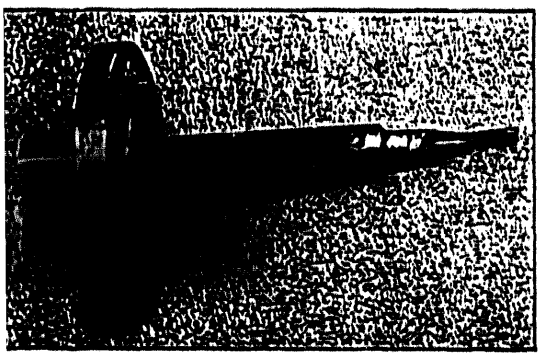

A major chemical manufacturer produces chlorine and caustic by the electrolysis of brine solution in an electrolytic cell. The electrolysis is conducted at a temperature of 180-200 Deg. F., and produces chlorine, caustic, and hydrogen. The processes used are diaphragm, mercury, or membrane cell technology.

The cell conditions of high temperature and high humidity along with the brine, caustic and chlorine represents a highly corrosive environment. Metals in the cell are rapidly attacked by the corrosive media. The corrosion of the metal components such as stainless steel thermowells results in contamination of the brine and caustic. The corrosion also results in leaks and resulting unplanned down time for emergency repairs. Environmental and worker safety requirements necessitate that these leaks be eliminated by cost effective, reliable means.

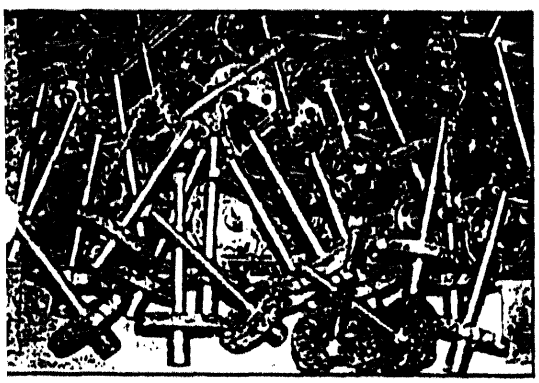

Electro Chemical applies a high performance Halar® dispersion coating system to the complex geometric shaped thermowells. The system is comprised of a specially formulated primer, intermediate and top coats for severe corrosion protection. These dispersions are organosols of Halar® E-CTFE powder dispersed in latent solvents. When the dispersions are spray-applied to a properly prepared metal substrate and oven baked at temperatures in the range of 450 Deg. F., to 500 Deg. F., the solvented particles coalesce to form a tough corrosion resistant Halar® film.

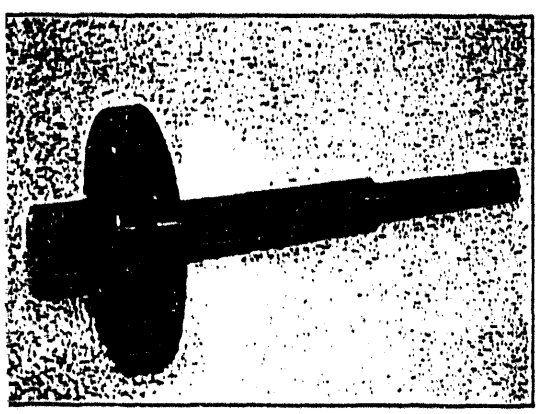

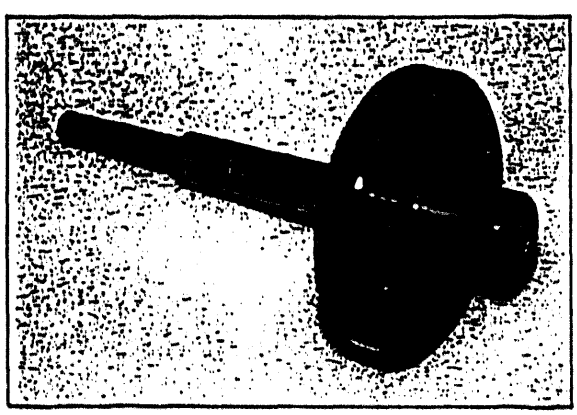

The resultant Halar® coated thermowells are significantly outlasting and out performing the 316 stainless steel thermowells used previously in the manufacture of chlorine and caustic.

FOR ADDITIONAL INFORMATION CALL:

ELECTRO CHEMICAL ENGINEERING AND MFG. CO.
750 Broad St., P.O. Box 509, Emmaus, PA 18049-0399
(215) 965-9061 Fax: (215) 965-2395

EL-CHEM CONSTRUCTION CO. LTD
937 Cumberland Ave., Box 354, Burlington, Ontario, Canada L7R 3Y3
(416) 634-5586 Fax: (416) 639-8088

CASE HISTORY 01.03.90

Electro CHEM

ENGINEERING & MFG. CO.

A manufacturer of high-purity sulfuric acid used as a cleaning solution by several large producers of semiconductor devices required a lined tank container for international shipments and long shipments within the U.S. The lining material would have to be resistant to 98% sulfuric acid and most importantly maintain the stringent purity requirements needed by the semiconductor industry.

The used 68" I.D. x 198" straight side "tank container" had been previously coated internally with another manufacturers spray applied system which had failed to prevent contamination of the load. In the case of semiconductor grade 98% sulfuric acid you cannot have even the minutest iron pickup. The chosen lining system would not only have to be acid resistant, but also not impose capacity restrictions because of it's weight, and be extremely resistant to both the thermal and mechanical shock associated with the container transportation.

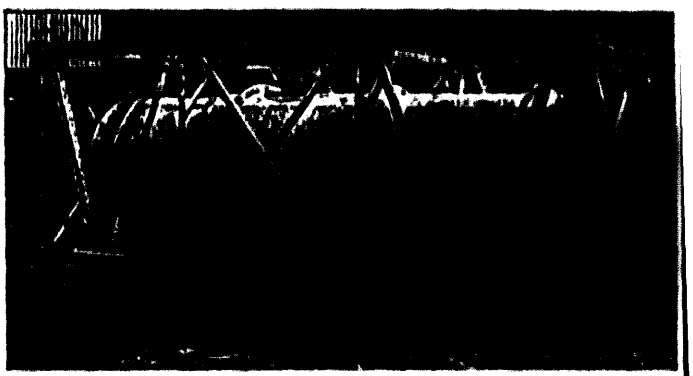

ELECTRO CHEMICAL forces stripped the internal areas of the container, neutralized the carbon steel substrate and grit blasted the surface to white metal. All internal areas of the container were then lined with a 60 mil thick EL-CHEM DURO-BOND E-CTFE knit glass backed HALAR® sheet lining. The lining was carried through all nozzles and out over all flange faces. All seams were welded using a hot gas process which incorporates a 1/8" diameter HALAR® weld rod and HALAR® cap strip. All internal areas were inspected and tested using a dielectric spark tester adjusted to 10,000 volts AC to guarantee that the lining was pinhole free. External areas of the container and framework were sandblasted, primed and painted with a paint system formulated to provide weather resistance and exterior durability.

The resultant DURO-BOND E-CTFE HALAR® lining has been successfully preserving the purity of the product - with no fillers or plasticizers to leach out and contaminate the service - it has proved to be an excellent choice for handling of high purity corrosive chemicals.

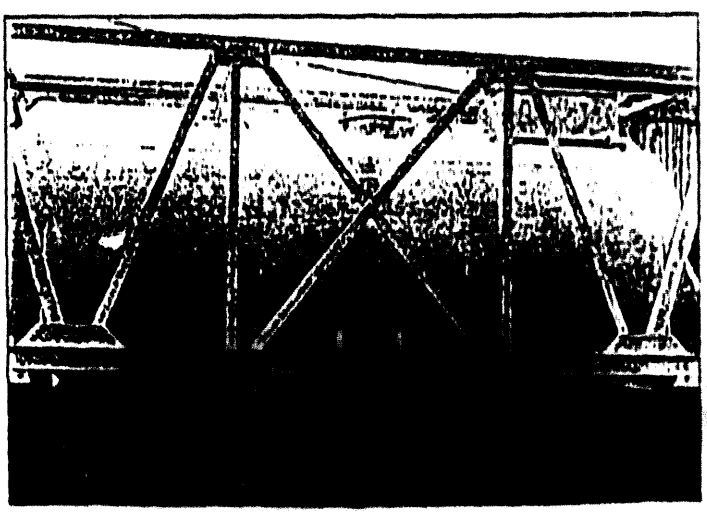

FOR ADDITIONAL INFORMATION CALL:

ELECTRO CHEMICAL ENGINEERING AND MFG. CO.
750 Broad St., P.O. Box 509, Emmaus, PA 18049-0399
(215) 965-9061 Fax: (215) 965-2595

EL-CHEM CONSTRUCTION CO. LTD
937 Cumberland Ave., Box 354, Burlington, Ontario, Canada L7R 3Y3
(416) 634-5586 Fax: (416) 639-8088

DOE/NREL/ORNL WORKSHOP LOW COST MATERIALS OF CONSTRUCTION FOR BIOLOGICAL PROCESSES
MAY 13, 1993

Chemical-Resistant Non-Metallic Materials of Construction for Biomass-to-Ethanol Process

Norman Huxley
Elf Atochem North America, Inc.
3 Park Way, Room 807
Philadelphia, PA 19102

ABSTRACT

A brief overview of Elf Atochem was given followed by a discussion of non-metallic chemical-resistant materials. Different types of linings, membranes and mortars were described along with the design considerations and construction methodology involved in using lining materials. The methodology for determining the thermal gradient across a lined vessel was also presented.

Additional information on the Elf Atochem Company can be found in the Appendix.

DOE/NREL/ORNL WORKSHOP

LOW COST MATERIALS OF CONSTRUCTION FOR BIOLOGICAL PROCESSES

15th SYMPOSIUM ON BIOTECHNOLOGY
FOR FUELS AND CHEMICALS

Thursday, May 13, 1993
Colorado Springs, CO

"Chemical-Resistant Non-Metallic Materials of Construction for Biomass-to-Ethanol Processes"

Norman Huxley, P.Eng.
Technical Manager - Sales
Corrosion Engineering Dept.
Elf Atochem North America, Inc.
Philadelphia, PA 19102

elf atochem
ATO

"Non-Metallic Chemical-Resistant Materials

Of Construction Are Unique Products

Used For Solving Unique Problems"

Chemical-Resistant Membrane And Masonry Lining Construction

- Support Structure

  Concrete, Steel

- Membrane

  Primary Protection To The Support Structure From Chemical Attack Which May Permeate Through The Porosity Or Cracks In The Masonry Construction.

- Masonry

  Chemical-Resistant Construction Units (Brick or Tile) Installed With Chemical-Resistant Mortar To Provide

  - Thermal Insulation
  - Physical/Mechanical Protection
  - Limits Chemical Environment Reaching The Membrane

Membranes

- Metals
  - Lead, Stainless Steel, Nickel Based Alloy Cladding
- Thermoset Resinous Systems
  - Baked Phenolics
  - Fiberglass Mat Reinforced Resin Linings
  - Glass Flake Filled Resin Linings
- Elastomers
  - Natural Rubber
  - Butyl Rubber
  - Chlorobutyl Rubber
  - Hypalon
  - Neoprene
  - Urethane Asphalt
  - Asphalt
- Plastics
  - Plasticized PVC
  - HDPE
  - HDPP
  - PVDF (KYNAR®)
  - E-CTFE (HALAR®)
  - TFE (TEFLON®)

  ] Fluoropolymers

Masonry

Brick/Tile

- Chemical-Resistant Masonry Units
  ASTM C279
- Chemical-Resistant Carbon Brick
  ASTM C1160

Mortars

- Chemical-Resistant Resin Mortars ASTM C395. (Furan, Epoxy, Phenolic, Vinyl Ester, Polyester).
- Chemical-Setting Silicate and Silica Chemical-Resistant Mortars ASTM C466. (Sodium Silicate, Potassium Silicate, Silica).
- Chemical-Resistant Sulfur Mortar ASTM C287.

Design Considerations

- The Support Structure Must Be Dimensionally Stable and Sufficiently Rigid to Support All Loads; Liquid Tight; and Hydro Tested Before Lining. Pressure Vessel Design Shall Be In Accordance With The Latest ASME Boiler And Pressure Vessel Code.

- Lining Materials Must Possess Suitable Physical, Thermal, and Chemical-Resistance Properties For The Design And Operating Exposures Called For In The Specifications.

- A Heat Transfer Profile Shall Be Calculated For Any Proposed Lining System To Ensure A Satisfactory Design.

- A Stress Analysis Of Any Proposed Lining System Shall Be Performed To Ensure A Satisfactory Design.

CHEMICAL-RESISTANT MEMBRANE AND MASONRY LINING CONSTRUCTION

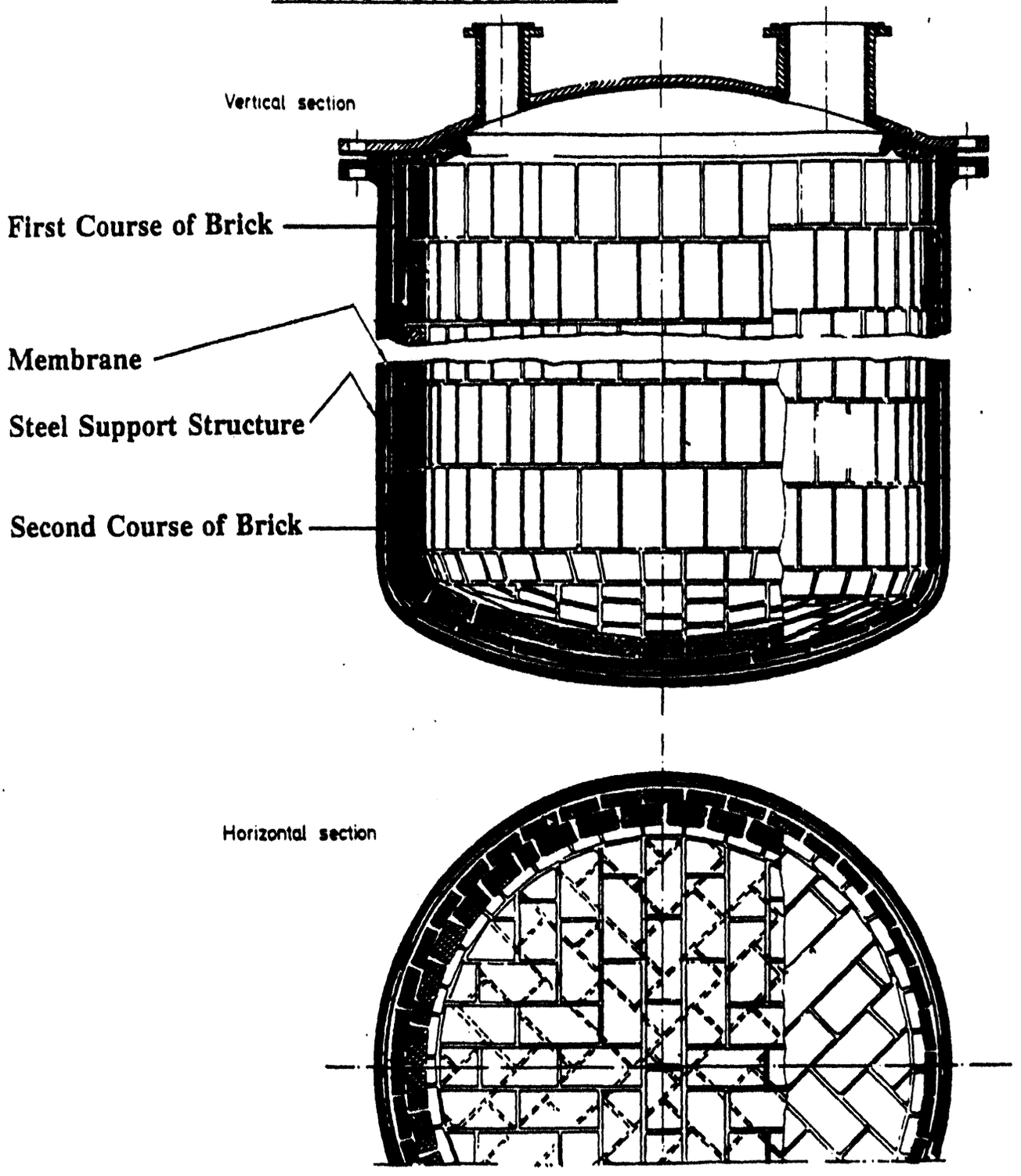

CHEMICAL - RESISTANT MEMBRANE AND MASONRY LINING CONSTRUCTION

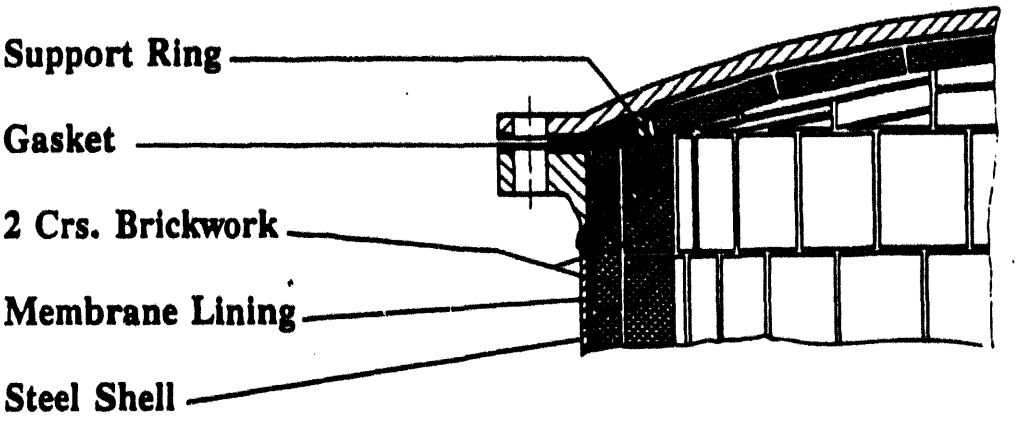

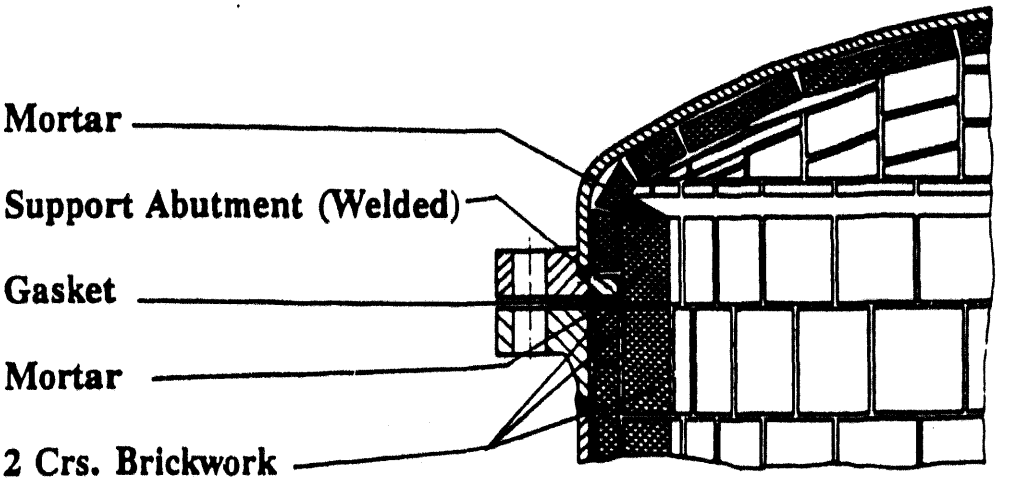

THERMAL GRADIENT ACROSS A CHEMICAL-RESISTANT MEMBRANE AND MASONRY LINED VESSEL

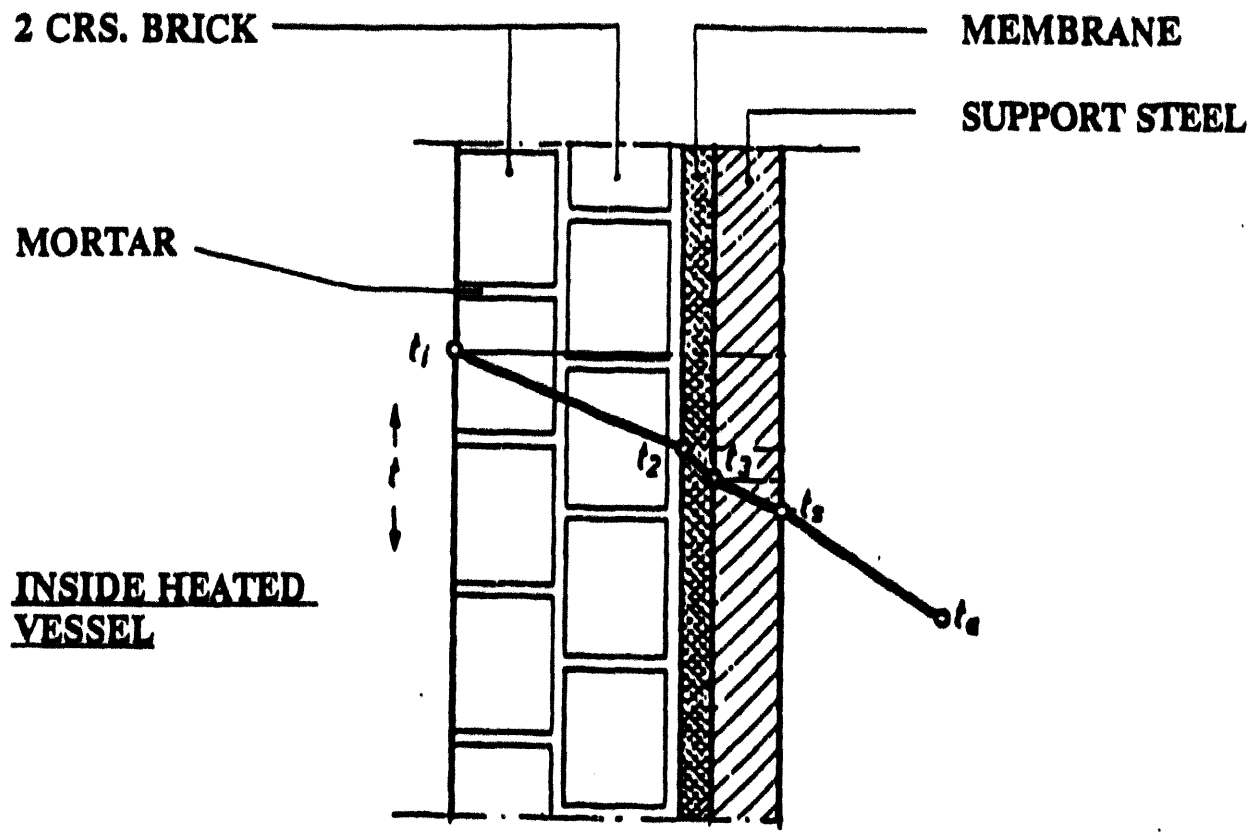

t_1 = Hot Face Surface Temperature of Brick
t_2 = Hot Face Surface Temperature of Membrane
t_3 = Cold Face Surface Temperature of Membrane
t_4 = Cold Face Surface Temperature of the Steel
t_a = Ambient Air Temperature

Other Non-Metallic Chemical-Resistant Materials of Construction

- Polymer Concretes
- Polymer Structural Grouts
- Thermoplastic Sheet Liners Anchored Into Concrete
- Resinous Flake Filled Coatings/Linings 12 Mils - 80 Mils
- Resinous Laminates Using Reinforcing Mats and Veils 125 Mils - 375 Mils
- Resinous Monolithic Floor Linings 250 Mils - 375 Mils
- Foamed Borosilicate Glass Acid Resistant Insulation
- Acid Resistant Potassium Silicate Formulations Applied By Dry Shotcrete Methods

Other Areas Requiring Protection From Chemical Exposures

- Waste Sewers And Trenches
- Sumps
- Secondary Containment
- Support Bases For Chemical Pumps
- Stacks
- Ducts Conveying Chemical Fumes Or Combustion Gases
- Concrete Floor Protection
- Structural Steel

WORK SESSION TOPICS

DOE/NREL/ORNL WORKSHOP LOW COST MATERIALS OF CONSTRUCTION FOR BIOLOGICAL PROCESSES

MAY 13, 1993

Standards for Biomass from ASTM Committee E-48 on Biotechnology

Larry Eitel
Wolder Engineers/Constructors
Denver West, Bldg. 4
1536 Cole Blvd.
Golden, CO 80401

ABSTRACT

The following information on the ASTM Committee E-48 on Biotechnology was presented to the National Renewable Energy Laboratory Workshop participants on May 13 to increase their understanding of standard test methods, practices and guidelines available for consideration in the biomass related fields being applied by NREL. E-48 has subcommittees for Biomass Conversion, environmental issues, biological fermentation and process control, materials of construction, biological species identification/characterization, biological materials preservation, process validation, and terminology. Cooperation between the NREL and ASTM standards development is encouraged since E-48 is chartered by ASTM to develop standards for this industry in coordination with academia, industry, consumers, general interests and producers.

CONFERENCE REPORT

WORKSHOP ON MATERIALS OF CONSTRUCTION FOR BIOMASS: STANDARDS FOR BIOMASS FROM ASTM COMMITTEE E-48 ON BIOTECHNOLOGY

Colorado Springs, CO May 13, 1993

Report Prepared by:
G. Larry Eitel
Chairman, ASTM E-48

The following information on the ASTM Committee E-48 on Biotechnology was presented to the National Renewable Energy Laboratory Workshop participants on May 13 to increase their understanding of standard test methods, practices and guidelines available for consideration in the biomass related fields being applied by NREL. E-48 has subcommitttees for Biomass Conversion, environmental issues, biological fermentation and process control, materials of construction, biological species identification/characterization, biological materials preservation, process validation, and terminology. Cooperation between the NREL and ASTM standards development is encouraged since E-48 is chartered by ASTM to develop standards for this industry in coordination with academia, industry, consumers, general interests and producers.

1. Overview of ASTM E-48

The American Society for Testing and Materials (ASTM) has produced standards for the past 90 years for testing a variety of materials including metals, plastics, water and many other industrial products. In 1985 ASTM responded to private and government interests to establish a committee to develop standards for the biotechnology industry. The number of U. S. biotechnology companies grew rapidly from about 100 in 1970 to over 1300 in 1992. The availability of standard methods for the industry to use fell behind this development curve and most major biotechnology firms prepared their own procedures for testing in a fragmented approach to using standard procedures.

In 1985 the organizational meeting of ASTM Committee E-48 on Biotechnology was held to prepare for developing voluntary, consensus approved standards. These standards include test methods, guides, practices, specifications, terminology and classifications. In 1990, the Biomass Conversion Subcommittee was transferred from the E-44 Solar Energy Committee, where it had originated in about 1981, to E-48 where it was more appropriate since it produced standards on converting grains and cellulostics to alcohols and fuel gas by biological ond other processes.

Six technical subcommittees are in place to develop standards in the following categories of interest:

Materials for biotechnology	Characterization of biolological species
Processes and their controls	Environmental issues
Biomass conversion	Validation and qualification of processes/facilities

Other subcommittees scopes include terminology, executive leadership and symposuim activities.

E-48 standards development include resources from international organizations such as from Japan and Europe. Over 100 scientists, engineers and biotechnology experienced personnel contribute their time to prepare and review new standards as well as review existing standards on a four year cycle.

The process ASTM uses to develop these standards is very thorough and is accomplished using voluntary consensus methods. The subcommittee drafts and ballots the draft version of a new standard. Not only must 60% of the subcommittee respond, but every negative vote or substantive comment must be resolved before the proposed standard can progress to the next level of review. Next, the Main Committee then the full ASTM Society ballots the new standard which reaches over 30,000 members from all industries and interests. After a final review by internal ASTM committees the new standard is published.

2. Where Is E-48 Heading Today?

Today, the E-48 Committee has developed over 30- standards in the above categories. About 26 new standards are being developed now. In the area of validation alone, there are over 100 potential standard practices and protocols that need to be developed for biotechnology activities to assist the industry to meet FDA and other agencies regulations. E-48 Committee is looking for volunteers to assist in this important process.

As stated in the attached purpose of E-48, the committee is promoting the knowledge and development of voluntary standards for biotechnology. Close coordination is maintained with other ASTM committees with related but not overlapping scopes of interest in biotechnology. Contact with other professional and technical organizations such as ASME, PMA, ABC, etc., provide coordination opportunities to avoid duplication of effort and focus on developing standards that are really needed by this industry. Members of E-48 also come from the Federal Agencies such as NIST, EPA, USDA, FDA, DOE and others.

The primary goal for 1993 is to increase participation by ASTM members and non-members to develop the high priority standards needed by this industry. It is intresting to note that although individuals assisting to prepare standards in E-48 are encouraged to join ASTM, they are not required to do so. However, voting rights, information mailing and officer assignments require membership.

The most effective standards can only be prepared by the best qualified persons on the topic from industry, academia and government. E-48 is seeking these volunteers to assist preparation of new standards in biotechnology to assist in this most important activity. By close linkage between E-48 and the industry members, we can provide the needed standards for the rapid explosion of activity in the biotechnology field.

ASTM COMMITTEE E-48

ON BIOTECHNOLOGY

E-48 COMMITTEE ON BIOTECHNOLOGY

PURPOSE

- Promotion of knowledge and the development of voluntary standards for biotechnology

- Coordinate work with other ASTM committees and organizations having mutual interests

NATURE OF VOLUNTARY STANDARDS

- Standards are developed by committees with balanced membership using consensus process
- Standards are documents of convenience
- Approved by majority of subcommittee, main committee and society ballot with 60% of ballots returned, 2/3 to 9/10 affirmative vote and all negative votes considered with no persuasive negatives
- Reviewed by Society Committee On Standards to assure correct procedures were followed
- Voluntary use in industry as documents of convenience unless mandated in regulations or contract

E-48 COMMITTEE MEMBERSHIP BALANCE

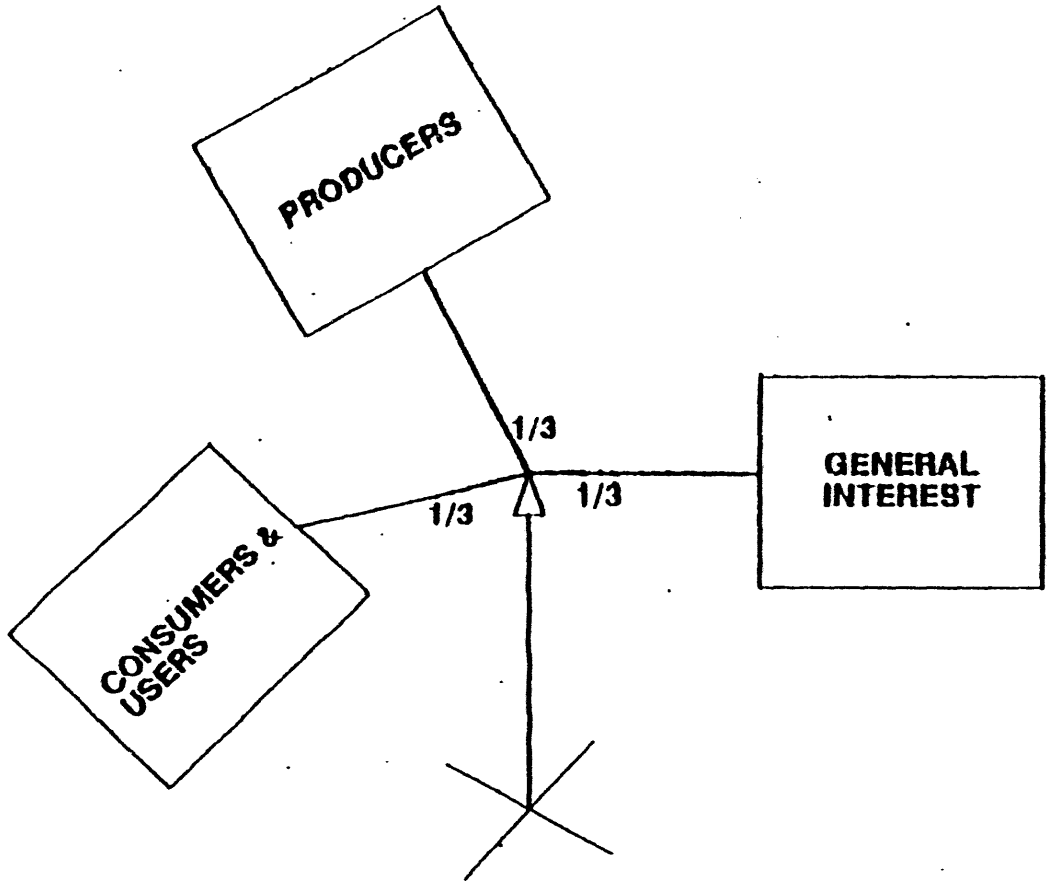

MAIN COMMITTEE E-48 ON BIOTECHNOLOGY

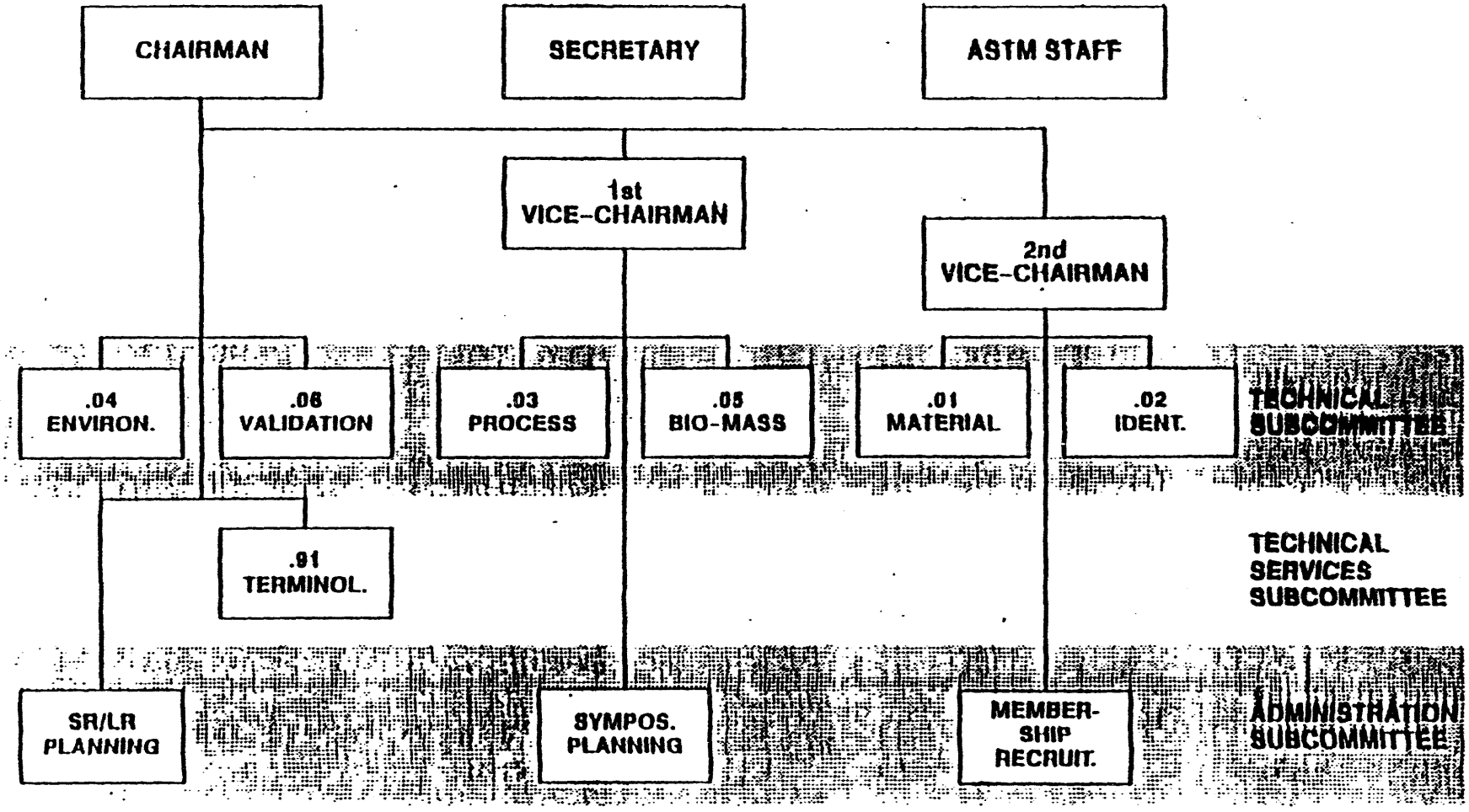

Standards for Biotechnology

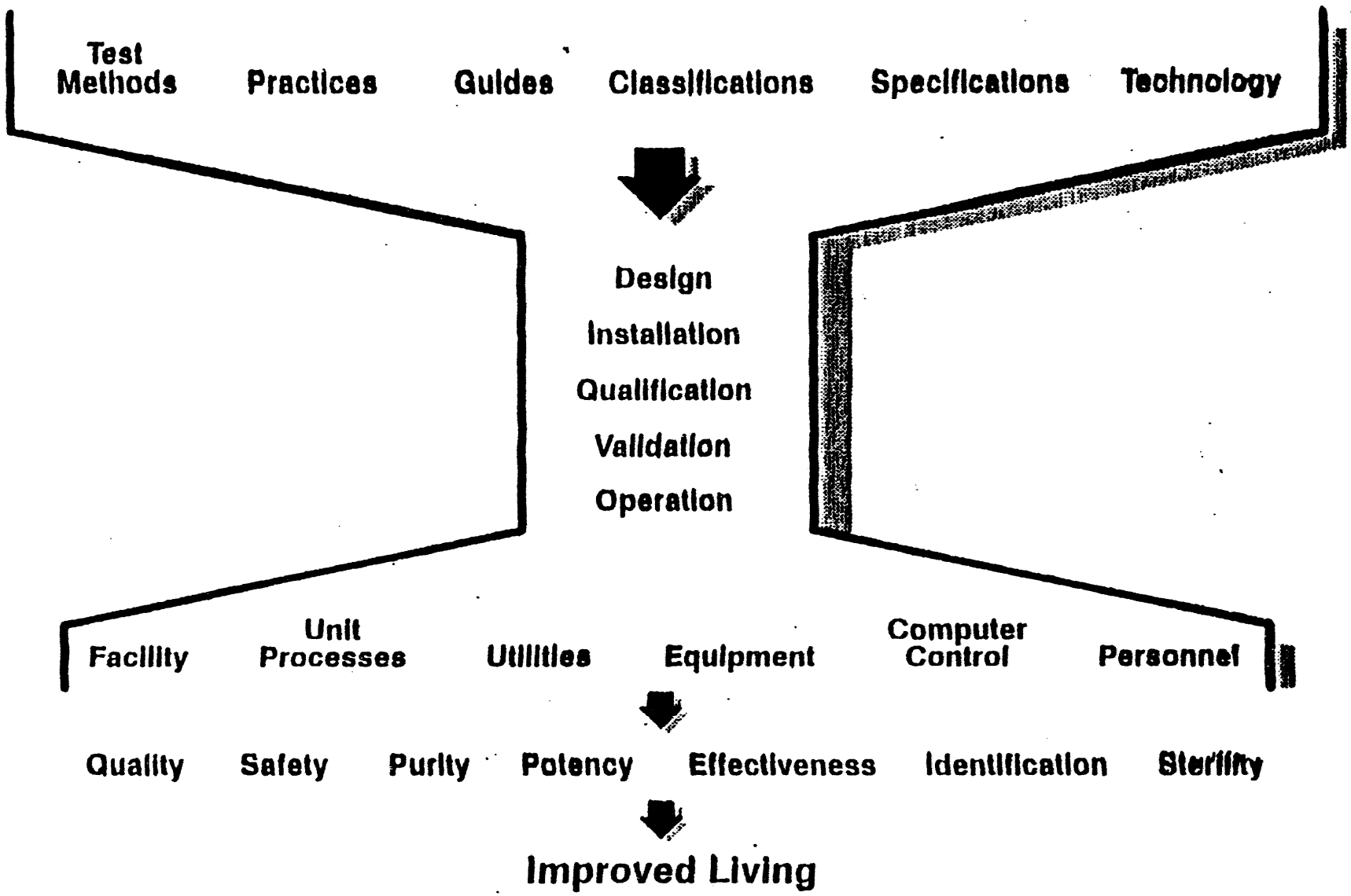

E-48 GOALS IN 1993

- Increase subcommittee task groups to develop more standards
- Plan the second E-48 symposium for 1994-95
- Promote standards with Japan and Europe
- Improve awareness of E-48 in the field of biotechnology
- Increase E-48 membership from government, producers, consumers, and general interest

ASTM E-48 SUBCOMMITTEE STANDARDS

		APPROVED	DRAFT/ PROPOSALS
.01	Materials	8	2
.02	Characterization	4	6
.03	Process/Controls	5	1
.04	Environmental		4
.05	Biomass	12	3
.06	Validation	1	9
.91	Terminology		1
		30	26

SUBCOMMITTEE: E48.0100 MATERIALS FOR BIOTECHNOLOGY

DESIG NR	TITLE
E1298-89	GUIDE FOR DETERMINATION OF PURITY, IMPURITIES, AND CONTAMINANTS IN BIOLOGICAL DRUG PRODCTS
E1531-93	PRACTICE FOR DIRECT DETECTION OF MYCOPLASMA IN CELL CULTURE BY BROTH ENRICHMENT AND AGAR GROWTH
E1532-93	PRACTICE FOR INDIRECT DETECTION OF MYCOPLASMA IN CELL CULTURE BY DNA BINDING WITH BISBENZAMIDE FLUOROCHROME STAIN
E1533-93	PRACTICE FOR INDIRECT DETECTION OF MYCOPLASMA IN CELL CULTURE BY 4' -6-DIAMIDINO-2-2 PHENYLINDOLE (DAPI) STAINING
E1536-93	PRACTICE FOR LARGE VOLUME TESTING OF SERUM FOR MYCOPLASMA CONTAMINATION
NEW STD	GUIDE FOR DESIGN AND MAINTENANCE OF LOW TEMPERATURE STORAGE FACILITIES FOR MAINTAINING CRYOPRESERVED BIOLOGICAL MATERIALS
NEW STD	GUIDE FOR INVENTORY CONTROL AND HANDLING OF BIOLOGICAL MATERIAL MAINTAINED AT LOW TEMPERATURES
NEW STD	GUIDE FOR HANDLING HAZARDOUS BIOLOGICAL MATERIALS IN LIQUID NITROGEN

TOTALS FOR: E48.0100

STANDARDS TOTALS:

APPROVED	=	5
NEW UNAPPROVED	=	0
PROPOSALS	=	0
EMERGENCY	=	0
WITHDRAWN	=	0
[illegible]	=	0

SUBCOMMITTEE: E48.0200 CHARACTERIZATION & IDENTIFICATION OF BIO SYST

DESIG NR	TITLE
E1288-89	GUIDE FOR IDENTIFICATION OF BACTERIOPHAGE LAMBDA ( ) OR ITS DNA
E1284-89	GUIDE FOR IDENTIFICATION OF HERPES SIMPLEX VIRUS OR ITS DNA
E1342-90	PRACTICE FOR PRESERVATION BY FREEZING, FREEZE-DRYING, AND LOW TEMPERATURE MAINTENANCE OF BACTERIA, FUNGI, PROTISTA, VIRUSES, GENETIC ELEMENTS, AND ANIMAL AND PLANT TISSUES
E1493-92	GUIDE FOR IDENTIFICATION OF BACTERIOPHAGE M13 OR ITS DNA

TOTALS FOR: E48.0200

STANDARDS TOTALS:

APPROVED	=	4
NEW UNAPPROVED	=	0
PROPOSALS	=	0
EMERGENCY	=	0
WITHDRAWN	=	0
OVERDUE	=	0

SUBCOMMITTEE: E48.0300 UNIT PROCESS AND THEIR CONTROL

DESIG NR	TITLE
E1287-89	PRACTICE FOR ASEPTIC SAMPLING OF BIOLOGICAL MATERIALS
E1294-89	TEST METHOD FOR PORE SIZE CHARACTERISTICS OF MEMBRANE FILTERS USING AUTOMATED LIQUID POROSIMETER
E1343-90	TEST METHOD FOR MOLECULAR WEIGHT CUTOFF EVALUATION OF FLAT SHEET ULTRAFILTRATION MEMBRANES
E1337-90	TEST METHOD FOR DETERMINING THE RATE OF BIOLEACHING OF IRON FROM PYRITE BY THIOBACILLUS FERROOXIDANS
E1470-92	TEST METHOD FOR CHARACTERIZATION OF PROTEINS BY ELECTROPHORETIC MOBILITY

TOTALS FOR: E48.0300

STANDARDS TOTALS:

APPROVED	= 5
NEW UNAPPROVED	= 0
PROPOSALS	= 0
EMERGENCY	= 0
WITHDRAWN	= 1
REVISIONS	= 0

SUBCOMMITTEE: E48.0500 BIOMASS CONVERSION

DESIG NR	TITLE
E0869-93	METHOD FOR PERFORMANCE EVALUATION OF FERMENTATION FUEL MANUFACTURINNG FACIL ITIES
E0870-82(1992)	TEST METHODS FOR ANALYSIS OF WOOD FUELS
E0871-82(1992)	METHOD OF MOISTURE ANALYSIS OF PARTICULATE WOOD FUELS
E0872-82(1992)	TEST METHOD FOR VOLATILE MATTER IN THE ANALYSIS OF PARTICULATE WOOD FUELS
E0873-82(1992)	TEST METHOD FOR BULK DENSITY OF DENSIFIED PARTICULATE BIOMASS FUELS
E1117-86(1990)	PRACTICE FOR DESIGN OF FUEL ALCOHOL MANUFACTURING FACILITIES
E1126-87(1992)	TERMINOLOGY RELATING TO BIOMASS FUELS
E1288-89	TEST METHOD FOR THE DURABILITY OF BIOMASS PELLETS
E1344-90	GUIDE FOR EVALUATION OF FUEL ETHANOL MANUFACTURING FACILITIES
E1358-90	TEST METHOD FOR DETERMINATION OF MOISTURE CONTENT OF PARTICULATE WOOD FUELS USING A MICROWAVE OVEN
E1534-93	TEST METHOD FOR DETERMINATION OF ASH CONTENT OF PARTICULATE WOOD FUELS
E1535-93	TEST METHOD FOR PERFORMANCE EVALUATION OF ANAEROBIC DIGESTION SYSTEMS
P0211	TERMINOLOGY RELATING TO BIOMASS FUELS

TOTALS FOR: E48.0500

STANDARDS TOTALS:		
	APPROVED	12
	NEW UNAPPROVED	0
	PROPOSALS	1
	EMERGENCY	0
	WITHDRAWN	0
	OVERDUE	1

SUBCOMMITTEE: E48.0600 BIOTECH EQUIP QUALIFICATION & PROCESS VAL.

DESIG NR	TITLE
NEW STD	GUIDE FOR BIOPHARMACEUTICAL FACILITIES ARCHITECTURAL DESIGN CONSIDERATIONS

TOTALS FOR: E48.0600

STANDARDS TOTALS:	APPROVED	0
	NEW UNAPPROVED	1
	PROPOSALS	0
	EMERGENCY	0
	WITHDRAWN	0
	OVERDUE	0

DISCUSSION SUMMARY

DISCUSSION SUMMARY - MATERIALS WORK SESSION

Due to the number of participants and their areas of expertise, one combined work session was held instead of the three originally planned.

Larry Eitel introduced the session with a brief overview of the E-48 Committee on biotechnology and the goals of the work session. Discussions then followed on each of the different unit operations; individual contributor notes are presented in chronological order.

Pretreatment

Discussion centered around the consensus that stainless steel would not be adequate for the temperature and pH conditions. Both more exotic metals and coatings/linings were suggested as possible materials. The toxicity of leached metals was of concern to most participants, particularly in regard to stainless steel alloys and chromium.

J. Keiser (ORNL) - There will be problems with stainless steels at a pH less than 3. Carpenter 20 is probably not good enough at pretreatment conditions.

C. Riley (NREL) - Thinks this operation will require some kind of lining.

J. Keiser (ORNL) - Still believes that metals should be looked at.

N. Huxley (Alf-Atochem) - Chemical resistance greater than stainless steels will be necessary to avoid chemical leaching. (Addresses area of toxicity of leached metals on microbial activity, which was of concern to most of the participants.)

D. Schell (NREL) - TVA uses zirconium for maximum chemical and corrosion resistance.

J. Keiser (ORNL) - To avoid problem of chemical leaching we need to look at top of the line coatings, any suggestions from manufacturers representatives? (No suggestions were offered.) J. Keiser suggested Siloxirane (J. Keiser has information and contact if further information is required - Tankinetics (Chuck Hoffman), (501) 741-3626.)

N. Huxley (Alf-Atochem) - Believes Siloxirane temperature performance may be overated by the manufacturer.

Neutralization

The discussion group felt that this area was of concern for materials selection due to the pH, temperature and components present in the liquid stream. SS alloys were considered questionable for this service also due to the leaching question.

J. Keiser (ORNL) - Flashing will concentrate some of the undesirable products in the liquid stream. Believes that 304 is not adequate and that 316 will need testing for this service.

G. Andermann (U. of HI) - Will still get chromium in the liquid even at a pH of 5.

DISCUSSION SUMMARY...(CONT'D)

Fermentation

The discussion group questioned the adequacy of carbon steel for the fermentation tanks and raised the issue that the composition of the fermentation broth needs to be known before a material can be adequately tested. Both concrete lined tanks and plastic or fiberglass tanks were suggested in addition to coatings for carbon steel tanks. It was felt that coatings may be useful on concrete or carbon steel vessels, but may have problems with pH and temperature swings. Fiberglass tanks may not have adequate resistance to alkaline chemicals used in Clean-In-Place sterilization; alternate sterilization processes were discussed. The suggestion was made to study the alcohol industry to find out what is currently being used.

L. Eitel (Wolder) - Reiterated that current NREL design calls for carbon steel, which is probably not adequate for long term service. We need to know the composition of the fermented material.

N. Huxley (Alf-Atochem) - Suggested that concrete tanks with a suitable liner could be used in place of metal tanks.

G. Tyson - Suggested that plastic tanks may be an option. They are used by the pickle industry, but not at the size required for fermenters. They are cheap, but there would be many issues involved in constructing large tanks suitable for fermenters.

G. Andermann (U. of HI) - Suggested that the Army may have information on constructing large plastic tanks.

Norm Klapper (Electro-Chem) - Suggested that field-erected fiberglass tanks may be an option, however, they would need to be formulated for resistance to CIP chemicals.

G. Tyson - Suggested that we look at "successful" alcohol plants to see what materials they used for their fermenters.

Norm Klapper (Electro-Chem) - Suggested using an ozone treatment for sterilization, this may be more compatible with alternative tank materials.

QUESTIONNAIRE SUMMARY

QUESTIONNAIRE SUMMARY - MATERIALS WORKSHOP

Following is the summary of responses to a questionnaire handed out to all workshop participants. 47% of the attendees returned the questionnaire. Respondents' background represented experience in corrosion testing, materials development and ethanol production, while their training varied between engineering, chemistry, materials science and metallurgy. Many had expertise with pilot plant and/or commercial facilities in the fossil energy, pulp/paper, chemical process, and biotechnology industries.

In general, most respondents recommended identifying currently available materials of construction and conducting an analysis to screen the most likely candidates. These materials should be tested in a standardized manner with the cooperation of researchers and experts in the materials industry to ensure the results can be directly applied. Specific comments to the questions are outlined below.

The majority of the respondents felt that the pretreatment area would benefit the most from materials research due to the extreme physical, chemical and thermal environment created, particularly with any acid pretreatment. Fermentation was also identified as an area in which materials research would benefit the economics of the process. Due to the unique environment in the fermentation tanks, applied testing (using a similar solution for testing) was stressed as important. To a lesser degree, abrasion studies would help to identify potential problems in the feedstock handling area. The suggestion was made to look at existing plants, both in the biomass to ethanol industry and in industries with similar processes to avoid doing research in already mature technologies.

Sample monitoring for material specimens in the pilot plant included both recommendations on chemical species to test for and testing methods to use. Chemical species included chlorine ions, sulfur, carbon and other metal deposits. Testing methods mentioned were ASTM procedures, evaluation of surface as well as interstitial changes in the material, weight change and compressive strength change of samples. A testing method used in determining engine wear by inspecting the oil drained from the engine was also suggested. Several respondents recommended accelerated testing of samples (coupons) in a laboratory setting followed by verification in the pilot plant. Sample placement in the pilot plant equipment, particularly in pretreatment, was a concern. It was also recommended to inspect the process solution for chemical species from the material specimens.

In addition to the ASTM and other test methods mentioned in the above responses, electrochemical studies were recommended for the accelerated testing, although the difficulty in simulating the entire pretreatment environment was noted. Instrumentation included electron microprobe, scanning electron microscopy (SEM), X-ray emission spectroscopy (XES), surface IR reflectance, and AC impedance. Keeping it simple and standardized was a theme suggested by many participants so that the results could be applied to a variety of situations through correlations.

There was a large variation among the respondents in extrapolating the pilot plant data to years of service, although most agreed that the extrapolation would be a function of the

QUESTIONNAIRE SUMMARY...(CONT'D)

quality of testing done. Several issues such as the length of testing (relative to corrosion rates), ability of pilot plant process to simulate the commercial process, and the philosophy of materials use were factors to consider in test planning.

Other issues in the biomass to ethanol process that would benefit from research more than the materials issue were noted as optimum microorganism application and research, alternate pretreatment and feedstock handling methods, solids separation, and waste disposal problems.

The most recommended materials for evaluation in the pretreatment area were polymeric and other coatings/linings. Specific materials were outlined by the material vendors. Acid brick and ceramic coatings were also listed for the pretreatment area. One possible drawback noted for coatings is the chance for erosion or chipping. In the fermentation area, lined carbon steel or concrete tanks were recommended. One respondent noted that metallic coatings could be an option if the economics were promising. Research needs to assess what is currently available in the materials arena by conducting a risk analysis and selecting the candidates with the highest probability of success. Carbon steel, the assumed material for the current base case, should be tested to prove/disprove its suitability.

Other areas recommended for additional research included catalyst materials, corrosion inhibitors added to the process stream, and the effect of metal ions on fermentation.

In the area of storage, other problems needing materials research included alcohol induced corrosion, adhesive systems, cleaning, contamination, impact of excess moisture formation (for gasohol) and fiberglass for gas tanks.

78% of the respondents felt the workshop was of value to them, although a longer program was suggested to cover all the issues. 78% also felt that they contributed to the workshop.

APPENDIX

OVERVIEW OF BIOMASS TO ETHANOL PROCESS

The conversion of biomass to biofuels is relatively well-researched in some aspects; other aspects are much less understood. One of the latter areas is materials selection for the process. Often, construction materials are chosen on the basis of past experience without taking the time to identify new and potentially cost-saving materials. This workshop will be the first in a series of steps to develop a research plan for a new program to identify and test possible low-cost materials of construction suited to the biomass to ethanol process. From the information presented on the conversion technology and information from workshop attendees in their fields of expertise, a preliminary research plan will be developed and potential participants identified for materials testing, economic analysis and other testing.

Biomass is a general term for lignocellulosic material; that is, it contains lignin and cellulose. Cellulose is a complex carbohydrate that when broken down into its monomeric form, glucose, can be used by various types of organisms to produce ethanol. Another component of lignocellulosic material is hemicellulose, which can also be utilized by organisms provided it is converted into monomeric sugars. Lignin cannot be fermented to ethanol.

The National Renewable Energy Laboratory (NREL) has developed a conceptual design for the biomass to ethanol process for the purpose of directing future research. A detailed process description and economic analysis are presented for a wood substrate. Capital costs are based primarily on carbon steel and stainless steel. Capital costs in this report refer to this NREL design case.

The general process for converting biomass to ethanol is comprised of the following steps: feedstock handling, pretreatment, biocatalyst production, fermentation, and ethanol recovery. Utilities, Wastewater treatment and off-sites support the process (see attachment 1). Of these areas, the utilities area makes up almost 42% of the total installed cost (TIC) for a plant (see below). Of the process areas, the highest percentage of installed equipment costs are in the pretreatment and the fermentation areas (source: the NREL design case). The capital estimate for the fermentation area assumes carbon steel tanks; if 316L is required, the relative percent of TIC becomes 36.5%. Is it these two areas which represent the greatest potential for savings from reduced equipment costs.

PROCESS AREA	% OF TIC
Feedstock Handling	5.6
Pretreatment	18.4
Biocatalyst Production	2.1
Fermentation	21.1
Ethanol Recovery	3.1
Utilities	41.3
WasteTreatment/Off-sites/Misc.	8.3

A preliminary economic analysis was performed to identify potential materials for inclusion into the research plan. The analysis included the major cost components in pretreatment and fermentation, namely the reactors and the fermentation tanks. The materials were selected on the basis of their compatibility with the particular process conditions in each area. These two areas will be further detailed along with Feedstock Handling, Ethanol Recovery and Waste Treatment.

It is important to keep in mind the general aspects of the entire process and their relevance to equipment construction and materials selection. Feedstock can range from wood chips to grasses to municipal solid waste (MSW), each with its own unique set of problems. For the purpose of this discussion, we will describe the process based on a wood feedstock with comments regarding other feedstock types. All of the feedstocks have abrasive characteristics and retain some solid content throughout the process. pH extremes are common due to the pretreatment strategies, fermentation conditions, and organic acids produced in an aqueous medium. Less difficult conditions exist with respect to temperature and pressure although even mild conditions can cause materials problems when coupled with low pH. Therefore, general process conditions can be described as:

- abrasive solids
- moderate to high solids levels (6 - 35%)
- low pH (1.3)
- acidic, aqueous medium
- ambient to moderate temperatures (20 - 200°C)
- atmospheric to low pressures (0 - 200 psig)

Pretreatment

Several basic pretreatment processes have been developed along with a myriad of variations for each. Any treatment prior to fermentation is typically used to hydrolyze the xylan to xylose and remove the lignin to increase the enzymatic digestibility of the cellulose (prehydrolysis) and, in some cases, to also hydrolyze the cellulose (hydrolysis). Pretreatment processes typically use acid combined with heat to break down the lignocellulosic structure and hydrolyze the carbohydrate chains, although other methods such as explosive decompression or the use of an alkali agent have been developed. For the purpose of this discussion, dilute sulfuric acid prehydrolysis will be detailed and other processes will be outlined.

Milled biomass (wood chips, grasses, MSW, etc.) is fed to a prehydrolysis reactor after being slurried to 35 wt. % solids, impregnated with dilute sulfuric acid (0.73-0.95 wt. %) and preheated to 100°C. The impregnated material is then heated to between 140 and 180°C with steam injection and held for 10 - 30 minutes, depending on the reactor temperature chosen. pH within the reactor is 1.3 - 1.4. Known reactions occurring within the reactor include the conversion of xylan to xylose (monomeric sugar), a small percentage of cellulose to glucose, xylose to furfural, and glucose to 5-hydroxymethyl furfural (HMF). The sugar degradation products, furfural and HMF are aldehydes which can react further to form carboxylic acids. Acetic acid is also formed from the acetyl groups present in the carbohydrate chains. Other by-products, such as lignin derivatives (from decomposition of lignin) and formic acid, which degrades easily to hydrogen gas (H_2) and carbon dioxide (CO_2) have been reported in literature. Other acids (nitric, phosphoric, hydrochloric) have also been investigated for use in dilute acid prehydrolysis.

Equipment used in dilute acid prehydrolysis includes feeders, impregnators and pressurized reactors, flash tanks with agitation, pumps and acid handling equipment. The impregnators and reactors comprise 88% of the purchased cost for this area. Equipment immediately downstream of the reactors must be specified for low pH service.

In determining suitable materials of construction for this process, the following negative and positive considerations must be taken into account:

-very low pH
-high solids concentration
-moderate temperatures
-erosion by the solid substrate
-leaching of construction material into process stream
+short residence time

Dilute acid pretreatment necessitates a subsequent **neutralization** step to bring the pH up to about 5.0, a range hospitable to yeast. This is done by adding solid lime to the process slurry after is has been flash cooled to 100°C and diluted to about 12 % solids. Gypsum is formed

in a reaction between the lime and sulfur groups in the process liquor. This by-product partially precipitates and is not removed to minimize cost. It may pose a problem downstream by adding to the abrasive nature of the process stream. Additionally, gypsum exhibits decreasing solubility at increasing temperatures and may foul the distillation columns.

Since the pretreatment step also serves to sterilize the process stream, all equipment downstream must be capable of being cleaned and sterilized prior to use as well as be designed to maintain aseptic conditions.

Equipment used in the neutralization step includes solids handling equipment for the lime as well as a neutralization tank with agitation, heat exchangers to cool the process stream, and slurry pumps.

Process considerations include:

-pH extremes, particularly in the neutralization tank
-precipitate formation
-maintenance of aseptic conditions
-leaching of metals into process stream
+moderate to low temperatures
+short residence time

In the NREL design case for the biomass to ethanol process, it is assumed that the pretreatment reactors are made of Carpenter-20, a low-carbon stainless steel alloy with molybdenum added for extra corrosion resistance. In the economic analysis it was not possible to cost the entire reactor (shell and internals) so the shell alone was quoted. It appears the best economic alternative to investigate is carbon steel lined with neoprene, acid brick, teflon, etc. It should be emphasized that these results are preliminary and do not take into account possible higher costs due to difficult manufacturing or lack of skilled manufacturing. For this reason, a more detailed analysis must be performed in conjunction with the materials research.

Although dilute acid prehydrolysis (DAP) combined with neutralization is the technology in which NREL has the most experience, other processes are being used or are under development. The figure below outlines various pretreatment schemes and a brief description of each is given below.

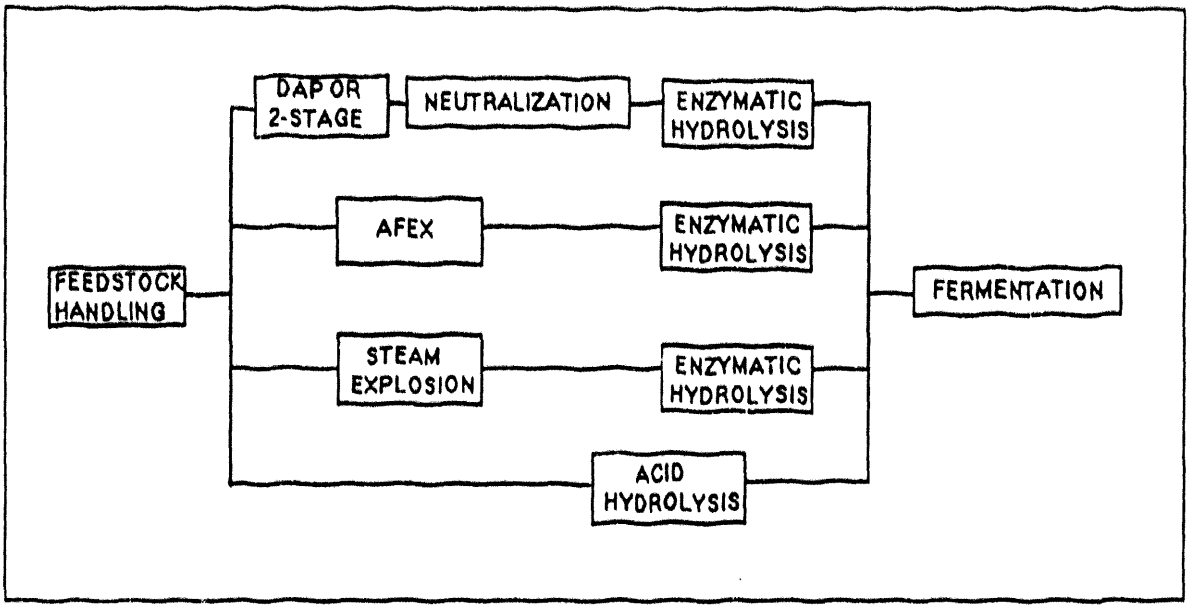

Pretreatment Schemes

2-stage acid prehydrolysis

This treatment is essentially the same as dilute acid prehydrolysis except that 2 different temperature levels are used. The reasoning behind this is that a large percentage of the xylan is hydrolyzed to xylose fairly rapidly; the remainder takes longer to hydrolyze. It is believed that the two temperature steps (140 and 170°C) with a washing step in-between facilitates the two hydrolysis rates with much less degradation of the xylose. Initial research indicates that up to 98% of the available xylan is hydrolyzed to xylose or xylose oligomers. Drawbacks to this process are, for the most part, the same as in dilute acid prehydrolysis - the low pH of the resulting stream requires acid-resistant materials selection and a neutralization step.

Ammonia fiber explosion (AFEX)

The AFEX method treats lignocellulosic material with liquid ammonia under pressure, followed by pressure release to evaporate the ammonia and explode the material. The major advantages of this process are that it negates the need for any pH neutralization, facilitates catalyst recovery (NH_3), and the low reaction temperatures (generally ambient) discourage by-product formation. From a materials standpoint, the reactor would be required to withstand liquid ammonia at pressures up to 200 psia at ambient temperature.

Steam explosion

By itself, steam explosion is a prehydrolysis method utilizing explosive decompression to exert a mechanical shear on the lignocellulosic fibers. The process uses high pressure steam (650 psia) to pressurize the reactor containing the feedstock. Due to the resulting high temperatures (250° C) a significant amount of degradation products are formed which are inhibitory to microbial growth and the solid must be washed to remove them.

By adding either sulfuric acid or sulfur dioxide as a catalyst in steam explosion, the yield of xylose from xylan can be increased; however, the same low pH problems arise as in dilute acid prehydrolysis. In addition, use of sulfur dioxide requires an extensive recovery system.

Acid Hydrolysis

This method actually replaces the enzymatic hydrolysis step. This process utilizes a higher temperature (265°C) than dilute acid prehydrolysis to facilitate autohydrolysis of the hemicellulose and cellulose. Due to this higher temperature, increased production and further degradation of the by-products seen at lower temperatures occurs, resulting in tars, levulinic and oleic acid by-products, believed to be inhibitory to the microbes, not to mention difficult to carry through a process. Low yields, typical of acid hydrolysis, result in poor process economics.

In grouping these various pretreatment methods with regard to materials of construction concerns, it becomes obvious that those employing acid require the most consideration, owing to the combination of low pH and temperature.

Fermentation

The second area which deserves close attention to equipment specification is the fermentation area. Fermentation is the heart of the biomass to ethanol process in which sugars are converted to ethanol through metabolic pathways of selected organisms. The process stream from pretreatment, mixed with enzyme, nutrients and a seed culture of microbes (yeast, bacteria or fungi) is held in large atmospheric tanks arranged in series for 5 - 7 days at a temperature between 35 - 40 °C. During fermentation, the pH of the broth typically drops from 5.0 to 3.5 or 3.0, depending on the organism being used. Production of organic acids, CO_2 and to a lesser extent, ethanol are responsible for the drop in pH. In some instances, pH is controlled by addition of calcium salts, ammonium sulfate, or hydroxides (ammonium, sodium, potassium), although this adds cost and is generally avoided.

By-products from the selected organism can include glycerol, acetic acid and lactic acid. Others, such as acetaldehyde, fusel oils (amyl, isoamyl, propyl alcohol), succinic acid, propionic acid, and formic acid, which degrades to CO_2 and H_2 have been reported in literature. Other potential sources of by-products are contaminant organisms, producing larger amounts of lactic (lactobacillus) or succinic acid (E. coli). pH control agents such as

ammonium-containing compounds can release ammonia, and salts can release chloride ions into the broth. Almost all of the by-products listed can have a negative effect on carbon steel fermentation tanks, either by corrosion or embrittlement.

Equipment in the fermentation area is comprised primarily of atmospheric fermentation tanks currently sized at 780,000 gallons each. Carbon steel fermentation tanks alone represent 56% of the purchased equipment cost for this area; 316L tanks would represent 78% of the cost. Heat exchangers, pumps and agitators are also required.

The primary process considerations stem from the low pH of the fermentation broth. Additionally, the negative and positive aspects must be taken into account when determining suitable materials:

-aqueous environment
-long residence time
-maintenance of aseptic conditions
-erosion from gypsum precipitate
-leaching of metals into broth
+low temperatures
+atmospheric pressure

Once again, we see the need for a low cost material, primarily for tank construction, that will handle an acidic pH and the presence of corrosive or embrittling chemicals.

For the fermentation vessels, 100,000 to 850,000 gallon atmospheric tanks were costed using various materials of construction. Carbon steel, used in the NREL design case analysis gives the lowest purchased cost, but there is some concern as to its suitability for the acidic conditions and abrasive solids encountered in fermentation. The next cheapest alternative is, again, carbon steel with some lining material resistant to organic acids. A subcontractor performed a similar study for NREL and found the same results - lining carbon steel tanks with a suitable low-cost lining such as epoxy or resin is more economically attractive than stainless alloys.

Three other process areas, feedstock handling, ethanol recovery and wastewater treatment deserve mention with respect to materials selection, not because a large savings in cost is possible, but because of the unique problems that the biomass presents.

Feedstock Handling

The two major concerns in the area of feedstock handling are erosion of equipment due to the abrasive nature of the feedstock and feedstock acidity. Biomass substrates such as wood and grasses can erode feeders, mills and other size reduction equipment. Contaminants in the feedstock (stones, grit, bark) can also cause erosion.

Stored feedstock can experience a drop in pH if kept for long periods of time or managed poorly, i.e. allowed to remain wet or compacted such that air cannot circulate within the pile. Normal wood pH (4.3 - 5.0) can drop to 3.0 in poor conditions. Although handling takes place at ambient temperatures and most feedstocks have a low moisture content, the drop in pH could cause slow corrosion of storage, conveying and size reduction equipment.

Ethanol Recovery

From fermentation, the process stream is sent to a series of distillation columns and solids separation equipment to recover the ethanol and concentrate the solids. The low concentration ethanol stream (3 - 4 wt.%) contains about 6 wt. % solids and most of the by-products from previous process steps. Process stream pH is still 3 - 5. The temperature in the atmospheric columns can reach 110°C in the bottoms of the columns and even higher temperatures at heat exchanger surfaces, which can cause the gypsum in the stream to become insoluble. Concentration of by-products in the column, such as acetic acid, can cause localized corrosion. Solids can cause fouling of the column and promote uneven flow through the trays. Solids separation equipment, primarily centrifuges, are exposed to the acids and other by-products present in the distillation bottoms.

Waste Treatment

Waste treatment must be capable of withstanding a mix of streams from solids separation, distillation and the Clean-In-Place/Chemical Sterilization system. In addition to the feed conditions, design of this area must take into account the long residence times required for digestion of the feed stream components by a mixed culture of organisms. Near ambient temperatures reduce the chance of corrosion from the acids in the feed. Large tanks and reactors dominate the equipment list, along with heat exchangers and pumps.

Summary

Throughout the biomass to ethanol process,solids content, pH, temperature and production of corrosive by-products dominate materials selection decisions. In particular, selection of the pretreatment method determines the level of corrosion resistance required.

In fermentation, the pH and the decision of whether or not to use pH control agents are the primary factors in determining candidates for materials. Careful selection of the control agent can avoid additional problems such as ammonia production or chloride ion release. Selection of the organism to minimize acid production can also play a role; however, organisms are generally selected first for their ability to produce ethanol with a high yield. Work is underway to alter organisms so that by-products are minimized.

Not to be overlooked is the economic factor that must come into play when evaluating processes or the equipment to carry them out. A material that can withstand low pH and elevated temperatures with acceptable corrosion rates may be so expensive that a profit cannot

be realized, no matter how long the useful equipment life. On the other hand, a change in conditions to reduce the corrosive nature of the process, while more costly than the unaltered process, may extend the life of a cheaper material and keep the process economics in a competitive range.

It is these two areas that must be explored simultaneously to determine the best selection of process and materials for the biomass to ethanol process. Research on the process side is underway; the materials research must start with a compilation of information from those most familiar with the area.

In summary, the outlined process conditions combined with the results of the preliminary economic study point to the need for additional options to be identified and screened for suitability and potential economic impact. Subjecting the best alternatives to a rigorous testing program including inhibition research and an in-depth economic analysis will provide candidates for long term testing and validation. These steps could reduce the cost of materials for alternative fuels processes.

OVERALL BLOCK FLOW DIAGRAM
Wood-to-Ethanol Process

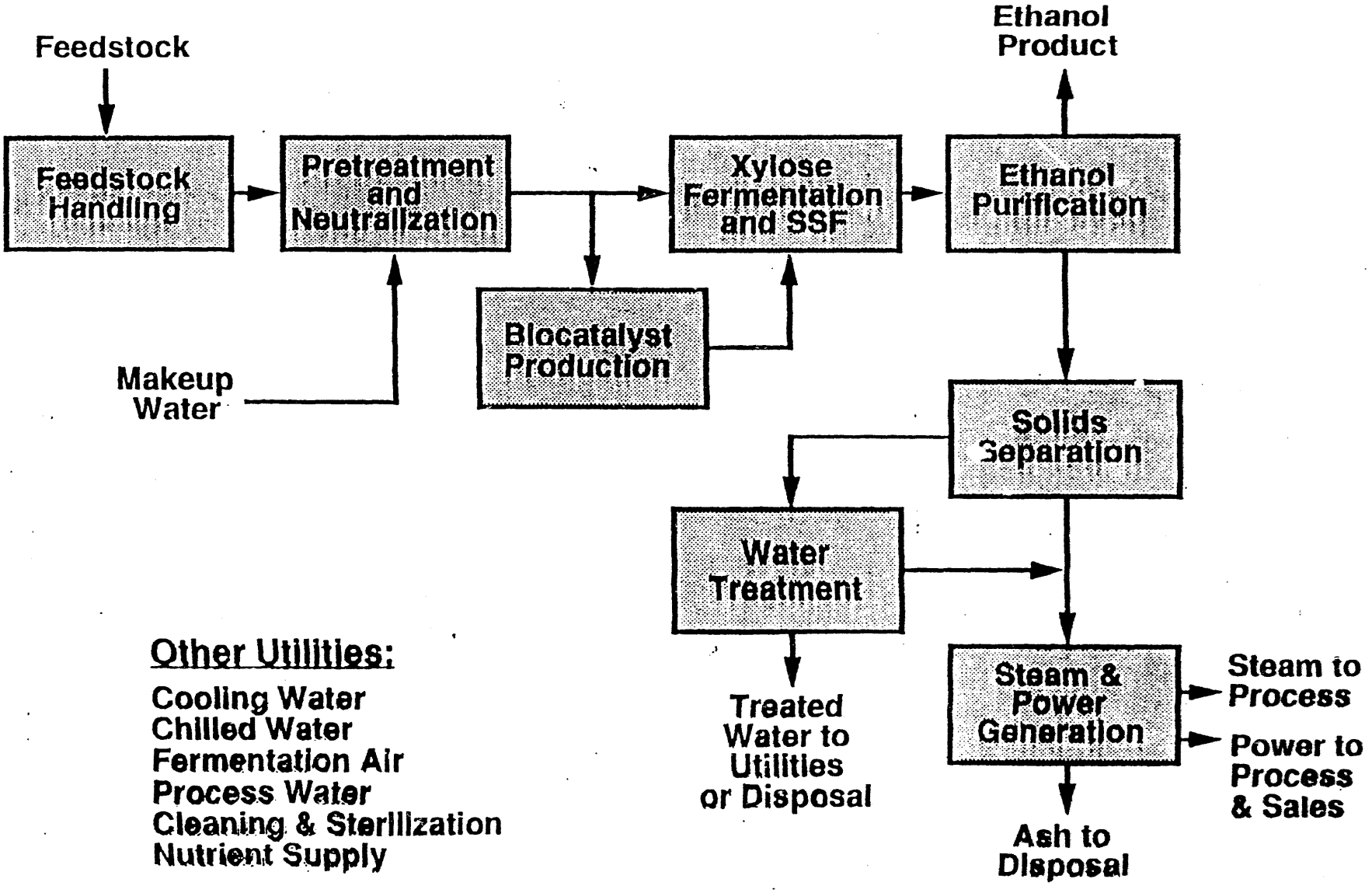

ATTACHMENT 1

OVERVIEW OF BIOMASS PROCESSES
DISCUSSION OUTLINE

•General Lignocellulosic Composition of Biomass
- ·Lignin, Cellulose, Hemicellulose, Glucose, Xylan and Xylose

•Description of the Biomass to Ethanol Process
- ·Feedstock Handling
- ·Pretreatment
- ·Biocatalyst Production
- ·Fermentation
- ·Ethanol Recovery
- ·Utilities
- ·Waste Treatment/Off-sites/Misc.

•General Process Conditions
- ·acidic, aqueous medium
- ·abrasive solids
- ·pH extremes
- ·moderate temperatures and pressures

•Pretreatment and Fermentation most capital intensive process areas

•Pretreatment
- ·Acid Prehydrolysis
  - -pressurized reactors with screw agitation
  - -very low pH process
  - -moderate temperature
  - -degradation products formed which can cause corrosion or embrittlement
  - -erosion by solids
- ·Neutralization
  - -large pH swings
  - -precipitate formation
  - -maintenance of aseptic conditions
- ·Other Pretreatment Processes
  - -2-Stage Acid Prehydrolysis
  - -Ammonia Fiber Explosion
  - -Steam Explosion
  - -Acid Hydrolysis

•Fermentation
- -10,000 to 1,000,000 gallon tanks
- -low pH process
- -low temperature
- -atmospheric pressure
- -organic acids and CO_2, H_2 formed
- -potential for contamination by-products
- -erosion from precipitate, solids
- - long residence time
- -maintenance of aseptic conditions
- -leaching of metals, corrosion products

•Feedstock Handling
- -storage and conveying equipment
- -size reduction equipment
- -erosion of equipment from abrasive solids
- -pH drop due to poor management techniques
- -ambient conditions

•Ethanol Recovery
- distillation columns
- -centrifuges
- -gypsum precipitation and column fouling
- -acidic, aqueous, slurry
- -concentration of by-products in columns
- -moderate temperature, low pressure

•Waste treatment
- -tanks and reactors
- -alkaline medium
- -long residence time
- -methane, CO_2 produced
- -low temperature, atmospheric pressure

•Process variables that most affect materials of construction selection
- ·Pretreatment
  - -method
    - -agents
    - -temperature
  - -substrate

- Fermentation
  - -pH and pH control
    - -selection of control agent
  - -organism selection/modification

- Preliminary Economic Analysis
  - Pretreatment reactors
    - -NREL design case economics based on Carpenter-20
    - -carbon steel with lining lowest purchased cost of identified alternatives
    - -other alternatives need to be identified
  - Fermentation tanks
    - -NREL design case economics based on carbon steel (CS), concern about suitability
    - -identified alternatives all more expensive than CS
    - -CS with linings next best economic alternative
    - -other alternatives need to be identified

- Summary
  - chemical, biological corrosion possibile, along with fouling
  - identification of additional materials needed with corresponding economic analysis
  - best alternatives chosen for testing program
  - simultaneous in-depth economic analysis required
  - additional testing to include effects of material on process - inhibitory to fermentation
  - long-term testing and validation

Biomass to Ethanol
Materials of Construction Worksheet

Stream	1	2	3	4
Name:	Biomass	Pretreated Feed	Flash Stream	Flashed Solids
Fluids, Wt%	0	65	0	88
		Water, Acids		Water, Glycerol
Solids, Wt%	100	35	0	12
		Cellulose, Lignin, Xylan		Cellulose, Xylan, Sugars, Lignin
Temp, C	Ambient	100-180	100	100
P,psig	Atm.	50-105	Atm.	Atm.
pH	3-5	1.3-1.4		1.3-1.4
Velocity/ Turbulence		High Energy		Mixer
Corrosives	Rocks, sap, grit, bark	H_2SO_4, furfual, HMF, carboxylic acids, H_3PO_4, HCl, HNO_3, formic acid, CO_2	Furfural	H_2SO_4, HMF, carboxylic acids, H_3PO_4, HCl, HNO_3, formic acid
Materials of Construction				
Primary:	CS	Carpenter 20	SS304	SS304
Alternates:		CS w/ lining		
Other	Abrasives	Abrasives		Abrasives

Biomass to Ethanol
Materials of Construction Worksheet

Stream	5	5A	6	7	8
Name:	Neutra-lized Solids	Lime/ Slurry	Neutral Xylose Sol'n	Ethanol From Xylose	SSF Feed
Fluids, Wt%	80	0-80	80	85-90	85-90
	Water, Glycerol	Water	Water, Glycerol	Water, Ethanol (1-2%), Glycerol	Water, Ethanol (1-2%), Glycerol
Solids, Wt%	20	100-20	20	10-15	10-15
	Cellulose, Xylan, Sugars, Lignin	Lime	Cellulose, Xylan, Sugars, Lignin	Cellulose, Xylan, Sugars, Lignin	Cellulose, Xylan, Sugars, Lignin
Temp, C	100	Ambient	35-40	35-40	35-40
P, psig	Atm.		Atm.	Atm.	Atm.
pH	5	10-12	5	3-3.5	3-5
Velocity/ Turbulence	Centrifuge	Mixer			
Corrosives	Acids, Bases	Lime	Acids, Bases	Acids, NH_3, Cl^-, Ethanol	Acids, NH_3, Cl^-, Ethanol
Materials of Construction					
Primary	SS304	CS	CS	CS	CS
Alternates			CS w/ Lining	CS w/ lining	CS w/lining
Other	Abrasives	Abrasives	Abrasives	Abrasives	Abrasives

Biomass to Ethanol
Materials of Construction Worksheet

Stream	8A	9	10	11
Name:	Cellulase Enzyme	SSF Product	Lignin Solids	Dilute Ethanol Solution
Fluids, Wt%	90-92%	90-92%	45-50%	92-96%
	Water	Water, Ethanol (4-5%), Glycerol	Water	Water, Ethanol (3-4%)
Solids, Wt%	8-10%	8-10%	50-55%	4-8%
	Cellulose, Xylan, Lignin, Sugars, Gypsum, Cellulase	Cellulose, Xylan, Lignin, Sugars, Gypsum	Lignin, Cellulose Xylan, Gypsum	
Temperature, C	25-30	35-40	35-40	35-110
Pressure, psig	Atm.	Atm.	Atm.	Atm.
pH	4.8	3-3.5	3-5	3-5
Velocity/ Turbulence				
Corrosives		Chlorides, Ammonia, Ethanol	Acids, Bases	Ethanol
Materials of Construction				
Primary:	CS	CS	CS	CS
Alternates:				
Other			Abrasives	

Biomass to Ethanol
Materials of Construction Worksheet

Stream	12	13	14	15	18
Name:	Distillation Waste Organics	Ethanol Product Stream	Waste Treatment	Organics to Boiler	Sludge to Boiler
Fluids: Wt%	100%	100%	95-98%	100% Gaseous	50%
	Water, Fusel Oils, Aldehydes	Ethanol (99.5%), Water	Water, Glycerol	Water (4%), CO_2 (53%), Methane (43%)	Water
Solids, Wt%	0	0	2-5%	0	50%
			Cellulose, Xylan, Lignin, Gypsum, Sugars		Cellulose, Lignin, Gypsum
Temper-ature C	35-80	75-80	35-40	35-40	35-40
Pressure, psig	Atm.	Atm.	Atm.	Atm.	Atm.
pH	DNA	5-7	6-8	DNA	DNA
Velocity/ Turbulence					
Corrosives		Ethanol			
Materials of Construc-tion					
Primary:	CS	CS	CS; CS w/ lining	CS	CS
Alternates:					
Other			Abrasives		Abrasives

Pretreatment

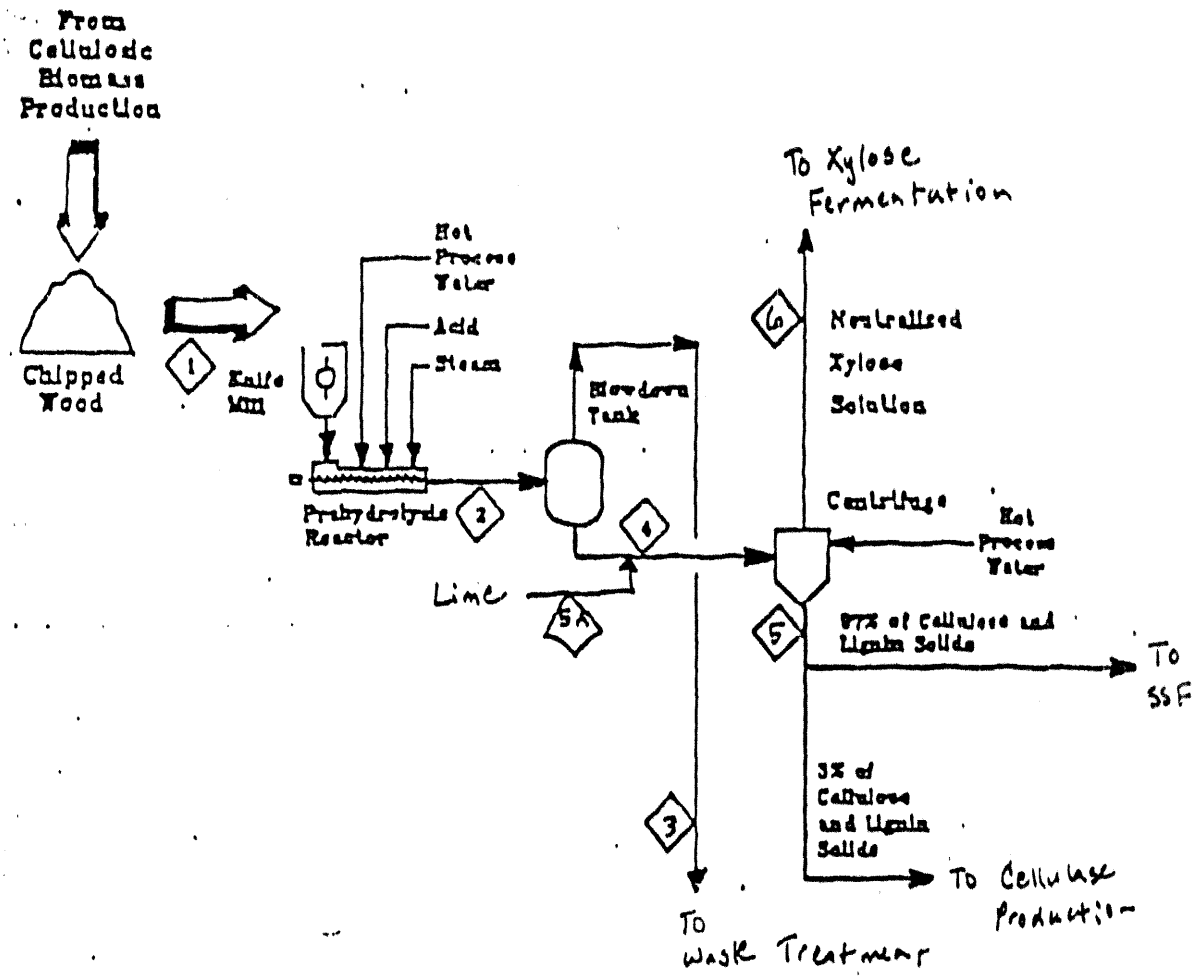

Fermentation and Ethanol Recovery

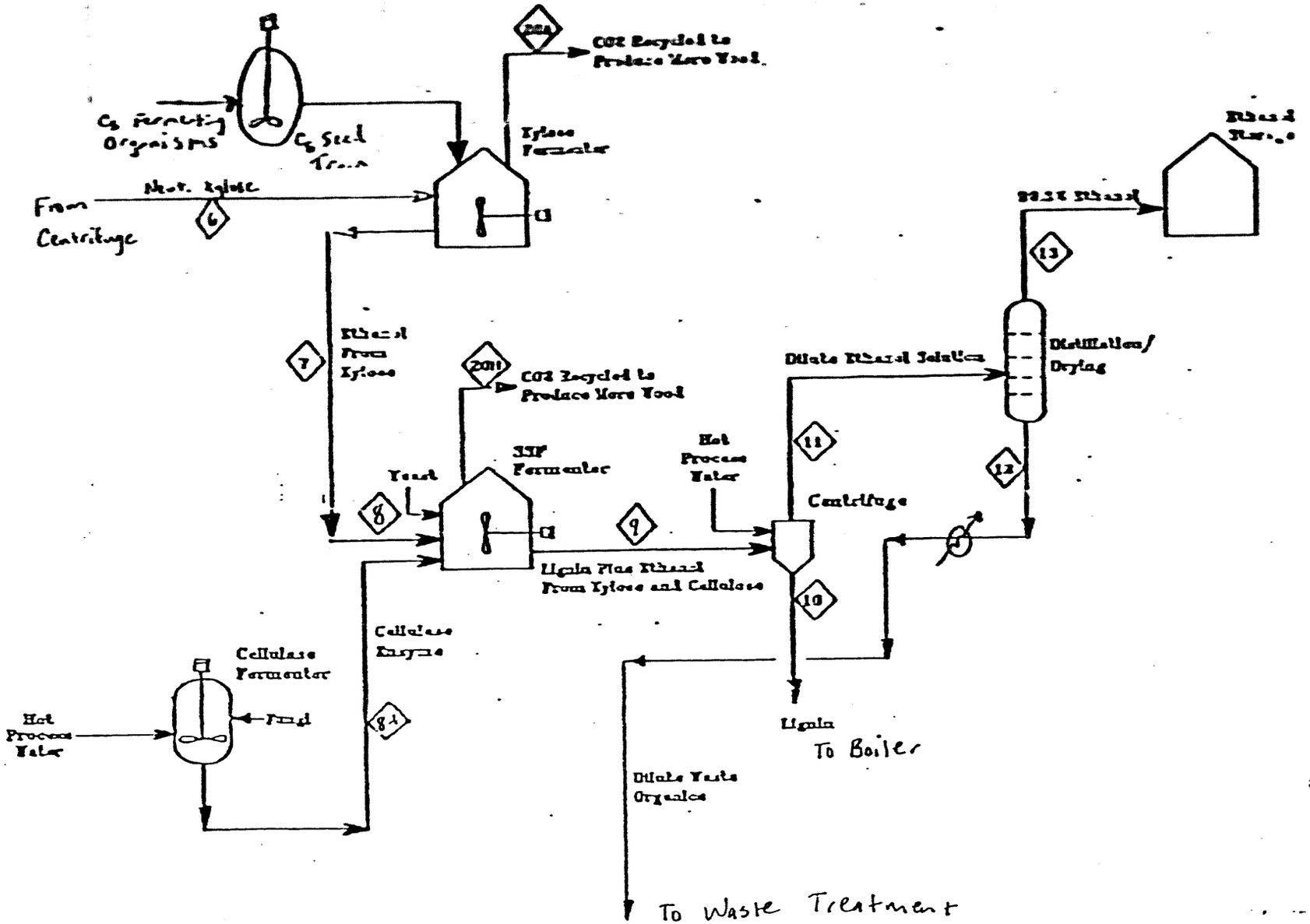

Waste Treatment and Electricity Generation

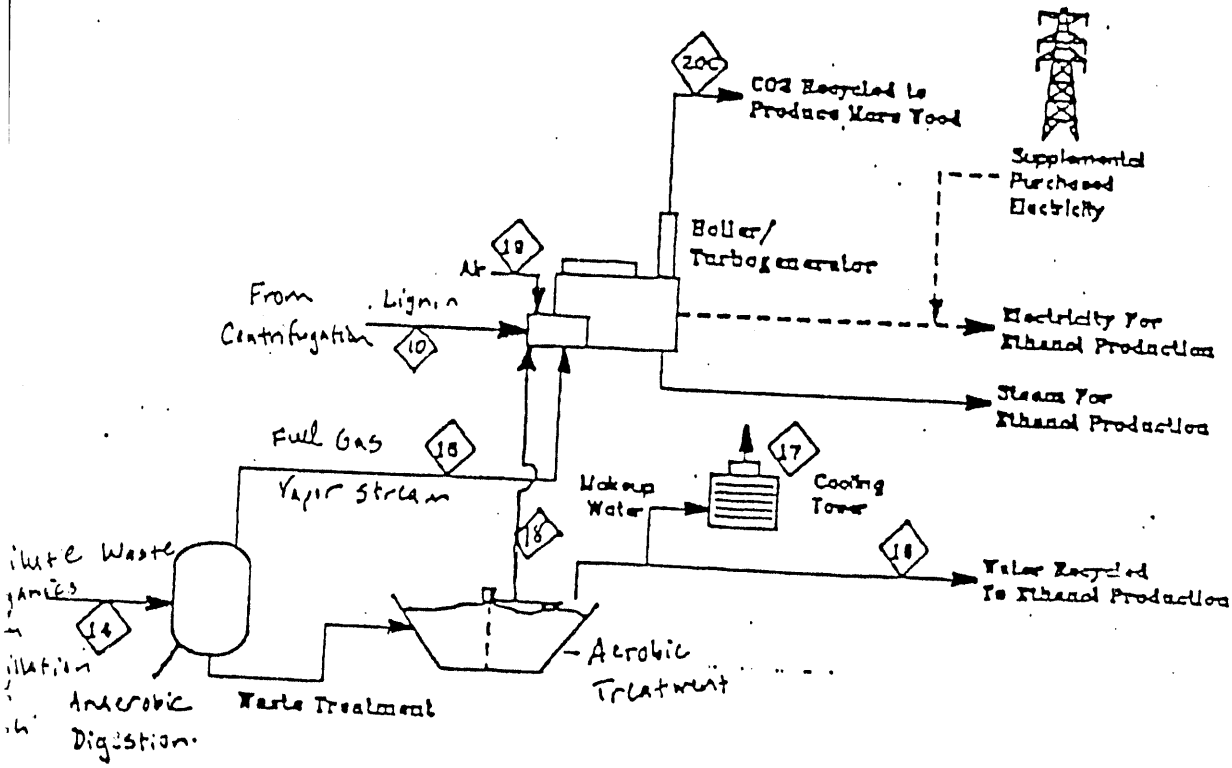

NAME:

YOUR PARTICIPATION IN THE WORKSHOP IS APPRECIATED AND WILL BE USEFUL IN DEFINING FUTURE PROGRAM IN THE ALTERNATIVE FUELS-COMPATIBLE MATERIALS AREA.

WORKSHOP on BIOMASS MATERIALS.
DOE/ORNL/NREL
May 13, 1993
Colorado Springs, CO

The following questions are aimed at identifying information on materials and corrosion that may help in the definition of program areas related to the Alternative Fuels-Compatible Materials Program.

EXPERIENCE:

Professionally trained as: [] Chemist [] Chem Eng [] Civil Eng [] Mech Eng [] Metallurgist [] Other:_____

1. Are you or have you been involved in biomass, alternative fuel, materials or corrosion research? [] Yes [] No

If yes, briefly describe your experience.

2. Have you had experience related to construction materials for either pilot plants or commercial facilities? [] Yes [] No

If yes, briefly describe your experience.

Alternatives/Path :

3. Based on the presentations, which areas related to the biomass processes described do you feel could significantly benefit from materials research.

[] Pretreatment:

[] Fermentation:

[] Feed-stock Handling:

[] Ethanol Recovery:

[] Waste Treatment:

Why:

4. If material specimens were to be evaluated as part of the pilot plant program next year, what sample monitoring would you recommend?

5. What instrumentation or tests would you recommend for evaluation of the samples? Why?

6. Do you feel it would be feasible to extrapolate the pilot plant laboratory tests to [] 5 years, [] 10 years, [] less years _____ , [] more years _____.

7. Do you feel that there are other areas that would benefit the Biomass Processing more than the construction materials issue? [] Yes [] No

If yes, which area.

8. Other than the materials described in the overview, what materials would you consider for the pilot plant evaluations and for which process areas?

Are any of the following paths would you recommend?

[] 1. Evaluate metallic coatings on lower cost metals.
[] 2. Evaluate polymeric coatings.
[] 3. Evaluate ceramic coatings.
[] 4. Evaluate other coatings.

9. Are there other areas that you would recommend additional research?

[] Catalyst materials [] Instrumental monitoring

[] Coatings [] Other Chemical SyNthesis

[] Other: _____

Comments:

Infrastructure:

10. One of the more important initial areas for research is storage, whether it be on vehicles, transportation or production storage. In addition to permeability and corrosion, are there other problems you see as needing materials research?

Other:

11. Do you feel that the workshop was of value to you?

12. Do you feel that you made a contribution to the workshop in defining needs or giving direction to future materials research areas?

13. Any other comments (Use additional Sheets if Necessary):

Cindy Riley
NREL
1617 Cole Blvd
Golden, CO 80401-3393

Dr. J.M. Perez, EE-34
USDOE
1000 Independence Ave, SW
Washington, DC 20585

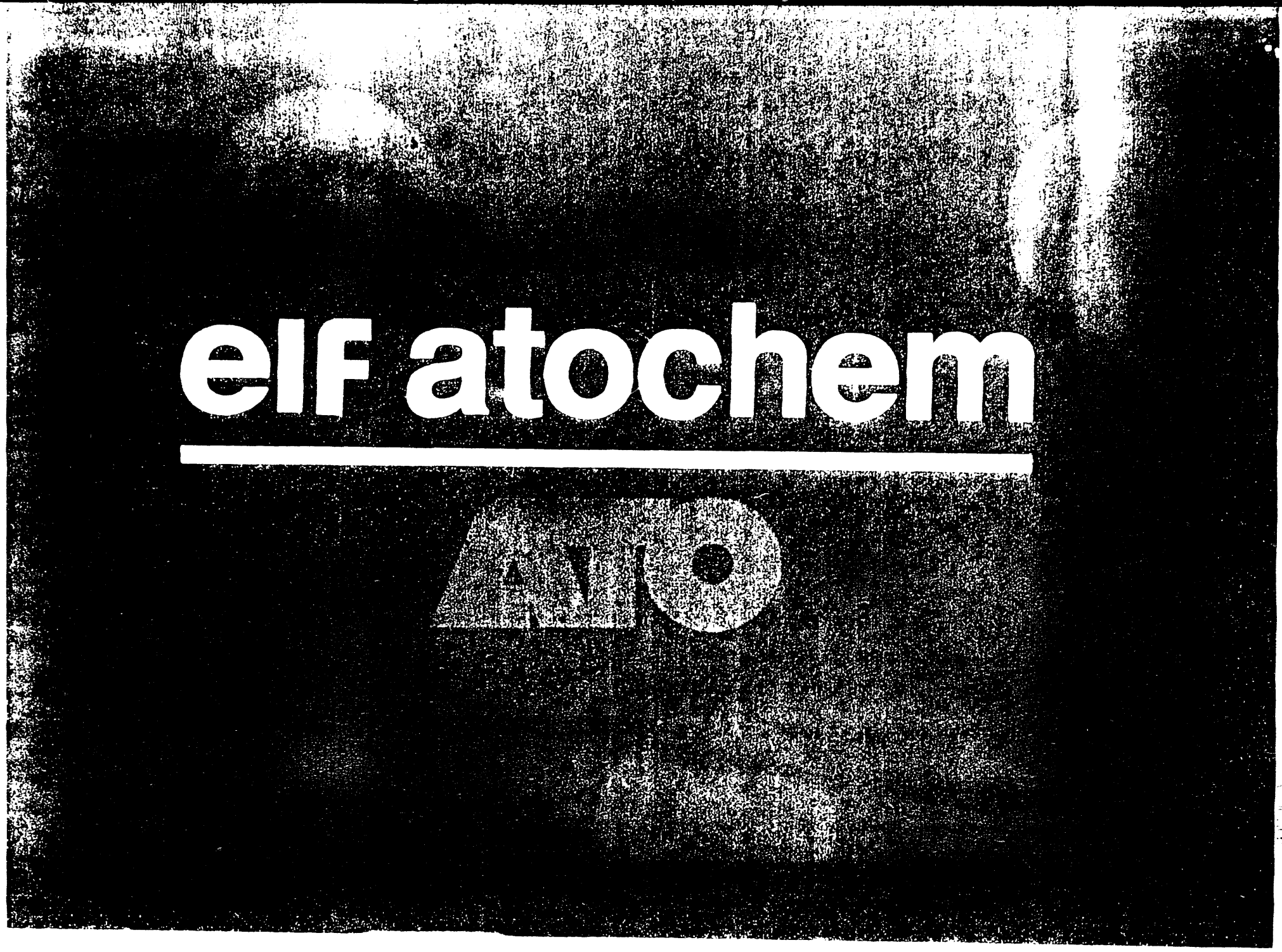
elf atochem
ATO

The Elf Group

1991 Results

Sales	$39 Billion
Net Income	$1.9 Billion

The Elf Group

Elf
(Hydrocarbons)

- Exploration and Production
- Refining and Marketing
- International Trading & Shipping

Elf Atochem
(Chemicals)

- Petrochemicals
- Chlorine Chemicals and PVC
- Fertilizers
- Specialty Chemicals
- Polymers and Fabricated Products
- Sulfur Chemicals

Elf Sanofi
(Health, Beauty & Biotechnology)

- Human Health/ Pharmaceuticals
- Food Additives
- Beauty Products/ Fragrances

The Elf Group in France

orld's La[illegible]t Chemical Companie[illegible]

1. BASF
2. Hoechst
3. Bayer
4. ICI
5. Du Pon[illegible]
6. Dow
7. Rhone Poulenc
8. Ciba Geigy
9. Shell Chemicals
10. Elf Atochem

elf atochem

Elf Atochem North America

1991 Results

Sales $1.5 Billion

Employees 5,500

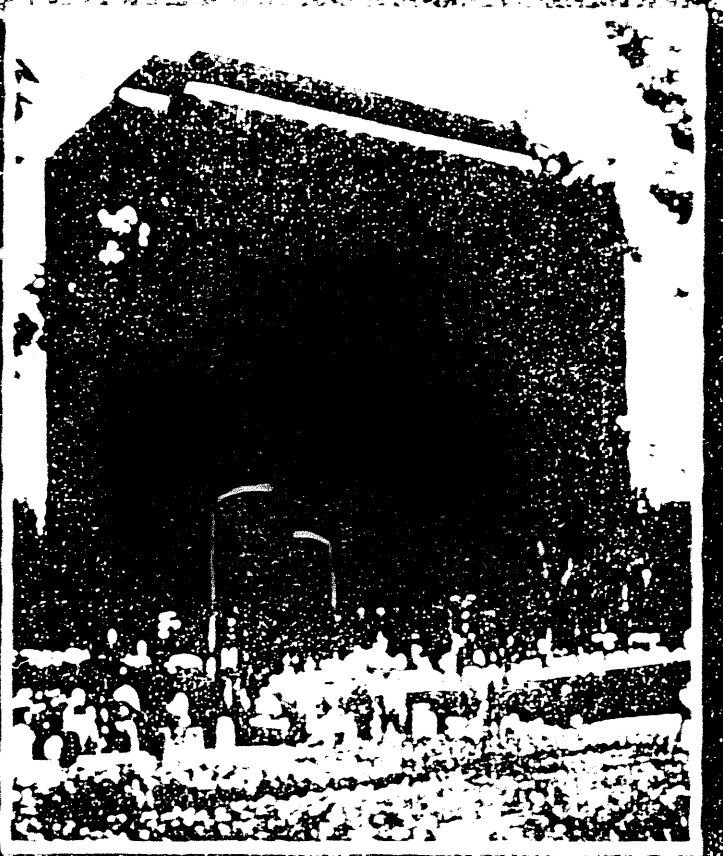

Where Will You Find the Products Made by the Specialty Chemicals Group?

Airplane Maintenance Chemicals

Toothpaste

Water Filters

Elf Atochem North America
Vision Statement

Elf Atochem North America will be the preferred supplier in its markets.

Our employees will take pride in providing quality products and superior service to every customer.

The company will be recognized for innovation, responsiveness, commitment to the environment and sensitivity to the community.

Elf Atochem North America Quality Policy

Elf Atochem North America will prosper and grow by being responsive to its customers, employees, communities and owners.

To our customers, we pledge quality products and superior service. We will strive to understand their requirements and to satisfy their expectations 100% of the time. We expect the same quality pledge from our suppliers.

To our employees, we pledge a quality workplace. Recognizing that our people are the means through which success is achieved, the company will provide functional and safe facilities and an environment that promotes opportunity, fulfillment and productivity. Our employees will receive developmental training and will be empowered to carry out their duties with objectives and methods that are established through open communication. We take pride in being an equal opportunity employer with a policy of promoting from within. Advancement and compensation will be based on performance that contributes to our ability to satisfy customers.

To our communities, we pledge responsible membership. We will contribute to regional and local development by providing employment and by encouraging our employees to participate in community, professional and service organizations. We will be a good neighbor committed to protecting the environment.

END

DATE
FILMED
2/24/94